Mechanical Ventilation Modelling and Optimisation

Erwin van Drunen

A thesis presented for the degree of

Masters of Engineering

in

Mechanical Engineering

at

The University of Canterbury,

Christchurch, New Zealand.

August, 2013

Acknowledgements

To my supervisors, Prof. Geoff Chase and Dr. Geoff Shaw, for their inputs and insights, as well as their valuable time.

To the bioengineering team for their ideas and help, in particular, Dr. Yeong Chiew.

To my family and friends for their love and support, in particular, Luci Swatton.

Table of Contents

List of Figures

List of Tables

Nomenclature

ABG	Arterial Blood Gas
ARDS	Acute Respiratory Distress Syndrome
CAT	Computer Axial Tomography
CM	Combined Method
CO_2	Carbon Dioxide
CT	Computed Tomography
dFRC	Dynamic Functional Residual Capacity
E_{cw}	Chest Wall Elastance
E_{drs}	Dynamic Respiratory System Elastance
$E_{dynamic}$	Dynamic Elastance
EIP	End-Inspiratory Pause
EIT	Electrical Impedance Tomography
EIV	End Inspiratory Volume
$E_{L,spec}$	Specific Lung Elastance
E_{lung}	Lung Elastance
E_{rs}	Respiratory System Elastance
E_{rsIB}	Respiratory System Elastance (Integral-Based Method)
E_{static}	Static Elastance
ET	Endotracheal (tube)
FRC	Functional Residual Capacity
ICU	Intensive Care Unit
IQR	Inter-Quartile Range

K	Expiratory Time-Constant Model Parameter
LIP	Lower Inflection Point
MV	Mechanical Ventilation
O_2	Oxygen
p	Wilcoxon Rank Sum Test Value
P_0	Offset Pressure
P_{0IB}	Offset Pressure (Integral-Based Method)
PaO_2/FiO_2	Arterial Partial Pressure of O_2 divided by the Fraction of Inspired O_2 (PF ratio)
P_{aw}	Airway Pressure
PEEP	Positive End Expiratory Pressure
PIP	Peak Inspiratory Pressure
P_L	Transpulmonary Pressure
P_{plat}	Plateau Pressure
PV	Pressure-Volume
Q	Volumetric Flow Rate
Q_0	Maximum Expiratory Volumetric Flow Rate
R^2	Trend Correlation Coefficient
RCT	Randomised Controlled Trial
R_{lung}	Lung Resistance
RM	Recruitment Manoeuvre
R_{rs}	Respiratory System Resistance
R_{rsIB}	Respiratory System Resistance (Integral-Based Method)
R_{static}	Static Resistance
SCSB	Single Compartment Single Breath
SSMB	Stress-Strain Multiple Breath
SSSB	Stress-Strain Single Breath

t	Time
TCP	Threshold Closing Pressure
TOP	Threshold Opening Pressure
UIP	Upper Inflection Point
V	Lung Volume
VILI	Ventilator Induced Lung Injury
VIR	Vibration Response Imaging
V_{P_0}	Additional Lung Volume due to PEEP
V_t	Tidal Volume
WoB	Work of Breathing
ZEEP	Zero End Expiratory Pressure
α	Ratio of E_{lung} to E_{cw}
β	Population Constant (SSMB Method, CM)
β_1	Population Constant (SSSB Method, CM)
τ	System Time-Constant

Abstract

Acute Respiratory Distress Syndrome (ARDS) is associated with lung inflammation and fluid filling, resulting in a stiffer lung with reduced intrapulmonary gas volume. ARDS patients are admitted to the Intensive Care Unit (ICU) and require Mechanical Ventilation (MV) for breathing support. Positive End Expiratory Pressure (PEEP) is applied to aid recovery by improving gas exchange and maintaining recruited lung volume. However, high PEEP risks further lung injury due to overstretching of healthy lung units, and low PEEP risks further lung injury due to the repetitive opening and closing of lung units. Thus, selecting PEEP is a balance between avoiding over-stretching and repetitive opening of alveoli. Furthermore, specific protocols to determine optimal PEEP do not currently exist, resulting in variable PEEP selection. Thus, ensuring an optimal PEEP would have significant impact on patient mortality, and the cost and duration of MV therapy.

Two important metrics that can be used to aid MV therapy are the elastance of the lungs as a function of PEEP, and the quantity of recruited lung volume as a function of PEEP. This thesis describes several models and model-based methods that can be used to select optimal PEEP in the ICU. Firstly, a single compartment lung model is investigated for its ability to capture the respiratory mechanics of a mechanically ventilated ARDS patient. This model is then expanded upon, leading to a novel method of mapping and visualising dynamic respiratory system elastance. Considering how elastance changes, both within a breath and throughout the course of care, provides a new clinical perspective. Next, a model using only

the expiratory portion of the breathing cycle is developed and presented, providing an alternative means to track changes in disease state throughout MV therapy. Finally, four model-based methods are compared based on their capability of estimating the quantity of recruited lung volume due to PEEP.

The models and model-based methods described in this thesis enable rapid parameter identification from readily available clinical data, providing a means of tracking lung condition and selecting optimal patient-specific PEEP. Each model is validated using data from clinical ICU patients and/or experimental ARDS animal models.

Deputy Vice-Chancellor's Office
Postgraduate Office

UNIVERSITY OF CANTERBURY
Te Whare Wānanga o Waitaha
CHRISTCHURCH NEW ZEALAND

Co-Authorship Form

This form is to accompany the submission of any thesis that contains research reported in co-authored work that has been published, accepted for publication, or submitted for publication. A copy of this form should be included for each co-authored work that is included in the thesis. Completed forms should be included at the front (after the thesis abstract) of each copy of the thesis submitted for examination and library deposit.

Chapter 5 (excluding the work on the SLICE Method):

VAN DRUNEN, E. J., CHIEW, Y. S., PRETTY, C., SHAW, G. M., LAMBERMONT, B., JANSSEN, N., CHASE, J. G. & DESAIVE, T. 2013. Visualisation of Time-Varying Respiratory System Elastance in Experimental ARDS Animal Models. *BMC Pulmonary Medicine*, (In Review).

VAN DRUNEN, E. J., CHIEW, Y. S., ZHAO, Z., LAMBERMONT, B., JANSSEN, N., PRETTY, C., DESAIVE, T., KNUT, M. & CHASE, J. G. Visualisation of Time-Variant Respiratory System Elastance in ARDS Models. Congress for the German Swiss and Austrian Society for Biomedical Engineering, 19-21 September 2013 Graz, Austria. BMT, 2.

Please detail the nature and extent of contribution by the candidate:

EJD assisted in the development of the E_{drs} model, generated the MATLAB code to create the E_{drs} maps, and drafted the manuscripts. EJD was thus the lead author and contributed at least 80% to these works under the supervision of JG Chase and YS Chiew with contributions (clinical, data, editing/comments and engineering) from other authors.

Certification by Co-authors:
If there is more than one co-author then a single co-author can sign on behalf of all. The undersigned certify that:

- The above statement correctly reflects the nature and extent of the masters candidate's contribution to this co-authored work.
- In cases where the candidate was the lead author of the co-authored work he or she wrote the text.

Name: *JG Chase*

Signature: 

Date: *August 6, 2013*

Deputy Vice-Chancellor's Office
Postgraduate Office

UNIVERSITY OF CANTERBURY
Te Whare Wānanga o Waitaha
CHRISTCHURCH NEW ZEALAND

Co-Authorship Form

This form is to accompany the submission of any thesis that contains research reported in co-authored work that has been published, accepted for publication, or submitted for publication. A copy of this form should be included for each co-authored work that is included in the thesis. Completed forms should be included at the front (after the thesis abstract) of each copy of the thesis submitted for examination and library deposit.

Chapter 6:

VAN DRUNEN, E. J., CHIEW, Y. S., CHASE, J. G., SHAW, G., LAMBERMONT, B., JANSSEN, N., DAMANHURI, N. & DESAIVE, T. 2013. Expiratory model-based method to monitor ARDS disease state. *BioMedical Engineering OnLine*, 12, 57.

VAN DRUNEN, E. J., CHIEW, Y. S., CHASE, J. G., LAMBERMONT, B., JANSSEN, N. & DESAIVE , T. Model-based Respiratory Mechanics to Titrate PEEP and Monitor Disease State for Experimental ARDS Subjects The 35th Annual International Conference of the IEEE Engineering in Medicine and Biology Society (EMBC"13), 3-7 July 2013 Osaka, Japan. IEEE, 4.

Please detail the nature and extent of contribution by the candidate:

EJD assisted in the development of the time-constant model, generated the MATLAB code to perform the validation of the model, and drafted the manuscripts. EJD was thus the lead author and contributed at least 80% to these works under the supervision of JG Chase and YS Chiew with contributions (clinical, data, editing/comments and engineering) from other authors.

Certification by Co-authors:
If there is more than one co-author then a single co-author can sign on behalf of all. The undersigned certify that:

- The above statement correctly reflects the nature and extent of the masters candidate's contribution to this co-authored work.
- In cases where the candidate was the lead author of the co-authored work he or she wrote the text.

Name: *JG Chase*

Signature: 

Date: *August 6, 2013*

Deputy Vice-Chancellor's Office
Postgraduate Office

UNIVERSITY OF CANTERBURY
Te Whare Wānanga o Waitaha
CHRISTCHURCH NEW ZEALAND

Co-Authorship Form

This form is to accompany the submission of any thesis that contains research reported in co-authored work that has been published, accepted for publication, or submitted for publication. A copy of this form should be included for each co-authored work that is included in the thesis. Completed forms should be included at the front (after the thesis abstract) of each copy of the thesis submitted for examination and library deposit.

Chapter 7 (excluding the work on the animal data):

VAN DRUNEN, E. J., CHASE, J. G., CHIEW, Y. S., SHAW, G. M. & DESAIVE, T. 2013. Analysis of different model-based approaches for estimating dFRC for real-time application. *BioMedical Engineering OnLine*, 12, 9.

Please detail the nature and extent of contribution by the candidate:

EJD developed the Combined Method, generated the MATLAB code to perform the validation of the models, and drafted the manuscript. EJD was thus the lead author and contributed at least 80% to this work under the supervision of JG Chase and YS Chiew with contributions (clinical, data, editing/comments and engineering) from other authors.

Certification by Co-authors:
If there is more than one co-author then a single co-author can sign on behalf of all. The undersigned certify that:

- The above statement correctly reflects the nature and extent of the masters candidate's contribution to this co-authored work.
- In cases where the candidate was the lead author of the co-authored work he or she wrote the text.

Name: *JG Chase*

Signature: 

Date: *August 6, 2013*

Chapter 1 – Introduction

1.1 RESPIRATORY SYSTEM ANATOMY AND PHYSIOLOGY

Cells are the basic structural and functional units of an organism and require a continuous supply of oxygen (O_2) to perform metabolic reactions to release energy. These reactions produce carbon dioxide (CO_2), which, in excessive amounts, can be toxic to cells and must be removed quickly. The respiratory system provides the means for gas exchange to occur, while the cardiovascular system transports the blood containing these gases between the lungs and the body cells. Thus, the respiratory system and the cardiovascular system cooperate to efficiently supply cells with O_2 and eliminate CO_2 (Tortora and Derrickson, 2006).

The respiratory system can be divided into two physiological zones. The first is the conducting zone, consisting of a series of interconnecting cavities and tubes that filter, warm, and moisten air as it is transported to the lungs. The second is the respiratory zone, where gas exchange occurs between the air and the blood. The respiratory system can also be divided into two anatomical regions. The first is the upper respiratory system consisting of the nose, pharynx, and associated structures. The second is the lower respiratory system consisting of the larynx, trachea, bronchi, and lungs (Tortora and Derrickson, 2006). These structures are shown in Figure 1.1.

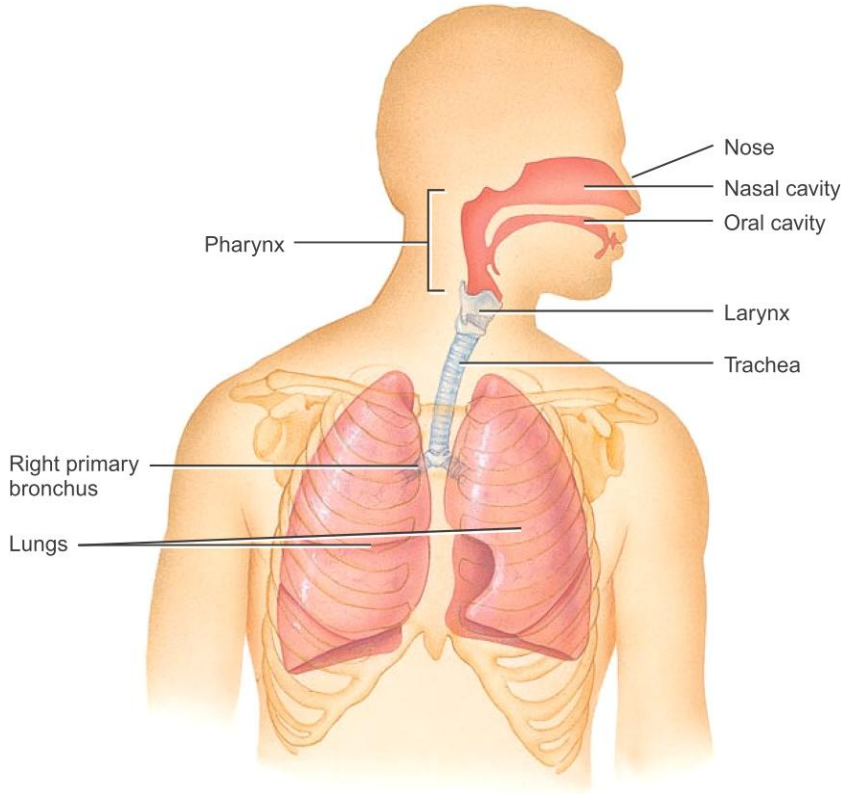

Figure 1.1 – Anterior view of the respiratory system (Tortora and Derrickson, 2006).

The lungs are paired organs situated within the thoracic cavity which is formed by the ribs, the muscles of the chest, the sternum, the thoracic portion of the vertebral column, and the diaphragm. The two lungs are located lateral to the heart with the left lung smaller than the right lung due to a concavity to accommodate the heart. Each lung is enclosed and protected by two layers of serous membrane, one lining the inner wall of the thoracic cavity, and the other lining the outer surface of each lung. Between these two membranes is a small space, known as the pleural cavity, containing pleural fluid that acts to reduce friction between the two membranes during breathing (Tortora and Derrickson, 2006).

During inspiration, air travels into the nasal cavity or oral cavity, through the pharynx and larynx, and into the trachea. The trachea is surrounded by horizontal hoops of cartilage, as shown in Figure 1.2, which act to support the tracheal wall from collapse. The inferior end of the trachea bifurcates into two primary bronchi, one for each lung. Upon entering the lungs, each primary bronchi branches to form smaller secondary bronchi, one for each lobe, where the right lung has three lobes and the left lung has two lobes. Secondary bronchi branch to form smaller tertiary bronchi that branch into smaller bronchioles, which, in turn, branch repeatedly, ultimately branching to form terminal bronchioles. The cartilage hoops are gradually replaced by cartilage plates in the primary bronchi and disappear completely in the distal bronchioles. The terminal bronchioles branch to form microscopic respiratory bronchioles, finally branching to form alveolar ducts. Approximately 25 generations of branching occurs between the trachea and the alveolar ducts (Tortora and Derrickson, 2006).

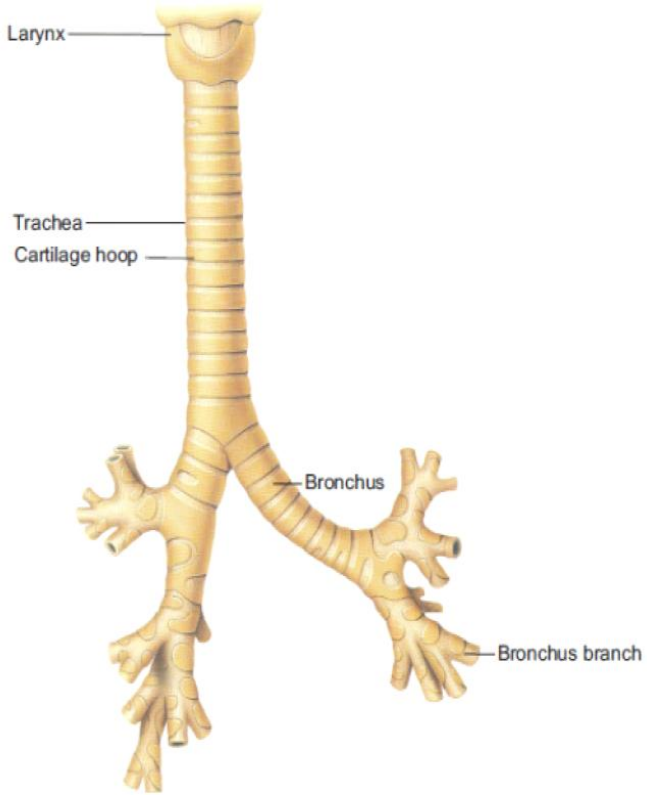

Figure 1.2 – Major proximal airways (Sebel, 1985).

Surrounding the alveolar ducts are numerous alveoli and alveolar sacs which consist of two or more alveoli sharing a common opening. Clusters of alveoli, known as lung units, are shown in Figure 1.3. The walls of alveoli consist of two types of epithelial cells. Type I cells are the primary sites of gas exchange, while type II cells secrete alveolar fluid that keeps the surface between the cells and the air moist. Included in the alveolar fluid is surfactant, a mixture of phospholipids and lipoproteins that lowers the surface tension of the alveolar fluid. Surface tension produces a force directed inward, reducing the diameter of the alveoli, and must be overcome to expand the lungs during inspiration. Therefore, a lower surface tension reduces the inspiratory effort by reducing the tendency of alveoli to collapse (Tortora and Derrickson, 2006).

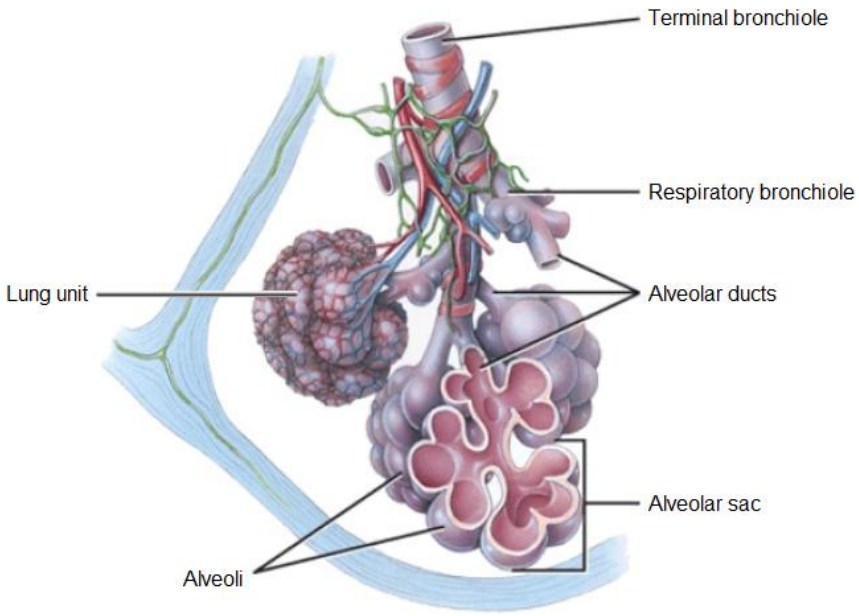

Figure 1.3 – Alveoli, alveolar sacs, and lung units (Tortora and Derrickson, 2006).

The lungs receive deoxygenated blood via the pulmonary arteries and oxygenated blood via the bronchial arteries. Return of oxygenated blood to the heart occurs via four pulmonary veins. The exchange of O_2 and CO_2 between the air in the lungs and the blood takes place in

available, or recruited, alveoli. Gas exchange is determined by the respective partial pressures of O_2 and CO_2 on either side of the alveolar and capillary walls, which together form the respiratory membrane. The respiratory membrane is very thin to allow for rapid diffusion of gases (Tortora and Derrickson, 2006).

1.2 PULMONARY VENTILATION

Pulmonary ventilation results in airflow between the atmosphere and the alveoli of the lungs due to pressure differences created by contraction and relaxation of respiratory muscles. The rate of airflow and the amount of effort required for breathing is also influenced by alveolar surface tension, stiffness of lung tissue, and airway resistance. Air travels into the lungs when the pressure inside the lungs is less than atmospheric pressure. Air travels out of the lungs when the pressure inside the lungs is greater than atmospheric pressure. These two scenarios define inspiration and expiration, respectively.

Pressure changes within the lungs are generated by changing the volume of the thoracic cavity. For inspiration, the lungs must expand in volume, thereby decreasing the alveoli pressure below atmospheric pressure. This negative pressure gradient is generated primarily by the diaphragm, which forms the base of the thoracic cavity, while the remainder is due to contraction of the external intercostals, which elevate the ribs and increase the anteroposterior and lateral diameters of the thoracic cavity. There is no physical connection between the lungs and the diaphragm or rib cage, so a negative pressure gradient must be created across the pleural cavity. Thus, movement of the lungs is completely passive.

Expiration begins when the inspiratory muscles relax. The recoil of elastic fibers stretched during inspiration, and the inward force of the surface tension due to the alveolar fluid, causes a decrease in lung volume. Thus, during quiet breathing, expiration is a passive process (Tortora and Derrickson, 2006). Figure 1.4 shows how movement of the diaphragm and ribs results in airflow between the atmosphere and the lungs.

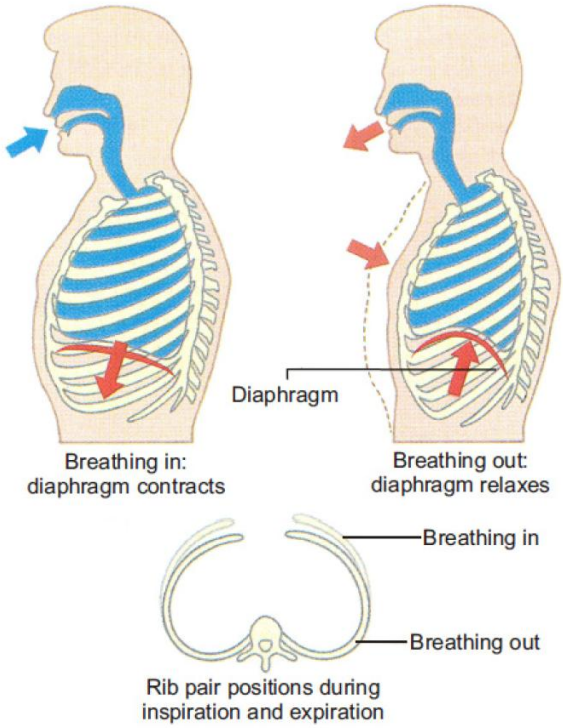

Figure 1.4 – Movement of the diaphragm and ribs during inspiration and expiration (Sebel, 1985).

1.3 ACUTE RESPIRATORY DISTRESS SYNDROME

Acute Respiratory Distress Syndrome (ARDS) (The ARDS Definition Task Force, 2012) is a condition where the lung is inflamed and fills with fluid, thereby losing the ability to exchange gas effectively. Inflammation leads to reduced surfactant production causing alveoli and/or bronchial passages to collapse and fill with fluid (Gattinoni and Pesenti, 2005).

Additional alveolar collapse is facilitated by an increase in pressure caused by the excess fluid in the lung (Ware and Matthay, 2000). Furthermore, injury to alveolar epithelial walls results in increased permeability between the blood and airspace, leading to pulmonary oedema, where the lungs flood due to excess build up of fluid.

ARDS affects the lungs heterogeneously, causing alterations in a patient's breath-to-breath respiratory mechanics (Puybasset et al., 2000, Gattinoni et al., 2001, Stenqvist et al., 2008). Injured lung tissue, combined with a build up of fluid, results in a stiffer, or less compliant lung (Gattinoni and Pesenti, 2005). Thus, an ARDS affected lung requires a higher pressure gradient to inflate, resulting in increased breathing effort, or Work of Breathing (WoB) (Chiew et al., 2011). Furthermore, loss of functional lung units reduces the intrapulmonary gas volume and results in O_2 deficient blood, reducing O_2 supply to tissues and increasing the risk of further organ failure and death.

Direct lung injury in the form of pneumonia, pulmonary aspiration/near drowning, inhalation lung injury, or lung contusion can lead to the onset of ARDS. Indirectly, ARDS can develop from a number of causes including sepsis, shock, major trauma, or massive blood transfusion (Ware and Matthay, 2000, Burleson and Maki, 2005). The annual number of ARDS incidences is reported to be between 5 and 74 cases per 100,000 people. The overall mortality rate has been reported to be between 34 % and 66 % (Reynolds et al., 1998, Luhr et al., 1999, Bersten et al., 2002, Manzano et al., 2005) and increases significantly with age (Manzano et al., 2005).

There are no specific criteria or tests to diagnose ARDS because there are no uniquely distinguishable disease symptoms (Artigas et al., 1998, Chew et al., 2012). However, the severity of ARDS is typically measured as the ratio of the arterial partial pressure of O_2 divided by the fraction of inspired O_2 (PaO_2/FiO_2 or PF ratio). The PF ratio assesses the ability of the lungs to oxygenate blood. ARDS is defined into three categories of severity (The ARDS Definition Task Force, 2012). A PF ratio $\leq$ 300 mmHg, but > 200 mmHg is characterised as mild ARDS. A PF ratio $\leq$ 200 mmHg, but > 100 mmHg is characterised as moderate ARDS, and a PF ratio $\leq$ 100 mmHg is characterised as severe ARDS. The acute time frame is also specified to be within one week. Severe hypoxemia (or low PF ratio) can prove fatal to vital organs if not treated immediately (Petty and Ashbaugh, 1971, Dunkel, 2006).

1.4 MECHANICAL VENTILATION

Patients suffering from ARDS are admitted to the Intensive Care Unit (ICU) where clinicians offer a supportive environment to aid recovery. Mechanical Ventilation (MV) is applied to partially or completely support the patients' breathing efforts. Modern ventilators, such as the Puritan Bennett 840 mechanical ventilator shown in Figure 1.5, use a wide range of positive pressure ventilation modes. Air is delivered to the lungs invasively through an endotracheal (ET) tube or a face mask.

Figure 1.5 – Puritan Bennett 840 mechanical ventilator.

1.4.1 Mechanical Ventilation Parameters

There are several important parameters that define the breathing cycle of a mechanically ventilated patient. These parameters include:

1. **Positive End Expiratory Pressure** (PEEP) is the remaining pressure within the lungs at the end of expiration and is an important parameter in MV therapy. ARDS affected alveoli are vulnerable to collapse due to inflammation and build up of fluid. Thus, PEEP maintains recruited lung units, improving gas exchange (Amato et al., 1998, The Acute Respiratory Distress Syndrome Network, 2000, McCann et al., 2001, Halter et al., 2003). However, there is a risk of overstretching healthy lung units during high PEEP (Bersten, 1998). Furthermore, if the PEEP is too low, injury is induced by the repetitive opening and closing of

alveoli units (Bates and Irvin, 2002, Retamal et al., 2013). Optimal PEEP remains highly debated with no conclusive results (Amato et al., 1998, Chiew et al., 2011, Sundaresan and Chase, 2011), and setting this parameter is thus a balance between avoiding over-stretching and repetitive opening of alveoli.

2. **Peak Inspiratory Pressure** (PIP) is the maximum pressure applied to the patient's proximal airway. However, high pressures can lead to further harm in the form of a pulmonary barotrauma.
3. **Functional Residual Capacity** (FRC) is the volume of the lungs at atmospheric pressure at the end of expiration and is shown schematically in Figure 1.6. Application of PEEP maintains additional lung volume above FRC known as dynamic FRC (dFRC) (Sundaresan et al., 2011b), increasing oxygenation.
4. **Tidal Volume** (V_t) is the net volume of air that enters the lungs with each normal breathing cycle, above the FRC, and is shown schematically in Figure 1.6. The FiO_2 of the air, together with the applied V_t, must be sufficient to provide adequate oxygenation (Allardet-Servent et al., 2009). However, the applied V_t is transferred from collapsed lung regions to healthy lung units. Thus, if the V_t is too high, the lungs can overinflate, leading to high PIPs and further harm in the form of a pulmonary volutrauma.

These parameters must be correctly managed to obtain maximum oxygenation, while avoiding excessive pressure, which is a balance that has proven difficult to obtain clinically.

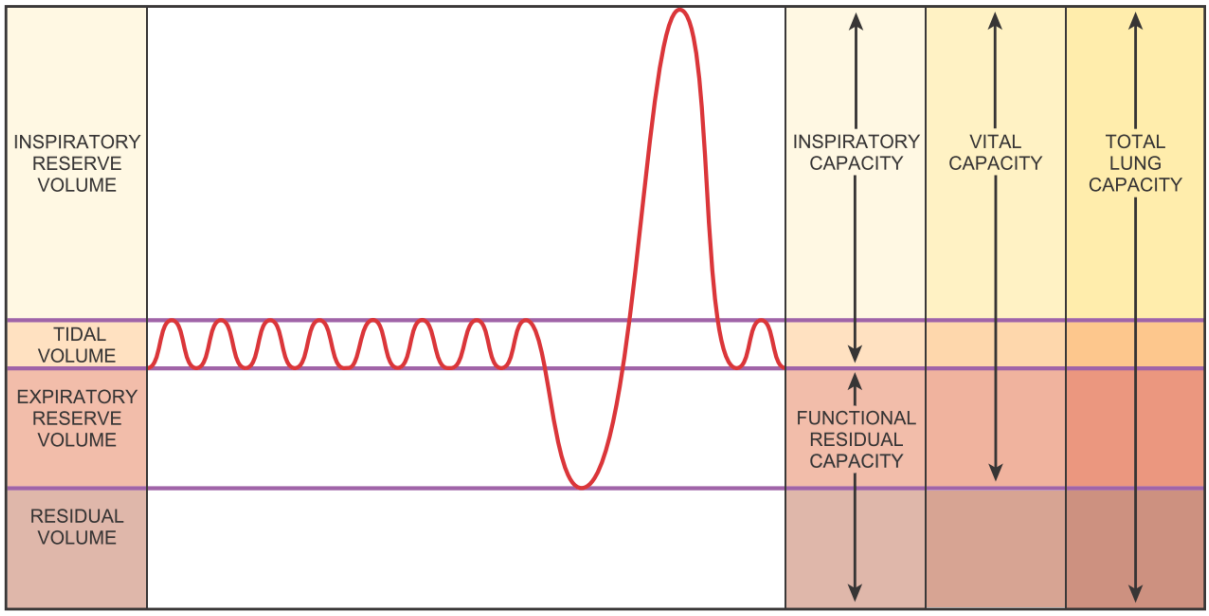

Figure 1.6 – Schematic of lung volumes and capacities with associated terminology (Tortora and Derrickson, 2006).

1.4.2 Mechanical Ventilator Control Modes

There are two basic modes of ventilation control (Mireles-Cabodevila et al., 2009):

1. **Pressure control mode** requires the PEEP and the PIP to be set directly by the clinician. The V_t is an indirect result of these settings. Thus, the volume change during inspiration is a passive process.
2. **Volume control mode** requires the PEEP and the V_t to be set directly by the clinician. The V_t is set using the volumetric flow rate since volume is the integral of volumetric flow rate with respect to time. The volumetric flow rate can be constant or varied during inspiration and the PIP is an indirect result of these settings. Thus, the pressure change during inspiration is a passive process.

MV should be applied for the shortest period of time necessary to prevent impairment of diaphragmatic function and other complications (Anzueto et al., 1997, Dries, 1997, Forel et al., 2012). Muscle atrophy can occur after as little as 18 hours of MV therapy (Levine et al., 2008), and prolonged MV requires a significant period of subsequent weaning (Anzueto et al., 1997). A reduced duration of MV also leads to substantial reductions in cost (Dasta et al., 2005).

1.5 PROBLEM SUMMARY

Currently, there is a lack of standardised protocols to base MV therapy in the ICU. In particular, difficulty arises in obtaining regular patient-specific insight into lung condition and disease progression (Malbouisson et al., 2001, Talmor et al., 2008, Zhao et al., 2009, Zhao et al., 2010b). Hence, ventilator settings and protocols are strongly dependent on the experience and intuition of the clinicians, resulting in variable protocols with limited effectiveness over broad cohorts (Grasso et al., 2007, Meade et al., 2008, Briel et al., 2010, Hodgson et al., 2011a). In addition, suboptimal MV can lead to Ventilator Induced Lung Injury (VILI) (Ware and Matthay, 2000). VILI can increase the mortality rate (Gajic et al., 2004, Carney et al., 2005) and is difficult to diagnose due to similarities with ARDS (Villar, 2005), providing a further incentive to improve control with minimum added pressure.

The heterogeneity of ARDS and variation in patient-specific response to MV means there is a need to determine optimal patient-specific MV parameters to maximise gas exchange and improve recovery time, while minimising the risk of VILI. Thus, it is clear that generic

solutions will have limited effectiveness, particularly over broad or diverse patient cohorts. Therefore, an optimal solution would see regular real-time adjustment of patient-specific MV parameters over clinically relevant time frames to provide continuous optimisation of therapy.

Simple analytical models incorporating engineering principles, lung physiology, and MV parameters can provide insight into a patient's condition, not readily available by other means. These model-based methods can provide real-time identification of optimal patient-specific MV parameters. Thus, the premise of this thesis is to present the development and application of models and model-based methods to optimise PEEP selection for mechanically ventilated patients in the ICU. In particular, models that capture patient-specific lung elastance (1/compliance) and recruitment can provide insight into otherwise un-measurable metrics of lung condition, thereby aiding clinical decision making. (Chase et al., 2006, Sundaresan et al., 2009, Chiew et al., 2011, Sundaresan et al., 2011b, Mishra et al., 2012).

Chapter 2 – Lung Mechanics

2.1 INTRODUCTION

Lung mechanics considers the respiratory system as a mechanical system to quantify clinically relevant mechanical properties. MV generates pressures that allow a volume of air to flow from the environment into the lungs. This pressure must be sufficient to overcome the superimposed pressure, the elastic tendencies of the tissues within the lungs and chest wall, and the resistance within the conducting airways (Bates, 2009). Thus, the mechanical properties of the lungs determine how pressure, airflow, and the resulting lung volume are related. This chapter describes the relevant properties of lung mechanics and how these properties can be used to gain insight into patient-specific lung condition. In turn, these properties can be used to develop relevant metrics to guide MV therapy.

2.2 PRESSURE, VOLUMETRIC FLOW RATE, AND VOLUME

Lung mechanics are generally developed using measurements of airway pressure and volumetric flow rate. These measurements are sampled together at essentially the same location, typically at the mouthpiece or directly at the ventilator (Karason et al., 1999). The volume of air entering the lungs is obtained by integrating the volumetric flow rate data with respect to time. Figure 2.1 shows a typical example of airway pressure, volumetric flow rate, and volume data for three breathing cycles. In this case, the ventilator is set to volume control mode with the volumetric flow rate set to a square-wave profile and a PEEP of 0 cmH_2O.

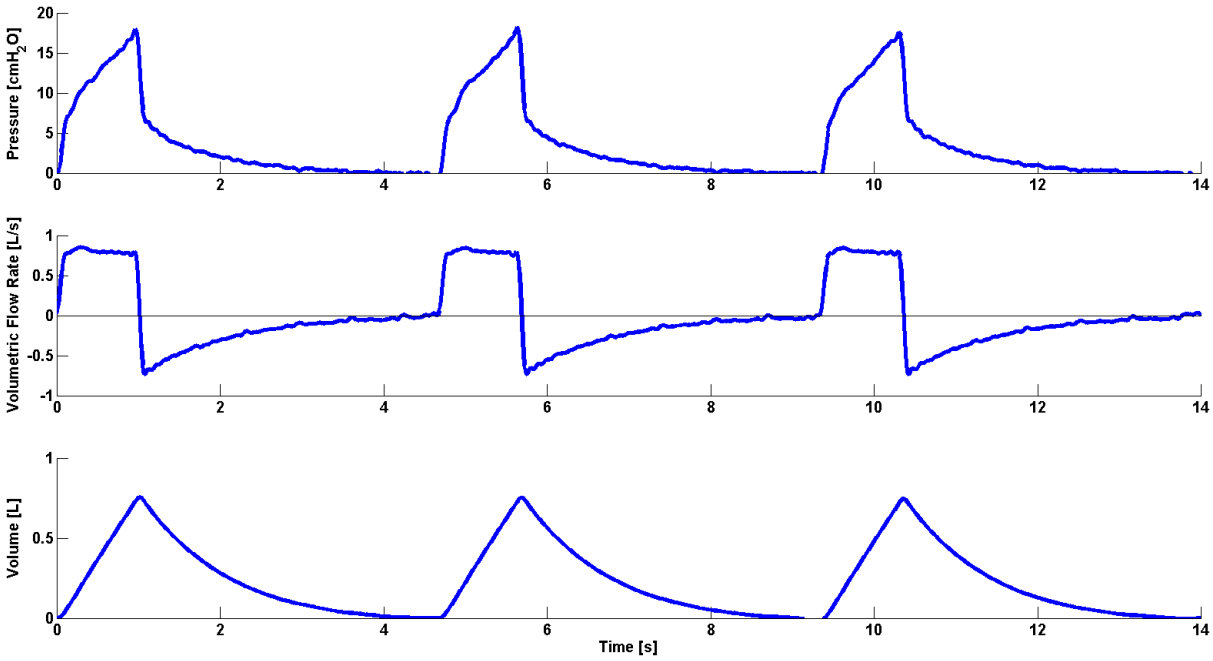

Figure 2.1 – Typical example of data from three breathing cycles. (Top) Airway pressure data. (Middle) Volumetric flow rate data. (Bottom) Volume data (Bersten, 1998).

For each breathing cycle, it is assumed that the volume of air that enters the lungs is equal to the volume of air that exits the lungs. However, small discrepancies often occur due to effects such as calibration error, dynamic pulmonary hyperinflation (Haberthur et al., 2009), changes in PEEP, measurement noise, leaks in the conducting tubes, differing rates of CO_2 production and O_2 consumption, and thermal expansion of air within the lungs. Therefore, integrating volumetric flow rate with respect to time leads to drift in the volume data. A typical example of volume drift is shown in Figure 2.2. However, volume data can be calibrated by assuming linear volume drift across each individual breathing cycle (Lauzon and Bates, 1991).

The transition from expiration to inspiration, and inspiration to expiration, involves the establishment of a new flow direction and is a rapid and dynamic process. Figure 2.3 shows a typical example of volumetric flow rate data for three breathing cycles sampled at 50 Hz. The

dynamic transition regions clearly show a reduction in the density of the sampled data. Therefore, these transition regions are more prone to errors, potentially reducing accuracy.

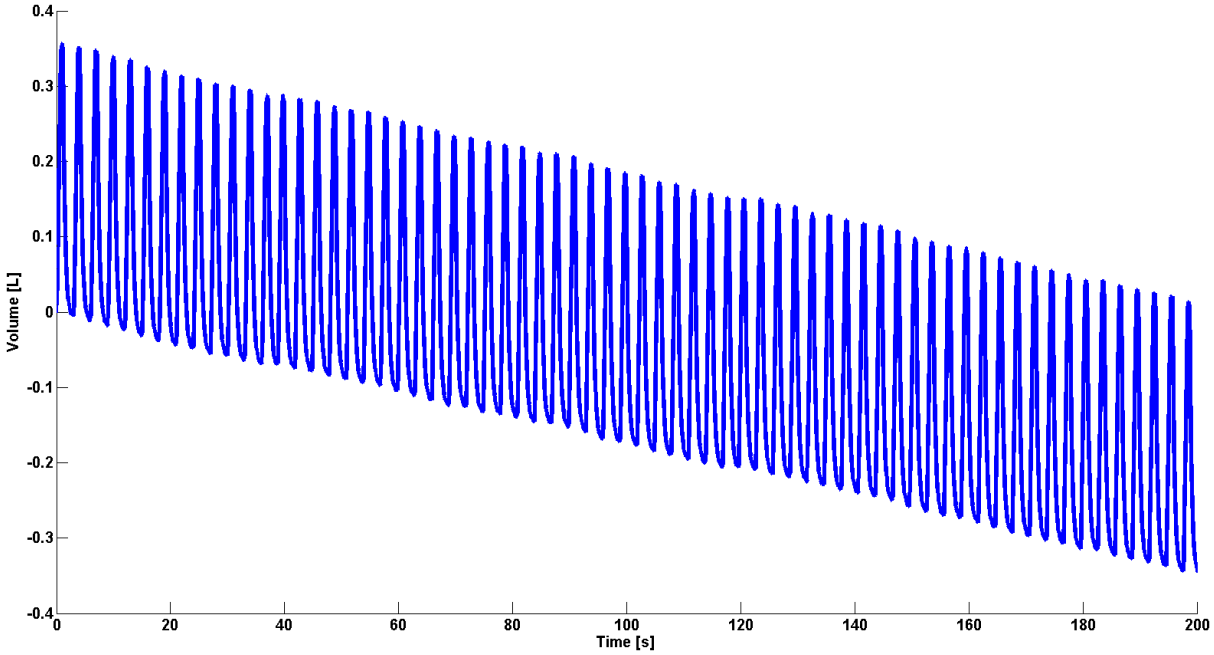

Figure 2.2 – Typical example of volume drift (Chiew et al., 2012a).

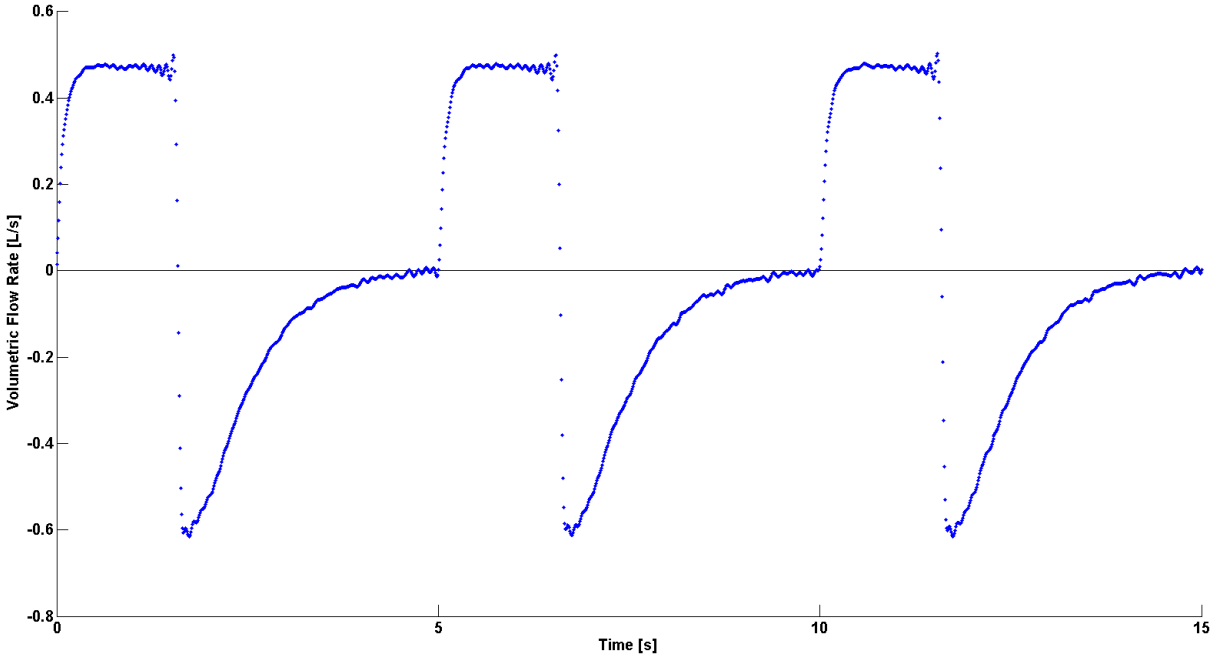

Figure 2.3 – The density distribution of volumetric flow rate data (Bersten, 1998).

2.3 THE PRESSURE-VOLUME RELATIONSHIP

Lung mechanics can be assessed by examining the patient-specific relationship between airway pressure and lung volume. Plotting airway pressure verses lung volume for a complete breathing cycle results in a distinctly unique plot known as the Pressure-Volume (PV) loop (Venegas et al., 1998, Harris, 2005, Albaiceta et al., 2007). PV loops represent a composite of pressure and volume for the entire lung, and are used by clinicians to estimate a patient's recruitment status, lung condition and response to MV.

PV loops are highly dependent on the volume history of the lungs. Thus, care must be taken when comparing data from different days, different patients, or different studies (Harris, 2005). Furthermore, there is much debate surrounding the clinical interpretation of PV loops due to the lack of a clear, well accepted explanation of lung mechanics at the alveoli level, where recruitment, aeration, and gas exchange take place (Maggiore et al., 2003, Cagido and Zin, 2007, Albaiceta et al., 2008). Hence, there is a need to provide an objective framework around interpreting this data by assessing the mechanics that relate airway pressure and lung volume.

Inspiration begins with increasing pressure in the proximal airways. The rigid cartilage hoops surrounding the proximal airways do not expand or stretch significantly, so no appreciable change in lung volume occurs. Furthermore, lung units experience a superimposed pressure from the weight of the lung units above them, which must be overcome before an increase in volume can occur. This superimposed pressure is especially prominent in ARDS patients

where there is additional weight from excess fluid in the lungs (Ware and Matthay, 2000). This initial process establishes airflow into the lungs and corresponds to an initial region of higher elastance (lower compliance).

Once sufficient pressure is achieved, air flows to the distal airways resulting in an increase in volume as pressure increases, corresponding to a lower, linear region of elastance (higher, linear region of compliance). At the end of inspiration, the lungs may be inflated to near maximum capacity. Stretching of lung tissues, especially at the distal airways, where there is no supporting cartilage, corresponds to a final region of higher elastance (lower compliance). Thus, the inspiratory curve of the PV loop typically forms a sigmoid shape, with a point of minimum inspiratory elastance (maximum inspiratory compliance) located within the linear region. The Lower Inflection Point (LIP) is defined as the point where the slope of the curve increases and the Upper Inflection Point (UIP) is defined as the point where the slope of the curve decreases.

Expiration occurs when the ventilator's expiratory valve is opened and the recoil of elastic fibers stretched during inspiration, and the inward force of the surface tension due to the alveolar fluid, cause a decrease in lung volume (Tortora and Derrickson, 2006). Thus, expiration is essentially the passive unloading of the inspired tidal volume, V_t, over a resistance at a constant ventilator applied pressure (Moller et al., 2010a, Moller et al., 2010b). As the lungs do not act as a perfect elastic system, the applied energy is not immediately returned. Thus, there is unrecoverable, or delayed recovery, of energy applied to the system, resulting in hysteresis between the inspiratory and expiratory curves of the PV loop (Harris,

2005, Andreassen et al., 2010). Healthy lungs have a lower elastance and less hysteresis, while ARDS affected lungs have a high elastance and significantly more hysteresis.

2.3.1 The Static Pressure-Volume Loop

The static PV loop has been regarded as the gold standard tool for assessment of lung mechanics (Stenqvist and Odenstedt, 2007), and is measured across the entire inspiratory capacity of the patient. The term static refers to the fact that there is no airflow within the respiratory airways. Thus, there is no resistive component of pressure loss. In addition, all viscoelastic forces are equilibrated (Henderson and Sheel, 2012), resulting in reduced hysteresis. Static, or semi-static PV loops are generally obtained using the super-syringe technique, the constant flow method, or the multiple-occlusion method (Harris, 2005, Sundaresan and Chase, 2011). The gradient of the static PV loop is equal to $\frac{\Delta V}{\Delta P}$, i.e. the compliance (1/elastance) of the respiratory system. Figure 2.4 (Left) shows a schematic of a typical static PV loop with the LIP and UIP indicated.

2.3.2 The Dynamic Pressure-Volume Loop

Under normal breathing and MV, plotting airway pressure against volume for a complete breathing cycle results in the dynamic PV loop. Dynamic PV loops are more frequently used than static PV loops as they are more readily available at the bedside. A typical example of three dynamic PV loops, taken at three separate PEEPs, is shown in Figure 2.4 (Right).

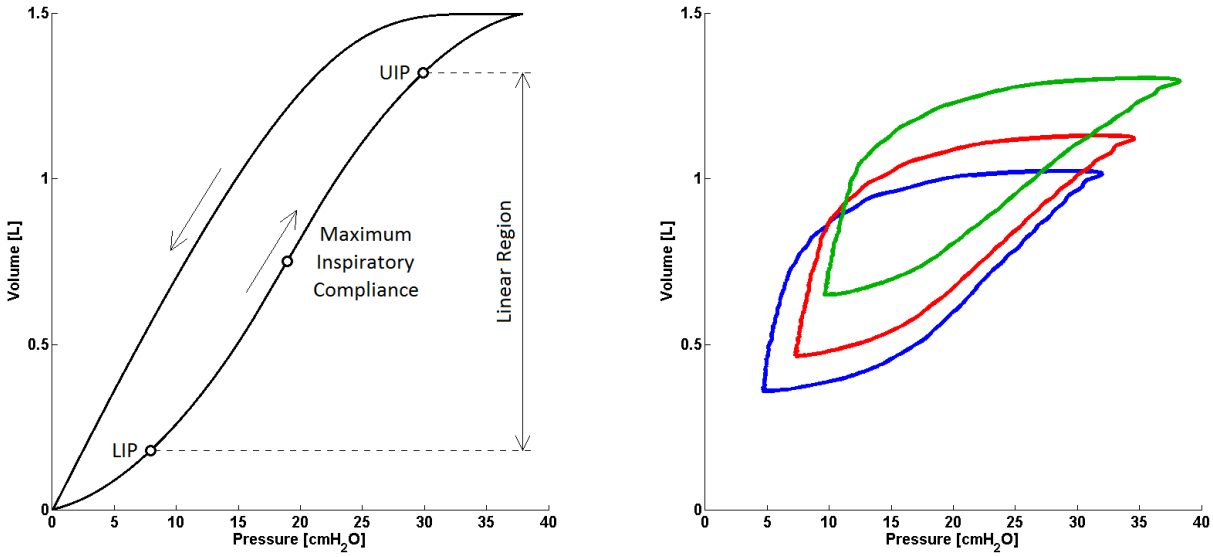

Figure 2.4 – PV loops. (Left) Schematic of a static PV loop. (Right) Typical example of three dynamic PV loops (Bersten, 1998).

Dynamic PV loops are limited by the resistive effects of the conducting airways. ARDS patients are ventilated through an endotracheal (ET) tube or face mask, where the ET tube provides significant airway resistance under certain flow patterns. A typical example of the effect of the ET tube on airway pressure measurements is shown in Figure 2.5, where data measured at the Y-piece, prior to the ET tube, is compared to data measured at the trachea (Karason et al., 2000). In addition, the physiological conducting airway further extends the total conducting airway. Thus, dynamic airway pressure measurements may contain considerable resistive pressure losses that can obscure the true mechanics of the lungs.

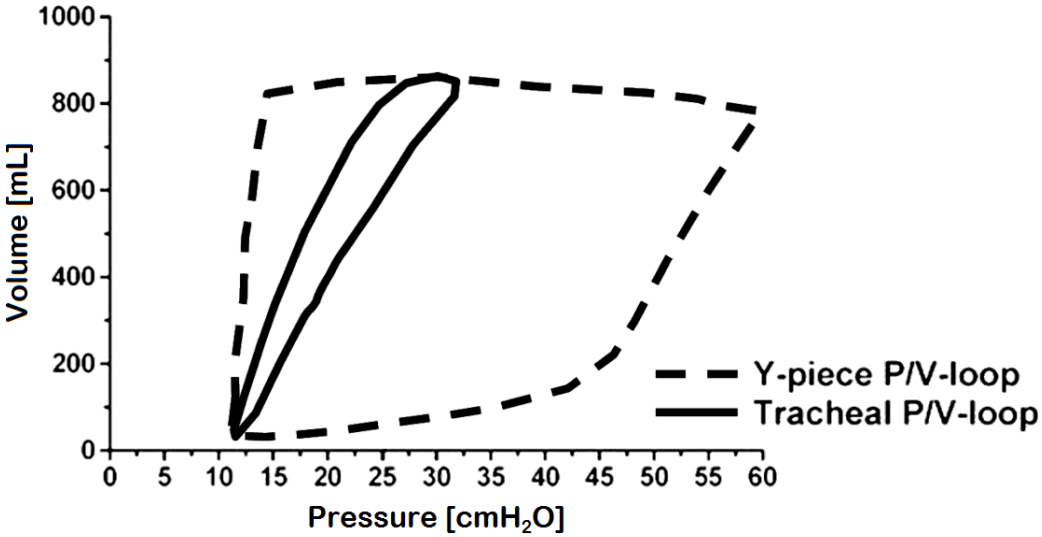

Figure 2.5 – Typical example of the resistive pressure loss associated with the ET tube. The outer loop shows measurements taken at the Y-piece, prior to the ET tube. The inner loop shows measurements taken at the trachea (Karason et al., 2001).

2.4 RECRUITMENT AND DERECRUITMENT

ARDS results in pulmonary oedema and inflammation, causing lung units to collapse due to additional pressure (Ware and Matthay, 2000, Gattinoni and Pesenti, 2005). Lung recruitment occurs when an applied pressure overcomes the superimposed pressure, and the pressure required for recruitment, causing the lung units to abruptly open. This pressure is referred to as the Threshold Opening Pressure (TOP). Above the TOP, lung units show very small isotropic expansion with further increases in pressure (Carney et al., 1999, Schiller et al., 2003). Derecruitment occurs when an applied pressure becomes lower than the minimum pressure required to maintain lung units at a non-zero volume. This pressure is referred to as the Threshold Closing Pressure (TCP). Below the TCP, lung units effectively assume a volume of zero. The TOP distribution and the TCP distribution for individual lung units are normally distributed with pressure across the entire pressure range (Crotti et al., 2001, Pelosi

et al., 2001, Harris, 2005). Thus, recruitment occurs continuously throughout the inspiratory static PV curve (Jonson et al., 1999, Sundaresan and Chase, 2011).

The in vivo microscopic study by Schiller et al. (Schiller et al., 2003) characterised lung units into three categories based on the level of injury:

1. **Type I alveoli** do not change in volume significantly during tidal ventilation. These alveoli are already recruited at the beginning of inspiration and do not collapse at the end of expiration.
2. **Type II alveoli** undergo a slight, but significant, change in volume during tidal ventilation and may collapse at the end of expiration.
3. **Type III alveoli** undergo a significant change in volume during tidal ventilation and collapse at the end of expiration. In severe cases, some alveoli may remain collapsed for the entire breathing cycle.

Healthy lungs contains only Type I alveoli. Type II and Type III alveoli are associated with ARDS, where Type III alveoli are the most severely injured.

2.5 LUNG VISCOELASTISITY

Lung tissues can stretch, especially in the distal airways where there is no supporting cartilage (Sebel, 1985), contributing to the increase in lung volume during inspiration. The

energy imparted to the lungs is initially stored elastically, but dissipates with time as lung tissue elements gradually rearrange themselves toward a state of lower global energy (Bates, 2007). Bates (Bates, 2007) proposed that stress relaxation in lung tissue occurs via a sequence of micro-rips that propagate stresses from one region to another. A typical example of this effect is shown in Figure 2.6, where the PEEP has been increased from 10 cmH_2O to 15 cmH_2O. Each successive breath shows a reduced Peak Inspiratory Pressure (PIP), indicating the time-dependent nature of the lung's viscoelastic properties. This effect highlights the importance of continuous monitoring in the ICU as lung mechanics vary continuously over various time scales.

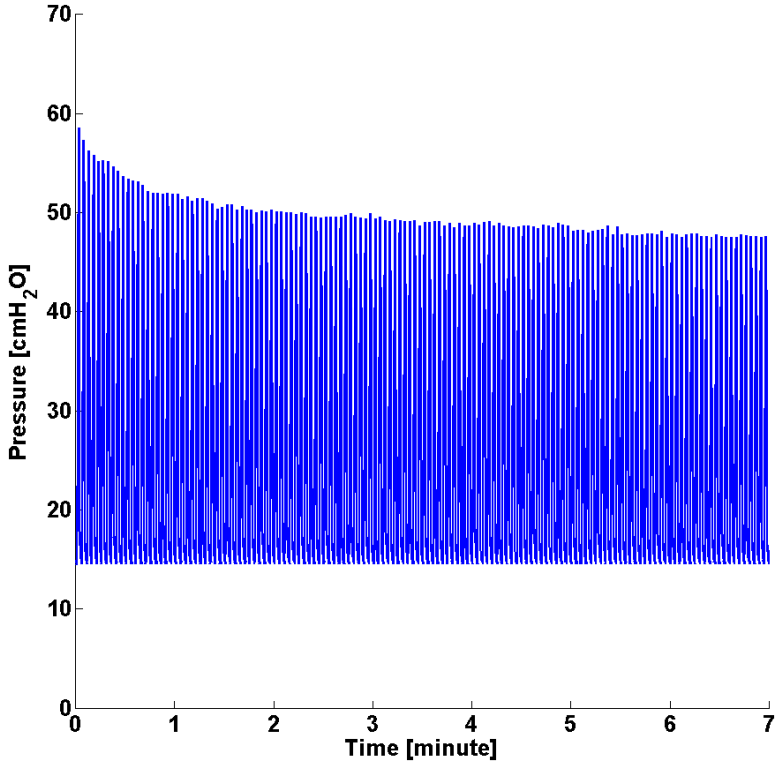

Figure 2.6 – Airway pressure data showing a time-dependent PIP (Chiew et al., 2012a).

2.6 SUMMARY

Lung mechanics is the use of engineering principles to describe lung physiology. Determining relationships between airway pressure, airflow, and the resulting lung volume allows lung properties and characteristics to be established. However, insight into clinically relevant metrics of patient condition and MV therapy can be limited by the quality of the measured data. Additionally, the circumstances under which the data is obtained, such as during dynamic breathing or a static manoeuvre, must be known to provide context and clinical meaning to parameters of lung mechanics.

Chapter 3 – Model-Based Decision Support

3.1 INTRODUCTION

Currently, optimal patient-specific ventilator settings are difficult to determine. This chapter describes the need for a model-based approach to guide patient-specific MV therapy for ARDS patients in the ICU. Physiological modelling is used to provide clinical insight into the behaviour of the lungs where it is impractical or impossible using direct measurements (Sundaresan and Chase, 2011). The mechanical properties of the lungs are described using mathematical models, such that clinically relevant aspects of patient condition are captured. In addition, the clinical and experimental data sets used for validating the models presented in this thesis are described in detail.

3.2 DIRECT IMAGING OF LUNG CONDITION

3.2.1 Computed Tomography

Computed Tomography (CT) scans, or Computer Axial Tomography (CAT) scans, are considered a gold standard for determining lung condition (Lu et al., 2001, Malbouisson et al., 2001, Gattinoni et al., 2006b). In particular, CT scans can determine if alveoli are recruited, de-recruited or overinflated (Sundaresan and Chase, 2011). However, regular CT scans are costly, impractical for continuous monitoring, and expose the patient to radiation and other risks (Wiest et al., 2002, Lee et al., 2004). Thus, CT scans are clinically and ethically unrealistic as a bedside tool for continuous monitoring of MV therapy.

3.2.2 Electrical Impedance Tomography

Electrical Impedance Tomography (EIT) generates a cross-sectional image of the lungs using the spatial distribution of electrical conductivity (Denai et al., 2010, Luecke et al., 2012). Although EIT produces a lower resolution than CT scans, it is non-invasive, radiation-free, and can be used as a bedside tool for continuous monitoring of MV therapy (Cheney et al., 1999, Frerichs, 2000, Zhao et al., 2009, Denai et al., 2010, Zhao et al., 2010b). However, EIT scans have limited spatial resolution, require complex image reconstruction algorithms, and require skilled operators to implement. Furthermore, EIT scans are usually acquired in only one electrode plane and changes in other lung regions may not be captured (Lionheart, 2004, Hahn et al., 2007, Frerichs et al., 2010).

3.2.3 Vibration Response Imaging

Vibration Response Imaging (VRI) measures vibration energy of lung sounds during MV therapy (Cinel et al., 2006, Jean et al., 2006). The effect of lung vibration on regional lung distribution shows a strong correlation with CT scans. However, the image resolution of VRI is much lower than that obtained from either CT scans or EIT. Furthermore, current VRI recordings are limited to patients that are near sitting and may prove to be unsuitable for patients who need to be in a supine position (Vincent et al., 2007). Thus, to date, VRI has only been used as a research tool (Sundaresan and Chase, 2011).

3.3 STANDARDISATION OF PRESSURE AND VOLUME

Current methods to determine ventilator settings are based on trial and error, and the intuition and experience of the clinicians (Bernstein et al., 2013). The resulting variability in MV protocols has an adverse effect on the quality of care offered to patients (Sundaresan and Chase, 2011). The primary MV parameters identified to lower the mortality rate of ARDS patients are a low tidal volume, V_t (Amato et al., 1998, Villar et al., 2006, Malhotra, 2007, Terragni et al., 2007), and the application of appropriate PEEP (Gattinoni et al., 2001, Rouby et al., 2002, Takeuchi et al., 2002, Brower et al., 2004, Gattinoni et al., 2006a, Villar et al., 2006).

3.3.1 Standardisation of Volume

Under normal circumstances, optimal V_t allows maximum gas exchange to occur at minimum breathing effort (Otis et al., 1950). However, ARDS patients experience heterogeneous lung collapse (Puybasset et al., 2000, Gattinoni et al., 2001, Stenqvist et al., 2008). Therefore, where damaged alveoli are surrounded by healthy alveoli, the applied V_t may be transferred to healthy lung units, resulting in variations in local strains and overdistension (Dreyfuss and Saumon, 1998). Hence, the use of low V_t is thought to reduce the amount of induced lung stain (Brochard et al., 1998, The Acute Respiratory Distress Syndrome Network, 2000, Parsons et al., 2005, Kallet et al., 2006). However, not all studies have shown that a lower V_t lowers the outcome mortality rate (Brochard et al., 1998, Stewart et al., 1998, Brower et al., 1999, Schultz et al., 2007, Briel et al., 2010). Despite these conflicting results from different studies, the use of low V_t throughout MV is becoming increasingly accepted and common place within the medical community.

3.3.2 Standardisation of Pressure

Standardisation of pressure settings throughout MV focuses on the PEEP as the lower limit, and the Peak Inspiratory Pressure (PIP), or peak plateau pressure, P_{plat}, as the upper limit, where P_{plat} is the resulting airway pressure after an End-Inspiratory Pause (EIP) is performed (Fuleihan et al., 1976). The EIP is a period of no airflow at the end of inspiration, allowing the inspired V_t to distribute evenly throughout the lungs. The P_{plat} will be lower than the PIP as it is a static measure that is not affected by airway resistance.

The level of appropriate PEEP over a given cohort has never been properly established (Sundaresan and Chase, 2011). Amato et al. (Amato et al., 1998) reported a decrease in the mortality rate when the PEEP was set 2 cmH_2O higher than the Lower Inflection Point (LIP) of the static Pressure-Volume (PV) loop. Conversely, Villar et al. (Villar et al., 2006) reported a decrease in the mortality rate at high PEEP. Although high PEEP can improve oxygenation, setting the PEEP above the Upper Inflection Point (UIP) presents a risk of overstretching lung units, particularly healthy lung units (Brower et al., 2004, Mercat et al., 2008, Sundaresan and Chase, 2011). However, setting the PEEP too low results in cyclic recruitment and derecruitment of lung units, which is also potentially injurious (Bates and Irvin, 2002, Schiller et al., 2003, Ferguson et al., 2005, Retamal et al., 2013).

Clinicians typically set PEEP such that it is between the LIP and UIP. However, this offers a large range of potential values, where a single optimal and patient-specific PEEP value cannot be determined (Sundaresan and Chase, 2011). Furthermore, studies have suggested

that PEEP should be set according to the deflation curve instead of the inflation curve since unwanted derecruitment of lung units occurs during deflation (Hickling, 2001, Girgis et al., 2006). In any case, obtaining patient-specific static PV loops are generally invasive, time consuming, and cause interruption to therapy (Karason et al., 2001, Harris, 2005). In addition, the location of the LIP and UIP, as used clinically, are typically not identifiable during normal tidal ventilation (Lichtwarck-Aschoff et al., 2000). Thus, PEEP selection based on the static PV loop is limited in clinical use, and a dynamic method is required.

Studies have shown that PIP should not exceed 45 cmH_2O (Gattinoni et al., 2006a), or that P_{plat} should not exceed 30-35 cmH_2O (Slutsky, 1993, Barberis et al., 2003, Agarwal and Nath, 2007). Fundamentally, excess applied pressure that does not recruit lung volume will lead to lung damage. Thus, to prevent barotrauma, or long term negative effects, P_{plat} should remain below this upper bound (Gattinoni et al., 2003, Borges Sobrinho et al., 2006, Gattinoni et al., 2006a). However, other studies have found that a PIP of up to 60 cmH_2O may be beneficial in some circumstances (Borges et al., 2006, de Matos et al., 2012). High applied pressure may be beneficial provided significant lung volume is recruited. Thus, once more, a patient-specific approach is required.

3.3.3 Limitations

Lower mortality rate can be attributed to either high PEEP or low V_t because of the trade-off that exists between these two parameters in setting MV (Jonson and Uttman, 2007). Current MV protocol for preventing lung injury is achieved with a low V_t, an adequate PEEP, and a

limited P_{plat} (Villar et al., 2006). However, this approach tends to compromise oxygenation. Another significant issue with the use of these protocols is that they do not account for the unique condition of individual patients, such as age, gender, or pre-existing medical conditions. Furthermore, since the condition of a patient evolves with time, the use of simple, or simplified, standardised protocols may not be effective for all patients under all circumstances. Thus, there is a clear need for a real-time, patient-specific approach to guiding MV therapy. In particular for determining optimal PEEP, as it is one of the most important parameters in MV therapy.

3.4 MODEL-BASED APPROACHES

Model-based methods represent a novel means to assess patient-specific condition and guide therapy. The overall goal is to determine the optimal MV settings without the complications associated with direct imaging methods or the static PV loop (Sundaresan and Chase, 2011). Hence, an optimal solution would not introduce any significantly new hardware or systems into the ICU, nor would it require excessive cost, clinical time, or effort to implement. However, few modelling approaches have been rigorously tested (Carvalho et al., 2007, Sundaresan et al., 2011a), and their potential applicability in the ICU is not yet validated.

3.4.1 Finite Element Models

Ultimately, the behaviour of the entire respiratory system must be traceable to each individual component and their associated interactions. Finite element models of pulmonary gas flow have been developed that offer detailed resolution and realistic simulation of lung behaviour

(Tawhai et al., 2004, Burrowes et al., 2005, Swan et al., 2008, Tawhai and Burrowes, 2008, Werner et al., 2009, Swan et al., 2012). However, a patient-specific geometry still requires a CT scan, which carries additional costs and risk. Furthermore, model creation, and the high computational effort associated with these models, means that they are not feasible for real-time clinical application.

3.4.2 Lumped Parameter Models

In practice, a model cannot incorporate every aspect of the complete respiratory system since it is clinically unachievable to obtain all the data required to identify every parameter (Schranz et al., 2012). However, a model requires only enough adjustable parameters such that relevant details of global behaviour are adequately captured (Bates, 2009). Thus, models do not have to be complicated to be useful (Lucangelo et al., 2007). Lumped parameter models offer a simple and relatively inexpensive method of assessing lung mechanics and capturing essential dynamics. Furthermore, simple models, having a small number of parameters, are a necessary consequence of the fact that such models have to be matched to clinical data, which can typically only support a limited number of free parameters (Bates, 2009). Thus, these simpler models are easily implemented in the ICU, but at the expense of physiological detail.

ARDS affects the lungs heterogeneously, causing alterations in a patient's breath-to-breath respiratory mechanics (Puybasset et al., 2000, Gattinoni et al., 2001, Stenqvist et al., 2008). Therefore, ARDS affected lung units will exhibit different mechanical properties to healthy

lung units. Since measurements of pressure and volumetric flow rate are obtained at a single, exterior location, the respiratory system is effectively treated as a single compartment. Thus, healthy lung units cannot be differentiated from injured lung units, and clinically relevant information, such as the location and extent of ARDS affected lung units, cannot be directly extracted.

3.5 CLINICALLY RELEVANT METRICS

3.5.1 Lung Elastance

Lung elastance is a physiologically important metric since injured lung tissue, combined with a build up of fluid, directly influence the elastance of the lungs (Gattinoni and Pesenti, 2005). Lung elastance is also used to assess the level of lung injury (The ARDS Definition Task Force, 2012). Optimal MV occurs when the lungs are inflated at the minimum inspiratory elastance (Carvalho et al., 2007, Suarez-Sipmann et al., 2007, Lambermont et al., 2008). At this point, maximum intrapulmonary volume change is achieved, providing maximum oxygenation, at a minimum change in pressure, or stress. Therefore, PEEP should be set such that the dynamic PV loop is located at the minimum inspiratory elastance (maximum inspiratory compliance) of the static PV loop (Lichtwarck-Aschoff et al., 2000, Stenqvist and Odenstedt, 2007). Thus, there is a need for a simple, non-invasive method to determine lung elastance as a function of PEEP, preferably in a dynamic sense over a single breath.

3.5.2 Lung Recruitment

In ARDS, the percentage of potentially recruitable lung units is extremely variable and is strongly associated with the response to PEEP (Gattinoni et al., 2006a). CT scans have confirmed that the end expiratory lung volume is higher when PEEP is applied (Amato et al., 1998, The Acute Respiratory Distress Syndrome Network, 2000, Gattinoni et al., 2001, McCann et al., 2001, Halter et al., 2003). Furthermore, studies have shown that mortality and length of stay in the ICU are reduced by recruiting available lung units to increase oxygenation (Gattinoni et al., 2006a). Therefore, since recruitment occurs continuously, optimal patient-specific PEEP can also be described as producing maximum alveolar recruitment while retraining the greatest number of lung units at the end of expiration (Gattinoni et al., 2006a). Thus, there is a need for a simple, non-invasive method to determine the quantity of recruited lung volume as a function of PEEP.

3.6 DATA AND PROTOCOLS

In this thesis, two clinical data sets and two experimetnal data sets are used for the purpose of model development and validation.

3.6.1 Retrospective Clinical Data

Two retrospective clinical cohorts are considered, each consisting of ten fully sedated patients diagnosed with ARDS:

1. **Cohort 1** (Sundaresan et al., 2011a): The demographics and cause of ARDS for each patient is presented in Table 3.1. The criteria for ARDS was acute onset of respiratory failure, observation of bilateral infiltrates on chest radiographs, absence of left heart failure, and a PaO_2/FiO_2 (PF ratio) between 150 and 300 mmHg. Patients were ventilated using a Puritan Bennett PB840 ventilator (Coviden, Boulder, CO, USA) under volume control mode (V_t = 400-600 mL). Each patient underwent a staircase Recruitment Manoeuvre (RM) from Zero End Expiratory Pressure (ZEEP), with PEEP increments of 5 cmH_2O (Hodgson et al., 2011b), until a PIP limit of 45 cmH_2O was reached (Gattinoni et al., 2006a). Airway pressure and volumetric flow rate data were acquired using a heated pneumotachometer (Hamilton Medical, Switzerland). The PEEPs at which data was obtained are presented in Table 3.2. These clinical trials and the use of this data has been reviewed and approved by the South Island Regional Ethics Committee of New Zealand.

Table 3.1 – Characteristics of the patients in Cohort 1.

Patient	Sex	Age [years]	Cause of Lung Injury
1	Female	61	Peritonitis
2	Male	22	Trauma
3	Male	55	Aspiration
4	Male	88	Pneumonia
5	Male	59	Pneumonia
6	Male	69	Trauma
7	Male	56	Legionnaires
8	Female	45	Aspiration
9	Male	37	H1N1
10	Male	56	Legionnaires

Table 3.2 – PEEPs at which data was obtained for patients in Cohort 1.

		PEEP [cmH_2O]											
		0	5	10	15	16	20	22	25	27	28	29	30
Trial	1	●	●	●	●		●		●	●			
	2	●	●	●	●		●	●					
	3	●	●	●	●		●		●		●		
	4	●	●	●	●		●		●				●
	5	●	●	●	●		●		●				
	6	●	●	●	●		●		●			●	
	7	●	●	●	●		●		●				
	8	●	●	●	●		●						
	9	●	●	●	●	●							
	10	●	●	●	●		●		●				●
	11	●	●	●	●		●		●			●	●
	12	●	●	●	●		●		●	●			

2. **Cohort 2** (Bersten, 1998): The demographics and cause of ARDS for each patient is presented in Table 3.3. Patients were ventilated using a Puritan-Bennett 7200ae ventilator (Puritan-Bennett Corp., Carlsbad, CA, USA) under volume control mode (V_t = 8-10 mL/kg). Trials were initially performed at baseline PEEP. Trials were then repeated at 30 min intervals following random PEEP changes between 5 and 15 cmH_2O. The final 60 s of data from each PEEP was recorded. Airway pressure data was acquired using a (water manometer) strain gauge transducer (Bell and Howell 4-327-I; Trans America Delaval, Pasadena, CA, USA). Volumetric flow rate data was acquired using a heated, Fleisch-type pneumotachograph (HP-47034A, Hewlett-Packard, Palo Alto, CA, USA). The PEEPs at which data was obtained are presented in Table 3.4. These clinical trials were approved by the Committee for Clinical Investigation at Flinders Medical Centre.

Table 3.3 – Characteristics of the patients in Cohort 2.

Patient	Sex	Age [years]	Cause of Lung Injury
1	Male	74	Ruptured abdominal aortic aneurysm
2	Male	24	Lung contusion
3	Female	72	Legionnaires
4	Male	48	Pancreatitis
5	Female	68	Pulmonary embolus
6	Male	54	Aspiration
7	Male	73	Aspiration
8	Male	72	Pneumonia
9	Male	81	Aspiration
10	Male	47	Liver transplant

Table 3.4 – PEEPs at which data was obtained for patients in Cohort 2.

		PEEP [cmH_2O]					
		0	5	7	10	12	15
Trial	1		●	●		●	
	2	●	●		●		
	3		●	●	●		
	4		●	●	●		
	5		●	●	●	●	
	6		●	●	●	●	
	7		●	●	●	●	
	8		●	●		●	
	9				●	●	●
	10		●	●	●	●	
	11		●	●	●		
	12		●		●		●

3.6.2 Retrospective Experimental Data

Two retrospective experimental ARDS animal models are considered, each consisting of fully sedated pure piétrain piglets ventilated through a tracheotomy under volume control

mode (V_t = 8-10 mL/kg) with an inspired oxygen (O_2) fraction (FiO_2) of 0.5 and a respiratory rate of 20 breaths/min. The criterion for ARDS was limited to hypoxemia monitoring with the PF ratio less than 300 mmHg:

1. **Oleic Acid Models** (Chiew et al., 2012a): Nine subjects were sedated and ventilated using an Engström CareStation ventilator (Datex, General Electric, Finland). The Arterial Blood Gas (ABG) was monitored as ARDS was induced using oleic acid (Ballard-Croft et al., 2012). However, only three subjects reached ARDS due to difficulty in reproducing experimental ARDS using oleic acid (Chiew et al., 2012a). Airway pressure and volumetric flow rate data were acquired using the Eview module provided with the ventilator across three experimental phases:

    1.1 **Phase 1**: A healthy state staircase RM with PEEP settings at 5 – 10 – 15 – 20 – 15 – 10 – 5 cmH_2O (Hodgson et al., 2011b). Breathing was maintained for approximately 10-15 breathing cycles at each PEEP.

    1.2 **Phase 2**: Progression from a healthy state to an oleic acid induced ARDS state at a constant PEEP of 5 cmH_2O.

    1.3 **Phase 3**: An oleic acid induced ARDS state staircase RM with PEEP settings at 5 – 10 – 15 – 20 – 15 – 10 – 5 cmH_2O (Hodgson et al., 2011b). Breathing was maintained for approximately 10-15 breathing cycles at each PEEP.

2. **Lavage Models**: Three subjects were sedated and ventilated using a Drager Evita2 ventilator (Drager, Lubeck Germany) with intermittent positive pressure ventilation. Each subject underwent surfactant depletion using lavage methods as shown in Figure 3.1 (Ballard-Croft et al., 2012). The ABG was monitored and once diagnosed with ARDS, each subject underwent a staircase RM with PEEP at 1 – 5 – 10 – 15 – 20 – 15 – 10 – 5 – 1 mbar (Hodgson et al., 2011b). Breathing was maintained for approximately 10-15 breathing cycles at each PEEP. Airway pressure and volumetric flow rate data were acquired using a 4700B pneumotachometer (Hans Rudolph Inc., Shawnee, KS).

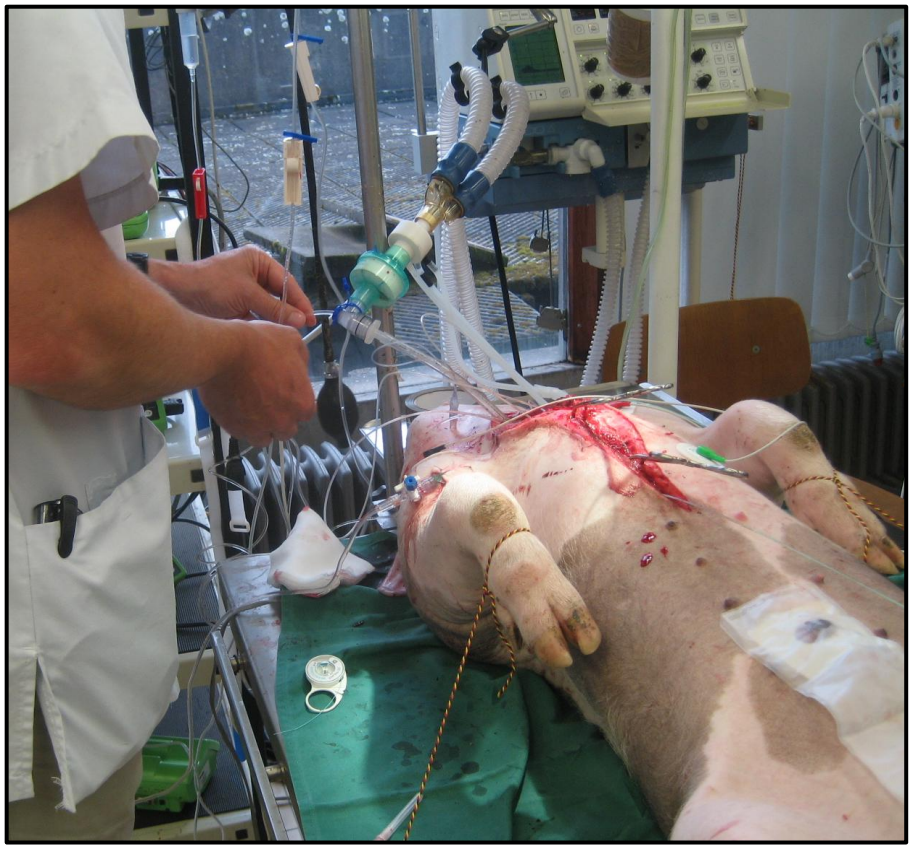

Figure 3.1 – An experimental ARDS piglet undergoing surfactant depletion using lavage methods.

These experimental procedures, protocols and the use of this data, for both ARDS animal models, has been reviewed and approved by the Ethics Committee of the University of Liège Medical Faculty.

3.7 SUMMARY

The major problem with MV lies with the lack of standardised protocols for treating ARDS patients in the ICU. Determining optimal PEEP throughout MV provides the greatest benefit to the patient at the lowest risk. This outcome can be achieved through the development of simple mathematical models that incorporate the mechanics of the lungs and relevant MV parameters. A model-based approach to guiding MV provides a low cost, non-invasive, and continuous means to gain insight into patient-specific condition and response to MV therapy.

Two important metrics that clinicians can use to effectively guide MV therapy are the elastance of the lungs as a function of PEEP, and the quantity of recruited lung volume as a function of PEEP. This thesis is aimed at using the metrics of lung elastance and recruited lung volume to develop and validate models and model-based methods to optimise PEEP selection in the ICU. These simple, real-time, dynamic, and patient-specific physiological models represent the first steps into a potential future clinical practice. In this thesis, these models and model-based methods are validated using the clinical and experimental data presented in this chapter.

Chapter 4 – Lung Elastance

4.1 INTRODUCTION

Lung elastance is an important parameter used to quantify the condition and response to MV therapy of a patient suffering from respiratory failure (Khirani et al., 2010, Chiew et al., 2012b). In particular, ARDS patients have relatively high elastance compared to healthy people (The ARDS Definition Task Force, 2012). This chapter introduces several methods to estimate lung elastance from clinically available data. Furthermore, the effect of PEEP on lung elastance, and its potential for guiding therapy, is also introduced.

4.2 EFFECT OF THE CHEST WALL

The human respiratory system can be divided into the conducting airways, the lungs, and the chest wall. The conducting airways can be described by a resistive component, whereas both the chest wall and the lungs are described by an elastic component. The chest wall is separated from the lungs by the pleural cavity, which contains pleural fluid. During inspiration, movement of the diaphragm and contraction of the external intercostals results in unique dynamics, specific to the chest wall, potentially concealing relevant aspects of lung elastance. Therefore, the measured airway pressure and volumetric flow rate data are immediately limited in their ability to provide direct insight into the true elastance of the lungs, instead providing an overall respiratory system elastance, E_{rs}, consisting of the sum of the chest wall elastance, E_{cw}, and the lung elastance, E_{lung}, as shown in Equation 4.1 (Bates,

2009). Other conditions, such as obesity and external injuries, can also alter the characteristics of the chest wall and may contribute to the complete respiratory system mechanics (Pelosi et al., 1996).

$$E_{rs} = E_{cw} + E_{lung}$$ **Equation 4.1**

One method to determine the chest wall elastance is to estimate the pleural pressure. Oesophageal pressure, measured using a balloon catheter (Karason et al., 1999, Bates, 2009), is used as a surrogate for the pleural pressure since measuring oesophageal pressure is easier and less invasive compared to measuring the pleural pressure directly. However, despite its potential to guide MV, this technique requires additional equipment, is considered uncomfortable for the patient, interrupts breathing and therapy, and is still additionally invasive. Thus, its application is limited in daily monitoring (Talmor et al., 2008, Khirani et al., 2010). Furthermore, a single oesophageal pressure measurement does not take into account the pressure gradient present throughout the thoracic cavity, which means its relevance is at least partly limited.

Generally E_{cw} is lower than E_{lung}, especially in ARDS patients (Chiumello et al., 2008). In addition, the effect of the chest wall for a fully sedated patient, who is completely dependent on the ventilator for breathing support, will be entirely passive. Thus, for a fully sedated patient, E_{cw} can be assumed constant, and changes in E_{rs} can be attributed directly to E_{lung} (Gattinoni and Pesenti, 2005).

4.3 CONVENTIONAL TWO-POINT METHODS

The static Pressure-Volume (PV) loop is regarded as the gold standard tool for assessment of lung mechanics (Stenqvist and Odenstedt, 2007). The majority of the inspiratory compliance (1/elastance) curve of the static PV loop consists of the linear region. Thus, in this approach, lung elastance can be assumed constant throughout inspiration.

4.3.1 Dynamic Elastance

Dynamic elastance, $E_{dynamic}$, is determined directly from the dynamic PV loop. A typical example of dynamic compliance (1/elastance) can be seen in Figure 4.1, where the dynamic compliance, shown by the red line, is calculated over the inspired tidal volume, V_t, between the PEEP and the Peak Inspiratory Pressure (PIP). This method is comparatively simple. However, $E_{dynamic}$ is often overestimated since the resistive effects of the conducting airways are included in the estimation (Storstein et al., 1959, Barberis et al., 2003, Lucangelo et al., 2007).

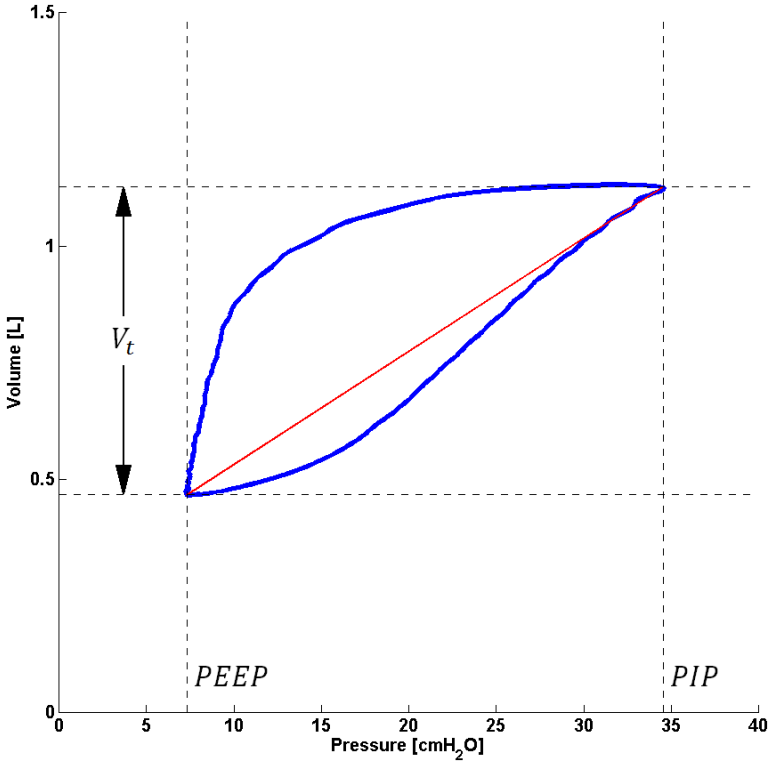

Figure 4.1 – A two-point method of estimating lung elastance. The estimated lung compliance (1/elastance) is indicated by the red line (Bersten, 1998).

Thus, $E_{dynamic}$ can be expressed symbolically:

$$E_{dynamic} = \frac{PIP - PEEP}{V_t}$$ **Equation 4.2**

4.3.2 Static Elastance

Static elastance, E_{static}, is determined using an End-Inspiratory Pause (EIP) (Fuleihan et al., 1976) where there is no airflow, allowing the inspired V_t to distribute evenly throughout the lungs. The resulting airway pressure after the EIP is called the plateau airway pressure, P_{plat}. Since there is no airflow, the resistive effects of the conducting airways are reduced to some

extent. However, when the automated EIP is too short, static conditions are not achieved, and airway pressure is not able to reach the true P_{plat}, greatly modifying the estimation of E_{static} (Barberis et al., 2003). In addition, the EIP interrupts care and breathing, and thus adds some invasiveness. A typical example of an EIP is shown in Figure 4.2 (Left). In Figure 4.2 (Right), the associated static compliance, shown by the red line, is calculated over the inspired V_t, between the PEEP and the P_{plat}.

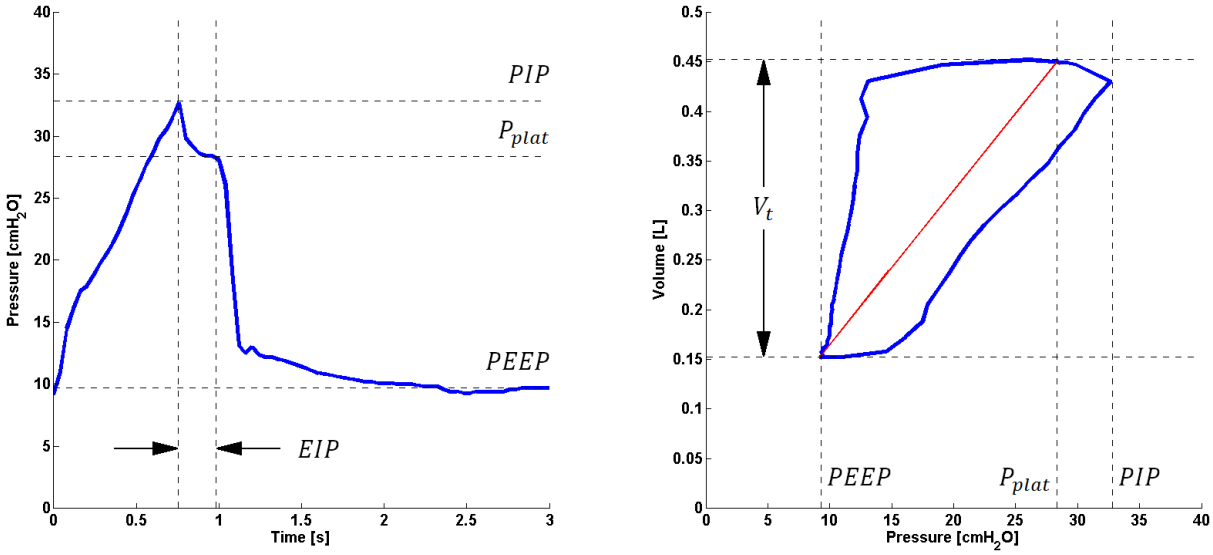

Figure 4.2 – A two-point method of estimating lung elastance with an EIP. (Left) Airway pressure data with an EIP. (Right) Dynamic PV loop where the estimated lung compliance (1/elastance) is indicated by the red line (Chiew et al., 2012a).

Thus, E_{static} can be expressed symbolically:

$$E_{static} = \frac{(P_{plat} - PEEP)}{V_t} \qquad \textbf{Equation 4.3}$$

4.4 SINGLE COMPARTMENT MODEL-BASED METHOD

4.4.1 Model Summary

Simple two-point methods are fundamentally limited since they consider only the end data points, neglecting the majority of available data. Thus, a method that uses all relevant and available data can be used to determine a more robust estimate of lung elastance. This method requires the formulation of a mathematical model to describe the behaviour of the lungs, relating airway pressure, airflow, and lung volume data.

The most commonly used model in clinical practice is the lumped parameter single compartment lung model (Mead and Whittenberger, 1953). In this model, the respiratory system is modelled as a combination of an elastic component and a resistive component, as shown schematically in Figure 4.3, where P_{aw} is the airway pressure, t is time, R_{rs} is the overall respiratory resistance consisting of the series resistance of the conducting airways, Q is the volumetric flow rate, V is the lung volume, and P_0 is the offset pressure (Bates, 2009).

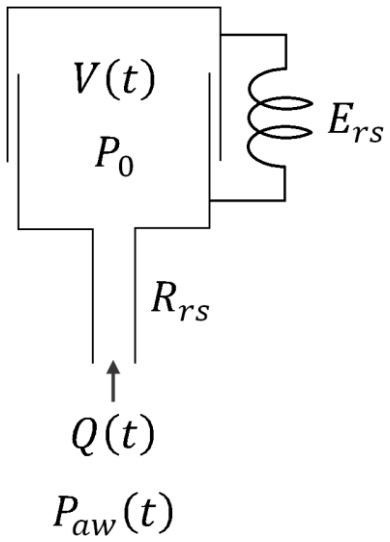

Figure 4.3 – Schematic of the single compartment lung model.

A real lung is significantly more complicated than the simple model shown in Figure 4.3. In particular, the model does not capture some specific physiological aspects, such as cardiogenic oscillations or regional differences in mechanical properties (Bates, 2009). However, it is clear that this model is anatomically and functionally analogous to a real lung. The pipe represents the conducting airways and the piston connected to an elastic spring represents the lungs, with the associated elastic tissues, that can be inflated and deflated through the pipe in the same way that the lungs inspire and expire (Bates, 2009). Furthermore, measurements of pressure and volumetric flow rate are obtained at a single, exterior location. Thus, based on the available clinical data, the respiratory system is already effectively treated as a single compartment.

The single compartment equation of motion describing the airway pressure as a function of the resistive and elastic components of the respiratory system is defined:

$$P_{aw}(t) = R_{rs} \times Q(t) + E_{rs} \times V(t) + P_0 \qquad \textbf{Equation 4.4}$$

where P_{aw} comprises the sum of the pressure required to overcome airway resistance ($R_{rs} \times Q(t)$), the pressure required to overcome the elastic tendencies of the lung tissues ($E_{rs} \times V(t)$), and the offset pressure (P_0).

Inspiration and expiration are different physiological processes, as described in Chapter 1 and Chapter 2. Thus, each process must be considered separately when determining lung properties (Moller et al., 2010a, Moller et al., 2010b). Furthermore, if expiratory airway pressure data is measured downstream of the ventilator's expiratory valve, it is expected to

contain no physiologically useful information (van Drunen et al., 2013c). Thus, the single compartment model, presented in the form of Equation 4.4, is limited to the inspiration process only. This issue is further discussed in detail in Chapter 6.

Respiratory resistance is due to the geometry of the conducting airways, and is typically dominated by the endotracheal (ET) tube, which is effectively constant during therapy (Karason et al., 2000). Thus, lung elastance provides significantly more variation with PEEP and time than airway resistance, allowing enhanced monitoring of lung overstretching and sub-optimal MV (van Drunen et al., 2013c).

4.4.2 Parameter Identification

In this research, the integral-based method (Hann et al., 2005) is used to identify the breath-specific parameters E_{rs} and R_{rs} that best fit Equation 4.4. Integral-based parameter identification is similar to multiple linear regression, where using integrals significantly increases robustness to noise (Hann et al., 2005, Chiew et al., 2011). Thus, integrating Equation 4.4 yields:

$$\int P_{aw}(t) = R_{rsIB} \times \int Q(t) + E_{rsIB} \times \int V(t) + \int P_0 \qquad \textbf{Equation 4.5}$$

where $P_{aw}(t)$, $Q(t)$, $V(t)$, and P_0 are known or measured quantities, and the respiratory system elastance (E_{rsIB}) and respiratory system resistance (R_{rsIB}) are unknown. Over a given time interval from t_0 to t_n, two or more such integrals, over different time ranges, may be calculated and reorganised to yield a linear system of equations, which can be easily solved:

$$\begin{bmatrix} \int_{t_0}^{t_1} (P_{aw}(t) - P_0) \\ \int_{t_0}^{t_2} (P_{aw}(t) - P_0) \\ \int_{t_0}^{t_3} (P_{aw}(t) - P_0) \\ \vdots \\ \int_{t_0}^{t_n} (P_{aw}(t) - P_0) \end{bmatrix} = R_{rsIB} \times \begin{bmatrix} \int_{t_0}^{t_1} Q(t) \\ \int_{t_0}^{t_2} Q(t) \\ \int_{t_0}^{t_3} Q(t) \\ \vdots \\ \int_{t_0}^{t_n} Q(t) \end{bmatrix} + E_{rsIB} \times \begin{bmatrix} \int_{t_0}^{t_1} V(t) \\ \int_{t_0}^{t_2} V(t) \\ \int_{t_0}^{t_3} V(t) \\ \vdots \\ \int_{t_0}^{t_n} V(t) \end{bmatrix}$$

Equation 4.6

Based on the simplicity of the single compartment lung model, the predicted airway pressure will never exactly match the measured airway pressure. However, optimising the identification of E_{rs} and R_{rs} will result in the predicted and measured airway pressures matching as closely as possible. The quality of the parameter identification is dependent on the signal-to-noise ratio of the airway pressure and volumetric flow rate data (Zhao et al., 2012).

The sensitivity of E_{rs} and R_{rs} to measurement noise is investigated by adding white Gaussian noise to an ideal arbitrary square-wave volumetric flow rate signal and an ideal airway pressure signal. The ideal airway pressure signal is generated from the ideal volumetric flow rate signal using Equation 4.4 with arbitrary values for E_{rs}, R_{rs}, and P_0. The volumetric flow rate signal is generated with a uniform data distribution of 50 data points over an inspiratory time of 1 s. The signal-to-noise ratio is gradually reduced over 10,000 increments such that

the level of noise relative to the signal increases from 0.1 % to 100 %, well beyond what would be expected clinically or considered usable.

Obviously, less noise should result in more accurate parameter identification. However, with added noise, identification of E_{rsIB} is generally overestimated, while identification of R_{rsIB} is generally underestimated, as shown in Figure 4.4. In clinical practice, the signal-to-noise ratio is expected to be high enough such that the estimation error shown in Figure 4.4 is minimal.

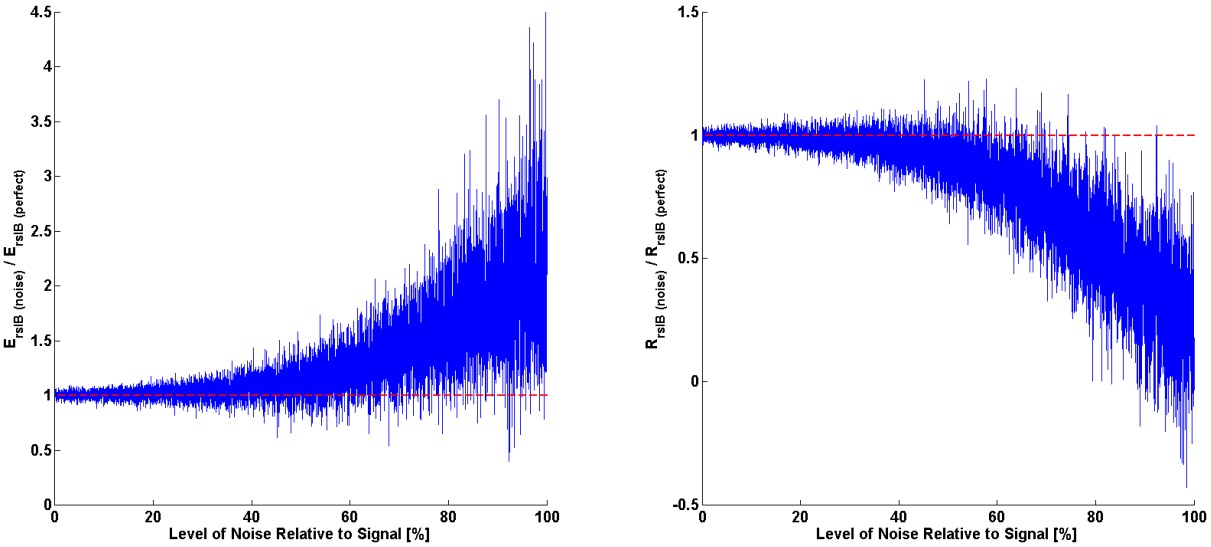

Figure 4.4 – Parameter sensitivity to noise. The red dotted line indicates exact parameter identification. (Left) $E_{rsIB\ (noise)}/E_{rsIB\ (perfect)}$. (Right) $R_{rsIB\ (noise)}/R_{rsIB\ (perfect)}$.

Accurate parameter identification is also limited by the square-wave profile of the volumetric flow rate data. From Equation 4.4, a constant volumetric flow rate effectively results in a constant term, $R_{rs} \times Q$. Thus, identification of the relative contributions of R_{rs} and E_{rs} to changes in $P_{aw}(t)$, particularly in real clinical and/or experimental data, is limited.

4.4.3 Validation of P_0

The offset pressure, P_0, represents the remaining pressure within the lungs at the end of expiration. Thus, P_0 represents the PEEP, yielding:

$$P_{aw}(t) = R_{rs} \times Q(t) + E_{rs} \times V(t) + PEEP \quad \textbf{Equation 4.7}$$

However, in patients with obstructive airway disease, gas can remain trapped in alveoli, resulting in an increased alveoli pressure at the end of expiration (Eberhard et al., 1992, Rossi et al., 1995, Ninane, 1997, Carvalho et al., 2007). This remaining pressure, known as intrinsic PEEP or auto-PEEP, has the effect of a sudden change in the level of recruitment once the PEEP exceeds the auto-PEEP. Thus, more generally, P_0 may represent the difference between the PEEP and the auto-PEEP, yielding:

$$P_{aw}(t) = R_{rs} \times Q(t) + E_{rs} \times V(t) + (PEEP - \textit{auto-PEEP}) \quad \textbf{Equation 4.8}$$

Furthermore, since application of PEEP recruits lung volume, P_0 can also be considered as the pressure required to increase baseline FRC. Thus, alternatively, the effect of P_0 may be accounted for by the addition of V_{P_0}, the additional lung volume increase due to PEEP:

$$P_{aw}(t) = R_{rs} \times Q(t) + E_{rs} \times (V(t) + V_{P_0}) \quad \textbf{Equation 4.9}$$

The validity of the interpretations and definitions of P_0 in Equation 4.7-Equation 4.9 are assessed using retrospective clinical data from 10 patients where auto-PEEP was present (Sundaresan et al., 2011a). The associated protocols are described in detail in Chapter 3. The integral-based method is used to estimate breath-specific values of respiratory system elastance (E_{rsIB}), respiratory system resistance (R_{rsIB}), and offset pressure (P_{0IB}) that best fit Equation 4.7-Equation 4.9.

The difference between the estimated P_0 (P_{0IB}) and the measured P_0 is shown in Figure 4.5. The maximum, minimum, median and Inter-Quartile Range (IQR) are used as summary statistics. Clearly, the case described by Equation 4.7 (P_0 = PEEP) produces the lowest deviation and is thus the best choice given this representative clinical data.

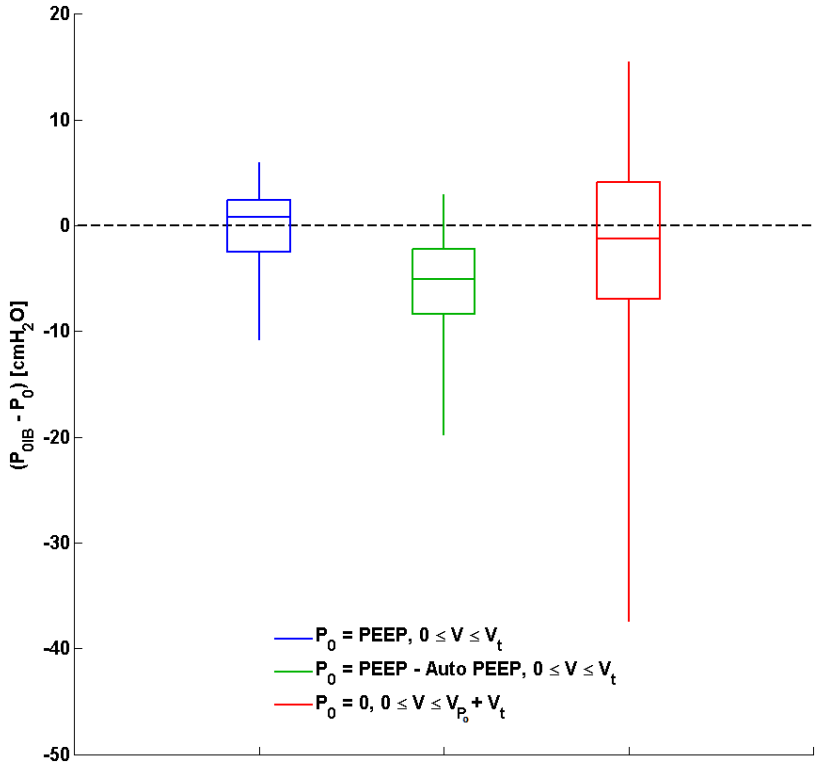

Figure 4.5 – Validation of the offset pressure, P_0, in the single compartment lung models of Equation 4.7-Equation 4.9.

4.5 EFFECT OF PEEP ON LUNG ELASTANCE

The inspiratory curve of the static PV loop typically follows a sigmoid shape, where a higher lung elastance is expected at the beginning and at the end of the inspiratory curve, and a lower lung elastance is expected in the middle. Optimal ventilation occurs when the lungs are inflated at the minimum inspiratory elastance (Carvalho et al., 2007, Suarez-Sipmann et al., 2007, Lambermont et al., 2008). At this point, maximum intrapulmonary volume change is achieved, providing maximum oxygenation at a minimum change in pressure. A method of determining the point of minimum inspiratory elastance, and consequently the optimal patient-specific PEEP, is to plot lung elastance as a function of PEEP. Figure 4.6 shows E_{rsIB} as a function of PEEP for retrospective clinical data from three patients (Sundaresan et al., 2011a) (Trials 1-3). The associated protocols are described in detail in Chapter 3. An optimal PEEP would be at or near the minimum E_{rsIB}, which can be easily identified.

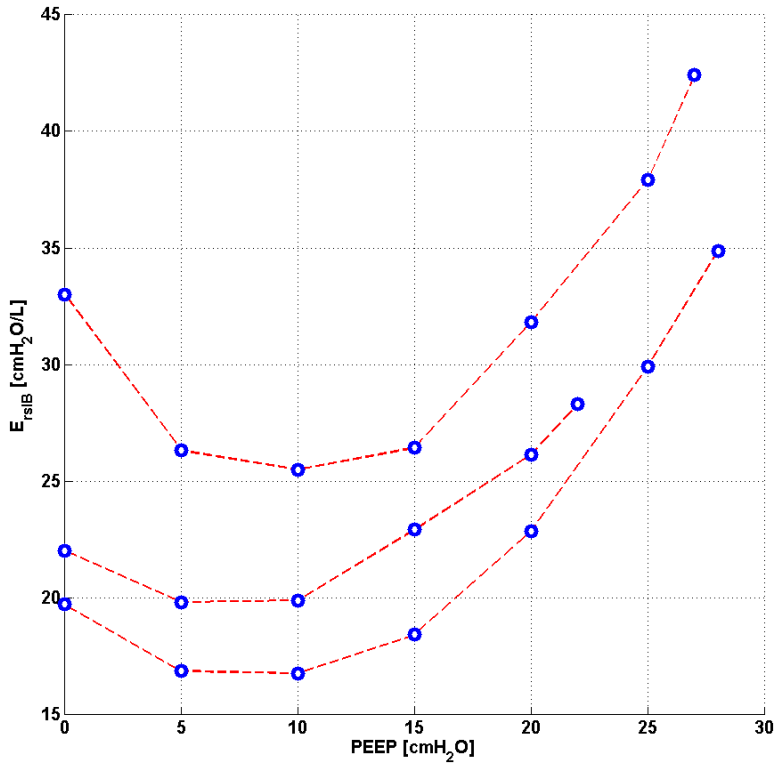

Figure 4.6 – Three examples of the effect of PEEP on lung elastance.

4.6 SUMMARY

Lung elastance is an important clinical metric used to gain insight into a patient's condition and response to therapy. The effect of PEEP on lung elastance provides a means of guiding PEEP selection. However, the methods presented in this chapter are limited in that they only provide single 'average' values of lung elastance, reducing the insight gained into the dynamics of lung elastance throughout inspiration. The single compartment lung model, combined with integral-based parameter identification, provides the most robust method of estimating parameters of lung mechanics. However, the physiological relevance of the identified parameters depends on the simplifying assumptions of the model.

Chapter 5 – Time-Varying Elastance Mapping

5.1 INTRODUCTION

This chapter presents a clinical application of dynamic respiratory system elastance (E_{drs}) proposed by Chiew et al. (Chiew et al., 2011). E_{drs} is a time-varying extension of respiratory system elastance (E_{rs}) with the aim of providing a higher resolution metric for use in guiding optimal PEEP selection. A novel method of visualising E_{drs} is presented using two separate experimental data cohorts. The bulk of this work has been submitted as a journal article (van Drunen et al., 2013d), and this method has been presented as a conference paper (van Drunen et al., 2013e).

5.2 BACKGROUND

Detrimental overstretching of healthy lung units can occur from high applied pressure. However, the heterogeneity of ARDS means that there is potential for overdistension even at low applied pressure. Dynamic respiratory system elastance (E_{drs}) is a breath-specific time-varying lung elastance (Chiew et al., 2011) and provides unique insight into a patient's breathing pattern, revealing lung recruitment and overdistension (Karason et al., 2001, Carvalho et al., 2006, Chiew et al., 2011, Zhao et al., 2012). In addition, identifying when E_{drs} is a minimum during PEEP titration can aid in identifying an optimal patient-specific PEEP to minimise Work of Breathing (WoB) and maximise recruitment without inducing further lung injury (Otis et al., 1950, Marini et al., 1985).

5.3 MODEL SUMMARY

As described in Chapter 4, a fully sedated, mechanically ventilated patient will have a near constant chest wall elastance, E_{cw}. Thus, changes in the overall respiratory system elastance, E_{rs}, are attributed directly to the patient's lung elastance, E_{lung}, as shown in Equation 5.1, providing insight into lung condition and ARDS severity (Gattinoni and Pesenti, 2005, Bates, 2009).

$$E_{rs} = E_{cw} + E_{lung} \quad \textbf{Equation 5.1}$$

The single compartment equation of motion describing the airway pressure as a function of the resistive and elastic components of the respiratory system for a fully sedated patient is defined (Bates, 2009):

$$P_{aw}(t) = R_{rs} \times Q(t) + E_{rs} \times V(t) + P_0 \quad \textbf{Equation 5.2}$$

where P_{aw} is the airway pressure, t is time, R_{rs} is the overall respiratory resistance consisting of the series resistance of the conducting airways, Q is the volumetric flow rate, V is the lung volume, and P_0 is the offset pressure.

The integral-based method (Hann et al., 2005) is used to estimate breath-specific values of respiratory system elastance (E_{rsIB}) and respiratory system resistance (R_{rsIB}) that best fit Equation 5.2:

$$\int P_{aw}(t) = R_{rsIB} \times \int Q(t) + E_{rsIB} \times \int V(t) + \int P_0 \qquad \textbf{Equation 5.3}$$

Studies have shown that R_{rs} can vary with PEEP and time due to opening or closing of airways (Mols et al., 2001, Carvalho et al., 2007, Suarez-Sipmann et al., 2007, Chiew et al., 2011), but is assumed constant throughout inspiration (Chiew et al., 2011). Thus, once R_{rsIB} is determined for a particular breath using Equation 5.3, it is substituted into Equation 5.4 where dynamic respiratory system elastance, E_{drs} (Chiew et al., 2011), is defined as a time-varying elastance, such that E_{rs} is effectively the average of E_{drs}.

$$P_{aw}(t) = R_{rsIB} \times Q(t) + E_{drs}(t) \times V(t) + P_0 \qquad \textbf{Equation 5.4}$$

Equation 5.4 can be rearranged for E_{drs}, yielding:

$$E_{drs}(t) = \frac{P_{aw}(t) - P_0 - R_{rsIB} \times Q(t)}{V(t)} \qquad \textbf{Equation 5.5}$$

Equation 5.5 determines a unique value of elastance for every available value of airway pressure and volumetric flow rate. In this way, significantly more insight is gained into the dynamics of lung elastance over the course of inspiration than can be provided by a single average value of E_{rs}. Furthermore, during a PEEP increase, recruitment of new lung volume outweighs lung stretching provided E_{drs} decreases breath-to-breath (Chiew et al., 2011).

Hence, the dynamic trajectory of E_{drs} captures the overall balance of volume (recruitment) and pressure (risk) within the lung.

5.4 MODEL VALIDATION

5.4.1 Data

This model is assessed using retrospective experimental data from six fully sedated ARDS induced piglets. In this chapter, Subjects 1-3 refer to those subjects induced with ARDS using oleic acid (Chiew et al., 2012a), while Subjects 4-6 refer to those subjects induced with ARDS using lavage methods. The associated protocols are described in detail in Chapter 3. The model is assessed across an ARDS state staircase Recruitment Manoeuvre (RM).

5.4.2 Visualisation of Dynamic Elastance

E_{drs} varies within a breath as recruitment and/or overdistension occurs. Similarly, E_{drs} will evolve with time as recruitment is time dependent (Bates and Irvin, 2002, Albert et al., 2009), disease state dependent (Pelosi et al., 2001, Halter et al., 2003), and MV dependent (Barbas et al., 2005, Albert et al., 2009). Arranging each breathing cycle's E_{drs} curve such that it is bounded by the E_{drs} curve of the preceding breath and the subsequent breath leads to a three-dimensional, time-varying, breath-specific E_{drs} map. This method of visualisation provides new insight into how the breath-to-breath lung mechanics change with time throughout the course of care. In a similar manner, the corresponding change in airway pressure from the PEEP to the Peak Inspiratory Pressure (PIP) is also displayed for each subject.

Each subject has approximately 160-360 recorded breathing cycles over the course of the RM. All breathing cycles are normalised to their total inspiratory time to provide clarity and to ensure consistency between breaths with different inspiratory times. Thus, each breath effectively begins at 0 % and ends at 100 %.

The dynamic elastance for each breath is calculated by dividing the numerator of Equation 5.5 by the inspiratory lung volume data vector. Therefore, at the beginning of inspiration, when the inspired volume is small, E_{drs} approaches physiologically unrealistic values. Since overdistension is unlikely to occur at low input volumes at the beginning of the breath, the initial 20 % of the inspiratory time for each breath is neglected for clarity. During this time, lung volume increases by approximately 0.04-0.06 L (less than 20 % of the total tidal volume, V_t) for each subject.

The time-varying breath-specific E_{drs} maps of the RM for Subjects 1-6 are shown in Figure 5.1-Figure 5.6 respectively, where blue indicates low E_{drs} and red indicates high E_{drs}. The corresponding airway pressure data and PEEP are shown in grey. The PaO_2/FiO_2 (PF ratio) for each subject is stated in the corresponding caption.

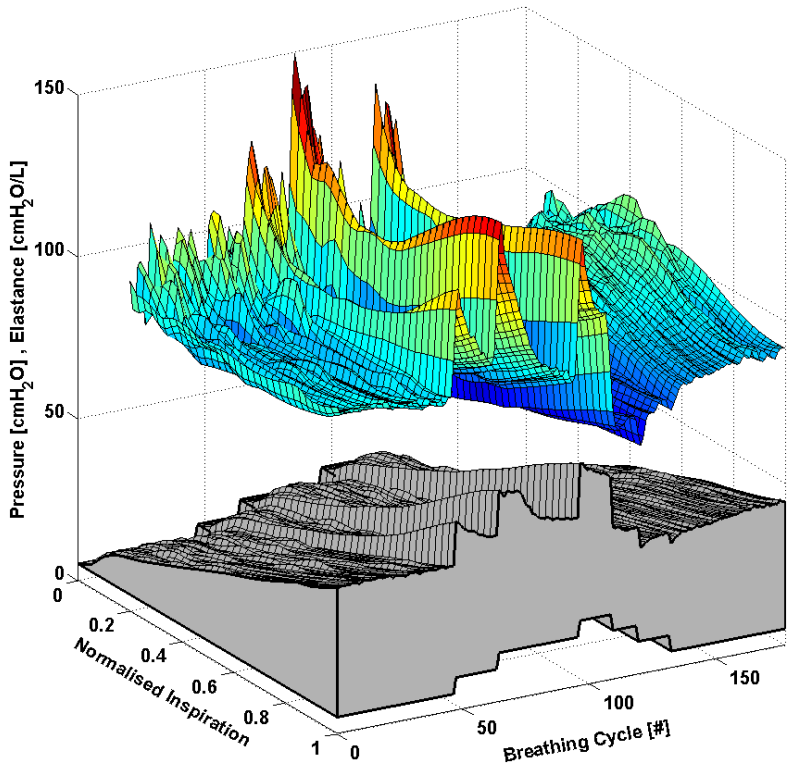

Figure 5.1 – Variation in E_{drs} across a normalised breath during a RM for Subject 1 (PF ratio = 126.6 mmHg). The change in airway pressure for each normalised breathing cycle is shown in grey. The model assumes a constant R_{rs} across each breath.

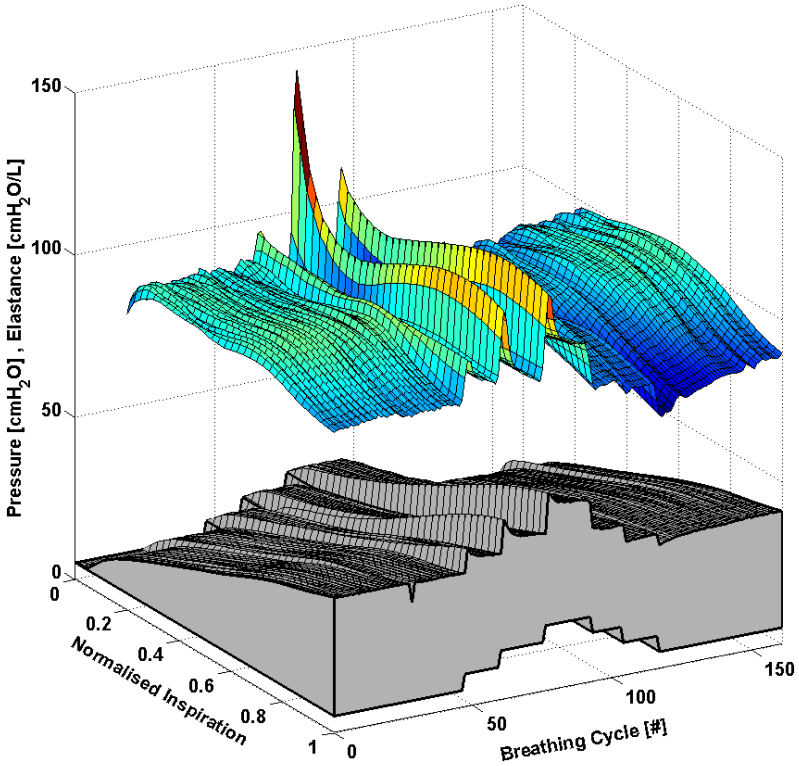

Figure 5.2 – Variation in E_{drs} across a normalised breath during a RM for Subject 2 (PF ratio = 183.6 mmHg). The change in airway pressure for each normalised breathing cycle is shown in grey. The model assumes a constant R_{rs} across each breath.

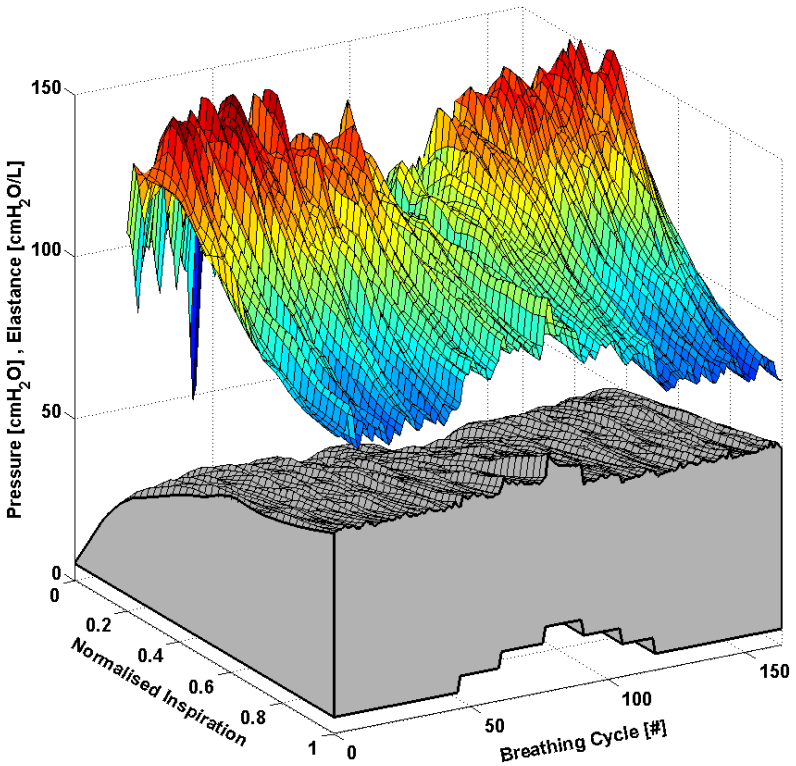

Figure 5.3 – Variation in E_{drs} across a normalised breath during a RM for Subject 3 (PF ratio = 113.6 mmHg). The change in airway pressure for each normalised breathing cycle is shown in grey. The model assumes a constant R_{rs} across each breath.

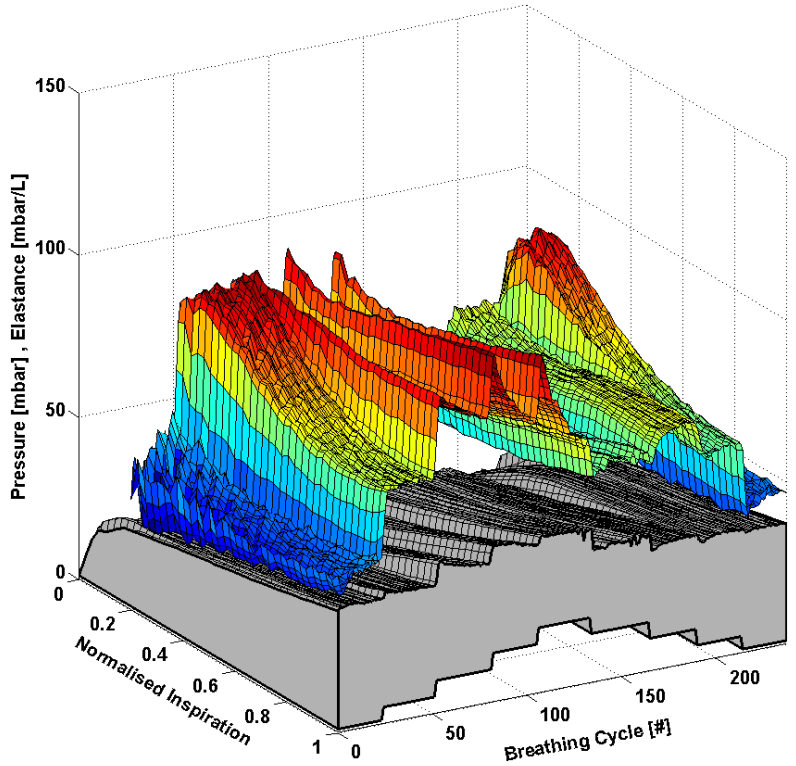

Figure 5.4 – Variation in E_{drs} across a normalised breath during a RM for Subject 4 (PF ratio = 155.2 mmHg). The change in airway pressure for each normalised breathing cycle is shown in grey. The model assumes a constant R_{rs} across each breath.

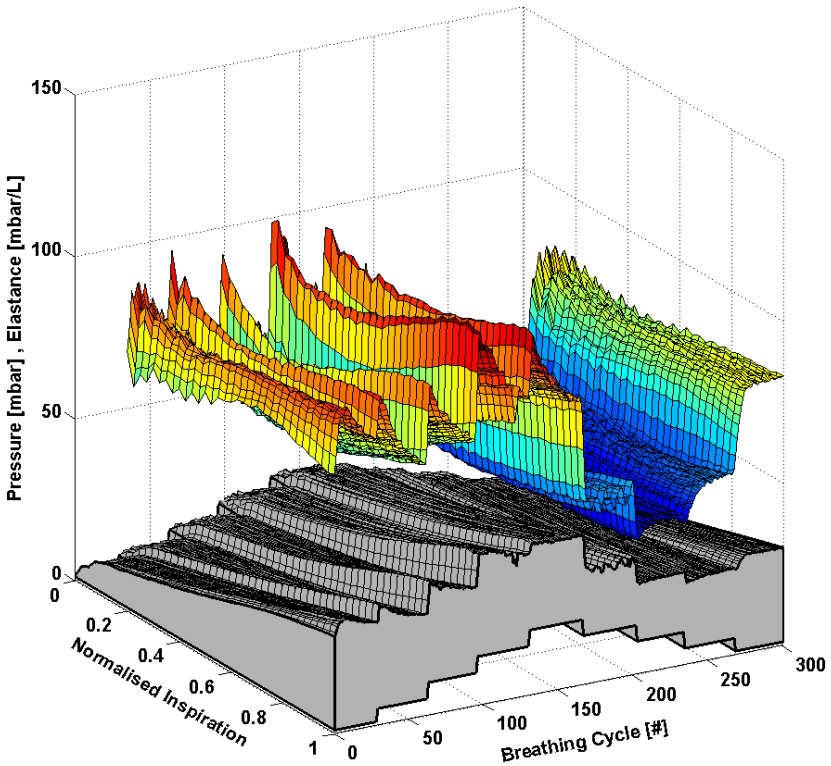

Figure 5.5 – Variation in E_{drs} across a normalised breath during a RM for Subject 5 (PF ratio = 85.9 mmHg). The change in airway pressure for each normalised breathing cycle is shown in grey. The model assumes a constant R_{rs} across each breath.

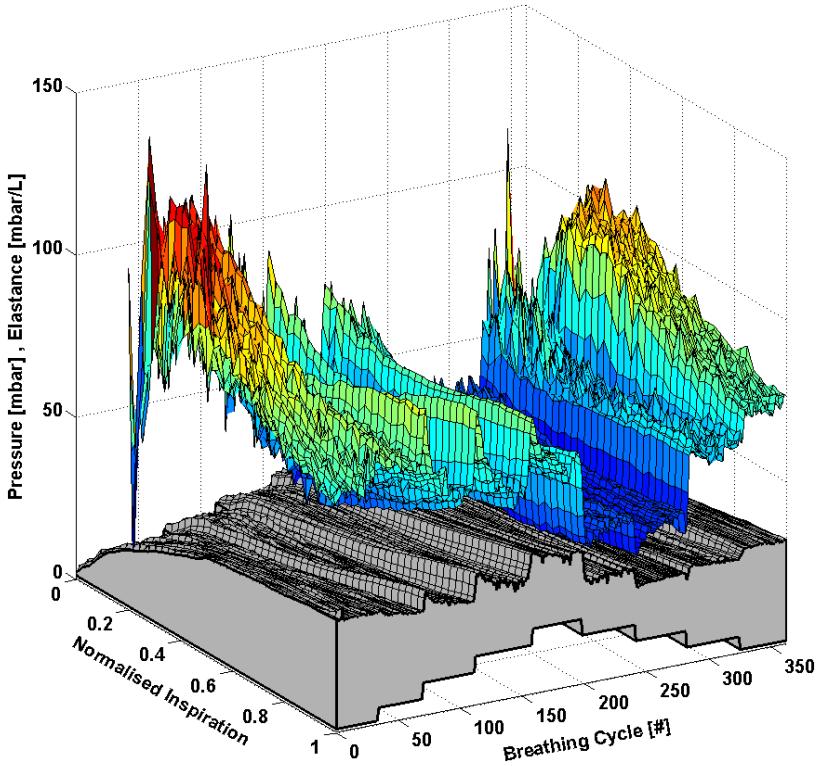

Figure 5.6 – Variation in E_{drs} across a normalised breath during a RM for Subject 6 (PF ratio = 110.4 mmHg). The change in airway pressure for each normalised breathing cycle is shown in grey. The model assumes a constant R_{rs} across each breath.

5.4.3 Validity of Constant Respiratory System Resistance

The effect of the resistive term in Equation 5.5 is mathematically limited in its impact (Chiew et al., 2011). However, there is evidence to suggest that in some cases R_{rs} may vary throughout inspiration (Mols et al., 2001). The determination of E_{drs} accommodates any R_{rs} value that is chosen such that the model perfectly fits the available airway pressure data. Therefore, the assumption of constant R_{rs} may limit the accuracy of the E_{drs} model.

The magnitude of the variation in R_{rs} can be quantified, to some extent, by dividing the inspiratory portion of each breath into multiple sections, or slices, and determining a unique value of R_{rs} (R_{rsIB}) for each slice (Zhao et al., 2012). This is known as the SLICE method (Guttmann et al., 1994). Thus, any variation in R_{rs} throughout inspiration can be approximated by a piecewise model. The SLICE method is applied to each subject and the number of volume slices increased iteratively from one to five. Integral-based parameter identification is applied, in turn, to each slice to determine a unique value for R_{rs}. Median and Inter-Quartile Range (IQR) values of R_{rs} are presented in Table 5.1.

Table 5.1 – The SLICE method of identifying in-breath R_{rs}.

		R_{rs} (Median, [IQR]) across ARDS RM [cmH_2Os/L]					
		Subject					
		1	2	3	4	5	6
Number of Slices	1	14.5 [11.0-17.1]	12.8 [6.0-16.6]	43.6 [25.6-45.9]	7.6 [6.2-25.0]	10.0 [8.2-12.6]	14.4 [10.8-19.0]
	2	15.2 [13.6-16.3]	12.2 [9.6-14.2]	29.1 [20.1-31.5]	9.0 [8.0-17.3]	11.5 [10.1-13.4]	14.8 [11.0-19.9]
		10.0 [0.0-24.8]	19.3 [1.7-27.1]	61.6 [42.1-69.4]	4.7 [0.0-35.5]	4.2 [0.0-9.7]	11.6 [5.4-17.9]
	3	14.5 [12.9-15.9]	12.1 [10.1-13.9]	24.9 [18.5-27.4]	9.4 [8.5-14.0]	11.7 [10.4-13.7]	13.8 [10.5-19.3]
		13.6 [8.4-18.3]	9.7 [0.5-14.9]	55.8 [36.4-67.8]	6.5 [3.7-36.7]	9.6 [6.8-12.2]	14.6 [10.8-18.8]
		7.4 [0.0-22.7]	27.6 [6.3-33.1]	61.6 [44.6-68.3]	4.9 [0.0-32.7]	1.5 [0.0-7.9]	9.6 [2.1-20.8]
	4	14.0 [12.8-15.4]	12.0 [10.7-13.5]	21.7 [16.5-23.5]	9.5 [8.6-13.0]	12.0 [10.6-14.2]	13.0 [10.1-18.9]
		14.7 [12.1-17.7]	12.4 [6.3-14.9]	46.4 [26.5-55.7]	8.4 [6.3-33.4]	11.0 [9.2-13.2]	16.2 [11.9-21.6]
		10.7 [1.4-22.2]	11.4 [0.0-21.4]	60.2 [40.8-71.6]	4.0 [1.1-37.8]	7.0 [3.0-11.0]	12.7 [8.5-17.6]
		3.7 [0.0-20.7]	29.4 [9.8-34.1]	57.5 [44.2-66.4]	5.8 [0.0-31.9]	0.0 [0.0-7.3]	8.0 [0.4-21.1]
	5	13.7 [12.5-14.9]	12.3 [11.0-13.3]	20.0 [15.5-22.0]	9.7 [8.7-12.9]	12.2 [10.7-14.6]	12.6 [9.7-18.4]
		15.9 [13.2-18.5]	12.7 [7.8-15.2]	41.0 [25.8-46.7]	8.7 [7.4-27.7]	11.2 [9.6-13.1]	16.3 [12.4-21.7]
		13.2 [7.6-18.4]	8.8 [0.0-15.1]	54.8 [35.3-70.5]	6.5 [3.3-37.7]	9.5 [6.8-12.1]	14.1 [10.6-19.0]
		10.3 [0.0-23.7]	19.6 [1.0-28.2]	57.9 [45.7-70.8]	3.9 [0.0-37.1]	5.1 [0.5-10.1]	11.4 [6.1-17.7]
		2.4 [0.0-18.9]	28.1 [8.6-33.4]	55.1 [44.4-63.1]	6.2 [0.0-30.9]	0.0 [0.0-6.0]	7.3 [0.0-21.9]

5.5 DISCUSSION

5.5.1 General Observations

All subjects show, to some degree, an increase in elastance immediately following a PEEP step increase of 5 cmH_2O/5 mbar. Each successive breath has a reduced peak elastance, indicating the time-dependent nature of recruitment and/or the lung's viscoelastic properties, which cause hysteresis (Ganzert et al., 2009, Andreassen et al., 2010). More specifically, there is a period of adaptation following an increase in PEEP that sees higher average E_{drs}, peak E_{drs} and PIP before the beneficial effect of lower E_{drs} is seen. Furthermore, the E_{drs} trajectory within a breath generally decreases during inspiration, suggesting in-breath recruitment.

Over the course of inspiration, and typically directly following a PEEP step increase, some subjects show a decreasing E_{drs} trajectory, followed by an increasing E_{drs} trajectory. Rising elastance indicates serious potential for lung damage due to overstretching, and may not be captured by a single value of E_{rs} (Chiew et al., 2011, Zhao et al., 2012). Thus, as a result of this study, PEEP increments of 1 cmH_2O/1 mbar, rather than increments of 5 cmH_2O/5 mbar, may avoid any damage due to the raised elastance in the early breaths and adaptation period following an increase in PEEP. During a RM, smaller PEEP increments, each followed by a short period of stabilisation, may substantially reduce the peak of the E_{drs} spikes at the end of inspiration. However, it is equally important to note that the occurrence of beneficial lower elastance after stabilisation may also be a direct consequence of the initial high overdistension immediately following an increase in PEEP. This finding warrants further

investigation where staircase recruitment is performed using smaller PEEP increments. Changes in ventilator pattern or mode also have the potential to modify the E_{drs} trajectory.

The E_{drs} map is significantly different between increasing and decreasing PEEP (using a Wilcoxon rank sum test, $p < 0.05$ for each subject), where decreasing PEEP titration generally results in lower overall elastance. When PEEP increases, recruitment, as well as potential lung overstretching occurs. However, as PEEP is reduced, the lung remains compliant and elastance drops to an overall minimum. Equally, this phenomenon is seen where the Threshold Opening Pressure (TOP) of collapsed lung units is higher than the Threshold Closing Pressure (TCP) (Crotti et al., 2001, Pelosi et al., 2001).

Considering increasing and decreasing PEEP separately, a local minimum elastance generally occurs at the same PEEP, suggesting that optimal PEEP can be selected either way. Recruitment is a function of PEEP and time (Barbas et al., 2005, Albert et al., 2009). Equally, the ARDS affected lung is prone to collapse due to the instability of affected lung units (Pelosi et al., 2001, Halter et al., 2003). Assuming that the severity of ARDS does not change within a short period, lung elastance during increasing PEEP titration is expected to reduce as time progresses to achieve stability. In contrast, lung elastance will increase with time during decreased PEEP to achieve stability. Hence, it is hypothesised that PEEP can be titrated to a minimum elastance either way, provided a stabilisation period is given at each PEEP to obtain a true minimum elastance. Such a process could be readily automated and monitored in a ventilator.

Setting PEEP at minimum elastance theoretically benefits ventilation by maximising recruitment, reducing WoB and avoiding overdistension (Carvalho et al., 2007, Suarez-Sipmann et al., 2007, Lambermont et al., 2008, Zhao et al., 2010a). However, selecting PEEP is a trade-off in maximising recruitment, versus minimising lung pressure and potential damage. The time-varying E_{drs} map is a higher resolution metric of dynamic adaptation to PEEP than a single E_{rs} value.

The PIP can be seen to follow the E_{drs} contour to some extent. However, it does not provide the same degree of resolution. In some cases, the PIP is seen to stabilise quickly or remain relatively constant following a change in PEEP, while E_{drs} continues to change significantly, indicating the occurrence of significant lung dynamics not readily apparent from monitoring airway pressure alone. This result shows the greater sensitivity of using E_{drs}, and that E_{drs} captures more relevant dynamics than airway pressure alone.

5.5.2 Oleic Acid ARDS Models

5.5.2.1 Subject 1

The response of Subject 1 to PEEP titration is seen in Figure 5.1. Elastance drops to an overall minimum at a PEEP of 15 cmH_2O, suggesting that maintaining this PEEP provides an optimal trade-off between maximising recruitment and reducing the risk of lung damage (Carvalho et al., 2007).

5.5.2.2 Subject 2

The response of Subject 2 to PEEP titration is seen in Figure 5.2 and is similar to that of Subject 1. However, the magnitude of the E_{drs} response to PEEP is reduced. Elastance drops to an overall minimum at a PEEP of 15 cmH_2O, implying optimal PEEP.

5.5.2.3 Subject 3

In Subject 3, E_{drs} rises to a maximum near the beginning of each breathing cycle, before rapidly decreasing, as seen in Figure 5.3. However, this trend is less pronounced at high PEEP. Subject 3 had a higher severity of ARDS (PF ratio = 113.6 mmHg) than Subject 1 (PF ratio = 126.6 mmHg) or Subject 2 (PF ratio = 183.6 mmHg), potentially resulting in the substantially different response to PEEP. The airway pressure curves initially show a rapid increase followed by a more gradual increase. Thus, it is possible that a different volumetric flow rate profile may eliminate the initial rapid pressure increase, reducing the rise in E_{drs}. The most uniform minimum elastance across a breath occurs at a PEEP of 15 cmH_2O (at both increasing and decreasing PEEP), implying optimal PEEP.

5.5.3 Lavage ARDS Models

5.5.3.1 Subject 4

Elastance increases significantly in Subject 4 when PEEP is increased from 1 mbar to 5 mbar as seen in Figure 5.4. The lowest elastance is encountered either side of the RM at a PEEP of 1 mbar. However, a local minimum elastance occurs at a PEEP of 15 mbar during decreasing

PEEP. Thus, in this case, minimum elastance would suggest that the subject should be ventilated at 1 mbar, rather than 15 mbar. However, it is important to note that ARDS patients should be ventilated at higher PEEP (> 5 cmH_2O/5 mbar) to prevent lung collapse (Hedenstierna and Rothen, 2000, The ARDS Definition Task Force, 2012, Briel et al., 2010). Thus, this E_{drs} map outlines a potential drawback of guiding PEEP selection based solely on minimum elastance, possibly resulting from a unique ventilation history prior to the RM. Clinicians should consider an alternate PEEP value when an unrealistically low PEEP is recommended by elastance alone. Alternatively, a modified elastance metric could be developed.

5.5.3.2 Subject 5

The response of Subject 5 to PEEP titration is seen in Figure 5.5. Elastance drops to an overall minimum at a PEEP of 10 mbar, implying optimal PEEP.

5.5.3.3 Subject 6

Unlike Subjects 4 and 5, the RM performed on Subject 6 was performed during an open chest surgery, thereby neglecting the effect of E_{cw} in Equation 5.1 and effectively capturing E_{lung} directly. It is apparent that more noise is present in this trial when compared to closed chest ventilation performed on Subjects 1-5, suggesting that the chest wall may provide some form of damping to high frequency physiological or mechanical effects. It is observed that minimum elastance occurs at a decreasing PEEP of 10 mbar, as shown in Figure 5.6.

5.5.4 Effect of Constant Resistance

The results presented in Table 5.1 indicate that the variation in R_{rs} across inspiration is generally minimal. However, the final slice, capturing the end of inspiration, is generally significantly different from the preceding estimates of R_{rs}. Thus, to investigate the impact of variable R_{rs} on E_{drs}, the SLICE method is extended to determine a piecewise E_{drs} map across inspiration as shown in Figure 5.7 for Subject 1. Both Figure 5.1 and Figure 5.7 show similar in-breath E_{drs} maps for higher, clinically relevant PEEPs. In addition, optimal PEEP occurs at 15 cmH_2O, regardless of the number of slices.

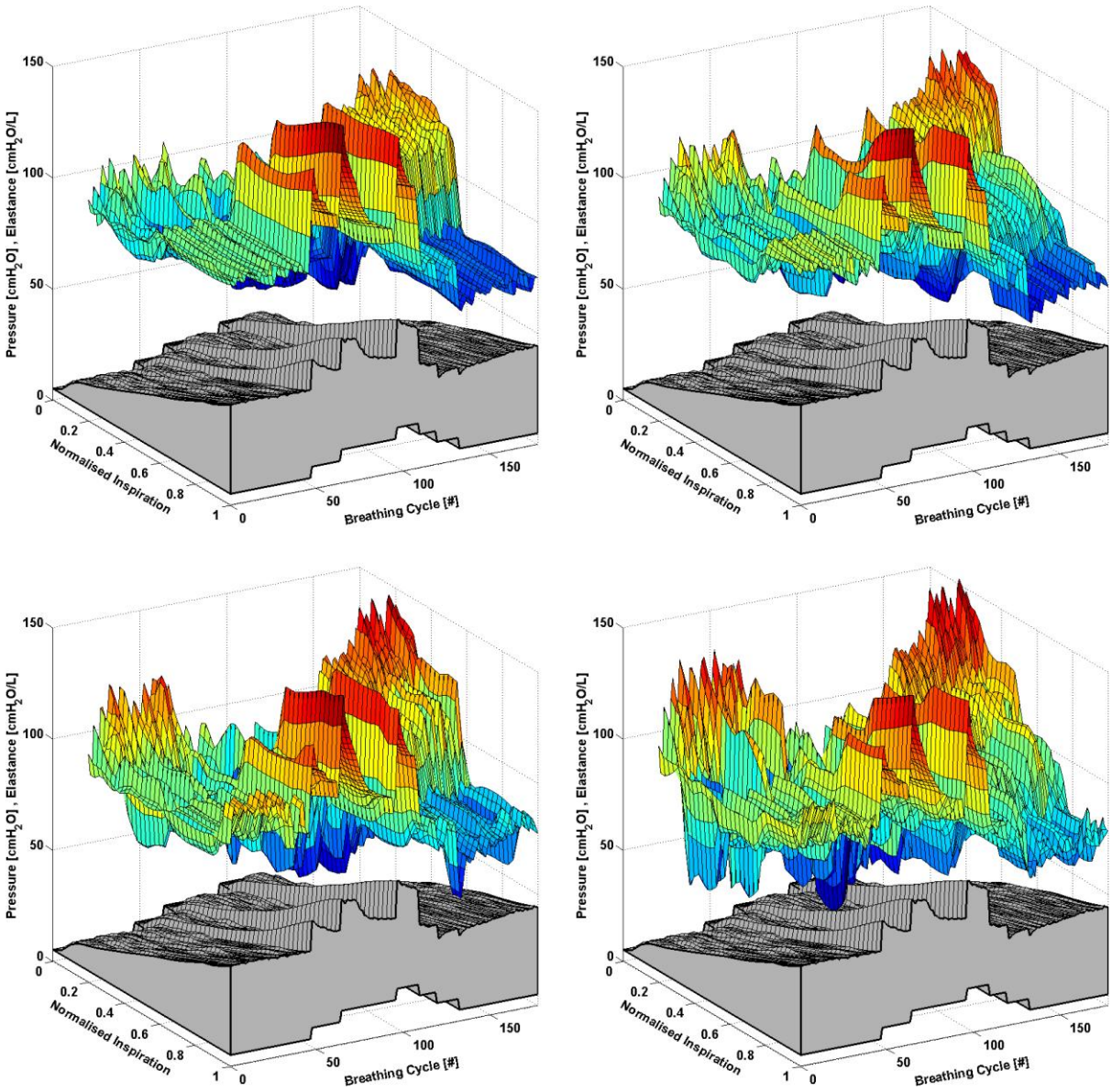

Figure 5.7 – Variation in E_{drs} across a normalised breath during a RM for Subject 1 with changes in R_{rs} identified using the SLICE method. The change in airway pressure for each normalised breathing cycle is shown in grey. (Top left) Two slices. (Top right) Three slices. (Bottom left) Four slices. (Bottom right) Five slices.

5.5.5 Limitations

The single compartment lung model used to derive the E_{drs} model does not capture some specific physiological aspects such as cardiogenic oscillations or regional differences in mechanical properties. Furthermore, the effects of non-linear flow or variations in airway

resistance over the course of inspiration are neglected (Bates, 2009). However, the SLICE method has shown that variation in R_{rs} across inspiration generally results in minimal changes in the trends of the E_{drs} map.

The SLICE method is not without limitation. Increasing the number of slices reduces the quality of the parameter identification within a slice due to a decrease in the number of available data points (Zhao et al., 2012). Thus, trend identification in Figure 5.7 is hindered by an increase in noise as the number of slices increase. The clinical potential of E_{drs} mapping requires a compromise between physiological accuracy and clarity. Assuming a constant R_{rs} across inspiration provides clearer trends that identify the same optimal PEEP as the SLICE method. Therefore, based on this study, assuming a constant R_{rs} across inspiration aids clinical decision making and provides potential for implementation in the ICU.

Both experimental ARDS animal models differed in many aspects. Thus, statistically significant comparisons between each model cannot be made. However, the main outcome of this research is that E_{drs} mapping of mechanically ventilated ARDS subjects can be monitored to provide a high resolution metric to describe disease state and physiological changes in response to PEEP. This outcome shows the robustness of both the model and the method of visualisation for application in the ICU. However, higher inter-patient variability is present in patients admitted to the ICU. Thus, application of this monitoring technique warrants further investigation in both human and animal studies.

A further limitation is that the findings of this research are based solely on observation of the E_{drs} maps. The findings require further investigation with additional imaging and monitoring tools such as in-vivo microscopy, Computed Tomography (CT) scans and/or Electrical Impedance Tomography (EIT) for validation. High resolution imaging technology is currently limited to regional investigation and clinically impractical for full and continuous monitoring (Malbouisson et al., 2001, Zhao et al., 2009, Zhao et al., 2010b). However, this analysis is predominantly based on the comparison of trends across a RM, where each subject is their own reference. Thus, the best validation is the ability to track clinically expected trends as shown here.

5.6 SUMMARY

Visualisation of dynamic respiratory system elastance (E_{drs}) provides significantly more insight into dynamic lung behaviour than can be provided by a single average value of respiratory system elastance (E_{rs}). Simultaneous monitoring of elastance across a breath and during a RM provides a new clinical perspective to guide therapy and provides unique patient-specific insight into the heterogeneous response to PEEP. The model is somewhat limited by its simplicity. However, trends match clinical expectation and the results highlight the inter-subject variability.

Chapter 6 – Expiratory Time-Constant Model

6.1 INTRODUCTION

This chapter presents and evaluates a proof of concept study of an expiratory time-constant model. Expiratory data is used to calculate a parameter, *K*, hypothesised to be a proxy for lung elastance. *K* has the potential to offer insight into lung mechanics in situations where conventional inspiratory metrics are not suitable. Furthermore, continuous monitoring of *K* allows changes in disease state to be tracked over time, aiding clinical decision making. This work has been published as a journal article (van Drunen et al., 2013c), and this method has been presented as a conference paper (van Drunen et al., 2013b).

6.2 BACKGROUND

Conventional metrics of lung mechanics are estimated based on the mechanics of breathing during inspiration, often neglecting expiratory data. However, passive expiration can be used to determine a metric based on the expiratory volumetric flow rate profile (Al-Rawas et al., 2013). Real-time monitoring of model-based lung mechanics throughout therapy can provide unique descriptions of a patient's disease progression and response to MV (Carvalho et al., 2007, Lucangelo et al., 2007, Suarez-Sipmann et al., 2007, Lambermont et al., 2008), offering the ability to optimise patient-specific PEEP selection.

6.3 MODEL SUMMARY

The single compartment equation of motion describing the airway pressure as a function of the resistive and elastic components of the respiratory system for a fully sedated patient is defined (Bates, 2009):

$$P_{aw}(t) = R_{rs} \times Q(t) + E_{rs} \times V(t) + P_0 \quad \textbf{Equation 6.1}$$

where P_{aw} is the airway pressure, t is time, R_{rs} is the overall respiratory system resistance consisting of the series resistance of the conducting airways, Q is the volumetric flow rate, E_{rs} is the overall respiratory system elastance, V is the lung volume, and P_0 is the offset pressure.

Inspiration and expiration are different physiological processes. Expiration is essentially the passive unloading of the inspired tidal volume, V_t, over a resistance at a constant ventilator applied airway pressure (P_{aw} = PEEP) with $P_0 =$ PEEP (Moller et al., 2010a, Moller et al., 2010b). Noting that volume is the integral of volumetric flow rate with respect to time, Equation 6.1 in expiration becomes:

$$PEEP = R_{rs} \times Q(t) + E_{rs} \times \int_0^t Q(t')dt' + PEEP \quad \textbf{Equation 6.2}$$

Differentiating Equation 6.2 yields:

$$0 = R_{rs} \times \frac{dQ(t)}{dt} + E_{rs} \times Q(t) \quad \textbf{Equation 6.3}$$

Dividing Equation 6.3 by R_{rs} yields a simple ordinary differential equation:

$$\frac{dQ(t)}{dt} + \frac{E_{rs}}{R_{rs}} \times Q(t) = 0 \qquad \textbf{Equation 6.4}$$

Solving Equation 6.4 yields the expiratory time-constant model:

$$Q(t) = Q_0 e^{-t/\tau} = Q_0 e^{-Kt} \qquad \textbf{Equation 6.5}$$

where Q_0 is the value of maximum expiratory volumetric flow rate and $\tau = 1/K = R_{rs}/E_{rs}$ is the system time-constant (Al-Rawas et al., 2013).

If R_{rs} is assumed constant (Chiew et al., 2011), then *K* is directly proportional to E_{rs}, where an increasing *K* implies a stiffer lung as ARDS progresses, as shown in Figure 6.1.

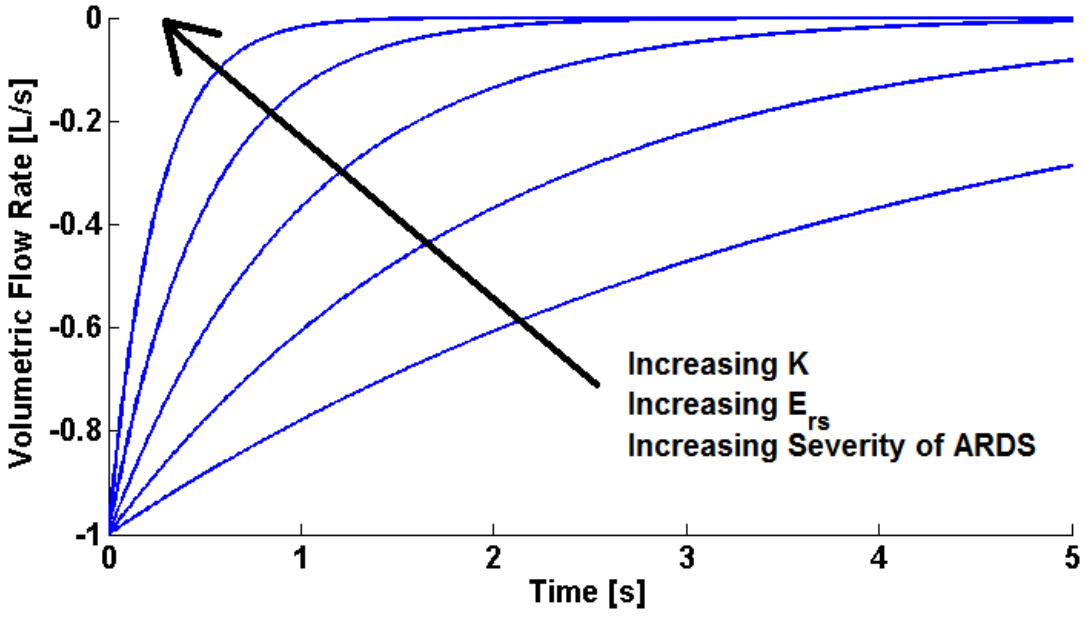

Figure 6.1 – How changes in the expiratory volumetric flow rate profile over time can be used to determine a patients' disease state, assuming R_{rs} is constant.

6.4 MODEL VALIDATION

6.4.1 Data

This model is assessed using retrospective experimental data from three fully sedated ARDS induced piglets. In this chapter, Subjects 1-3 refer to those subjects induced with ARDS using oleic acid (Chiew et al., 2012a). The associated protocols are described in detail in Chapter 3. The model is assessed across three experimental phases:

1. **Phase 1**: A healthy state staircase Recruitment Manoeuvre (RM).
2. **Phase 2**: Progression from a healthy state to an induced ARDS state at a constant PEEP.
3. **Phase 3**: An induced ARDS state staircase RM.

Each subject has approximately 1,600-3,500 recorded breathing cycles across all three phases, with a combined total of 6,800 breathing cycles. Using a large number of breathing cycles provides robust identification of trends.

6.4.2 Model Fitting

Values of K and Q_0 are determined from the least-squares best fit of Equation 6.5 to the expiratory volumetric flow rate data. Determining Q_0 simultaneously with K leads to robust parameter identification as the effect of outliers at, or near, the beginning of expiration is reduced. During expiration, the density distribution of data increases because the rate of

change of volumetric flow rate decreases. Therefore, towards the end of expiration, the model fit becomes more constrained. When combined with the presence of a long portion of near-constant volumetric flow rate at the end of expiration, caused by resistance in the ventilator's expiratory valve (Al-Rawas et al., 2013), poor model fitting can occur. Hence, model fitting is limited to the time span required for the respiratory system to reach 95 % of its equilibrium value, as illustrated for a representative breath in Figure 6.2 (Top).

The expiratory airway pressure data recorded in this study shows a sudden decrease to just above the applied PEEP, followed by a small trailing portion as shown for a representative breath in Figure 6.2 (Bottom). This data is expected to contain no physiologically useful information since it is measured downstream of the ventilator's expiratory valve. Furthermore, the change in airway pressure from 1.12 s to the end of expiration is minor. This outcome further justifies the approach of only considering volumetric flow rate data throughout expiration.

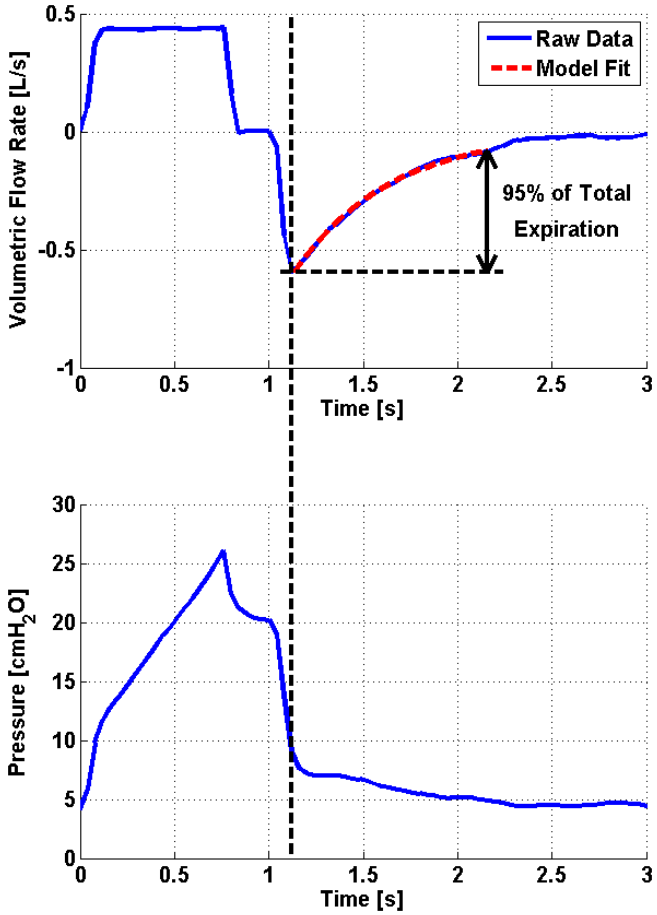

Figure 6.2 – A single representative breathing cycle. (Top) The expiratory time-constant model fitted to expiratory volumetric flow rate data. (Bottom) Airway pressure data of a single breathing cycle at PEEP = 5 cmH_2O. In this case, airway pressure data after 1.12 s is physiologically meaningless.

6.4.3 Validation Metrics

The expiratory time-constant model parameter, *K*, is determined continuously for every breathing cycle for each subject across each phase. Validation is performed by comparing trends in *K* to trends obtained using an End-Inspiratory Pause (EIP) method and trends obtained using an integral-based method. Both methods determine unique inspiratory estimates of respiratory system elastance and respiratory system resistance for each breathing cycle, providing more insight into lung mechanics than the single lumped parameter, *K*. In particular:

1. **EIP method**: Metrics of respiratory system mechanics are determined directly from the Engström CareStation ventilator (Datex, General Electric Healthcare, Finland) which automates a short EIP during controlled MV (Ingelstedt et al., 1972, Fuleihan et al., 1976, Pillet et al., 1993). The pause during EIP omits the resistance component in Equation 6.1 ($Q(t) = 0$) and prolongs inspiration, allowing the inspired volume of air to distribute evenly throughout the lungs. The resulting airway pressure after the EIP is called the plateau airway pressure, P_{plat}, and can be used to estimate static elastance, E_{static}, as shown in Equation 6.6. Equally, the pressure difference between the PIP and the P_{plat} can be used to calculate static resistance, R_{static}, as shown in Equation 6.7.

$$E_{static} = \frac{(P_{plat} - PEEP)}{V_t} \qquad \textbf{Equation 6.6}$$

$$R_{static} = \frac{(PIP - P_{plat})}{Q} \qquad \textbf{Equation 6.7}$$

2. **Integral-based method** (Hann et al., 2005): The integral-based method is used to estimate breath-specific values of respiratory system elastance (E_{rsIB}) and respiratory system resistance (R_{rsIB}) that best fit Equation 6.1:

$$\int P_{aw}(t) = R_{rsIB} \times \int Q(t) + E_{rsIB} \times \int V(t) + \int P_0 \qquad \textbf{Equation 6.8}$$

Thus, K can be compared with, E_{static} and R_{static}, as well as, E_{rsIB} and R_{rsIB}, both of which aim to capture the true elastance (E_{lung}) and resistance (R_{lung}) of the lung. This validation process is summarised graphically in Figure 6.3.

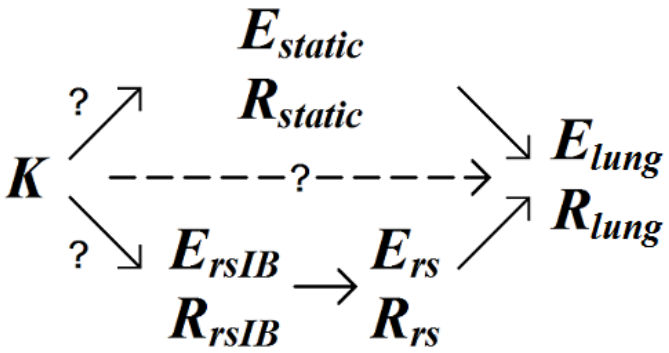

Figure 6.3 – Graphic representation of the relationship between various metrics of lung mechanics and the true elastance and resistance of the lung.

6.4.4 Analysis

For each breath, the expiratory time-constant model and both validation methods are compared to recorded volumetric flow rate and airway pressure data respectively. In particular, the parameters K and Q_0 are substituted into Equation 6.5 and the calculated volumetric flow rate is compared to the measured expiratory volumetric flow rate data used during model fitting. In the case of both validation methods, the estimated parameters, E_{static} and R_{static}, and, E_{rsIB} and R_{rsIB}, are substituted into Equation 6.1 and the calculated airway pressure is compared to the measured inspiratory airway pressure data. Median and Inter-Quartile Range (IQR) absolute percentage fitting errors are presented in Table 6.1. The integral-based method has the lowest overall median fitting error for each subject. The expiratory time-constant model has the second lowest overall median fitting error for Subjects 2 and 3. All overall median fitting errors are within likely measurement errors of 3-10 %.

Table 6.1 – Model fitting errors.

		Absolute Percentage Fitting Error (Median, [IQR]) [%]			
	Subject	**Phase 1**	**Phase 2**	**Phase 3**	**Overall**
Expiratory Time-Constant Model	1	5.01 [2.24-9.89]	7.24 [3.74-12.58]	5.19 [2.50-8.96]	6.99 [3.55-12.21]
	2	3.69 [1.68-7.58]	3.66 [1.59-6.78]	5.84 [2.77-9.62]	3.83 [1.67-7.12]
	3	4.38 [1.90-8.71]	4.37 [2.00-8.41]	10.57 [5.11-17.29]	4.72 [2.13-9.34]
EIP Method	1	2.61 [1.25-4.87]	3.85 [1.85-6.99]	4.07 [1.75-7.83]	3.77 [1.80-6.92]
	2	5.83 [3.28-10.26]	5.31 [2.69-9.13]	6.81 [3.84-9.91]	5.48 [2.83-9.34]
	3	5.59 [3.58-9.91]	6.32 [3.51-11.04]	12.71 [6.51-24.32]	6.61 [3.65-11.69]
Integral-Based Method	1	1.42 [0.59-3.18]	1.98 [0.92-3.84]	2.31 [1.03-4.12]	1.97 [0.90-3.81]
	2	1.81 [0.85-3.27]	1.48 [0.71-2.86]	2.04 [0.93-3.43]	1.55 [0.73-2.97]
	3	1.31 [0.68-2.36]	2.23 [0.95-4.95]	4.99 [2.14-8.59]	2.26 [0.96-5.11]

Continuous monitoring of K and the validation metrics, E_{static} and R_{static}, and, E_{rsIB} and R_{rsIB}, are shown for each Phases 1-3 in Figure 6.4-Figure 6.6 respectively. The corresponding airway pressure data is also shown. Trend comparison was assessed by trend correlation coefficient (R^2). Comparison between K and E_{static}, and, K and E_{rsIB}, for every available breathing cycle across all three phases is shown in Figure 6.7.

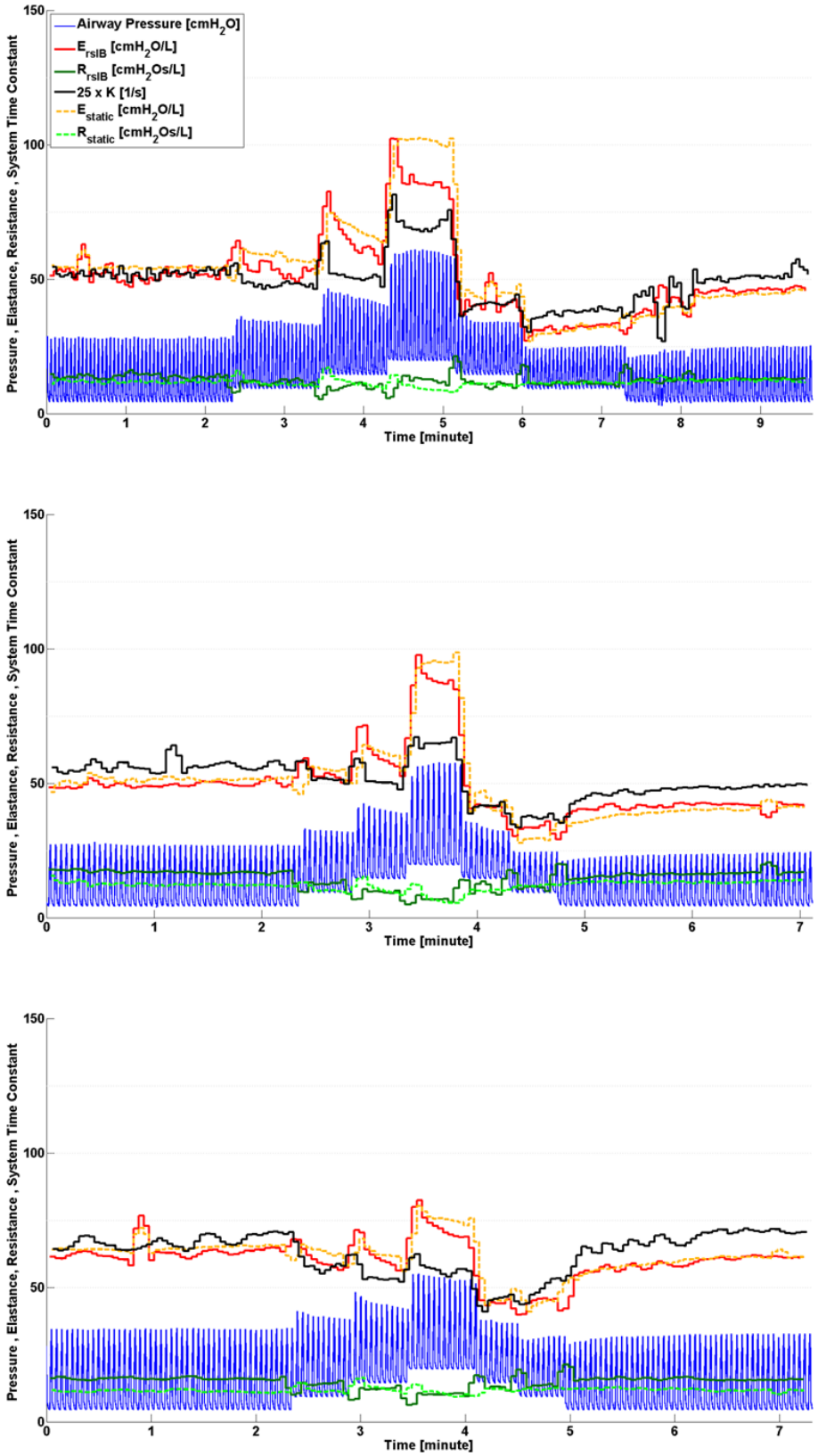

Figure 6.4 – Respiratory system mechanics monitoring during Phase 1, healthy state RM. (Top) Subject 1. (Middle) Subject 2. (Bottom) Subject 3. Values of *K* are scaled for clarity and serve only as an indication for trend comparison.

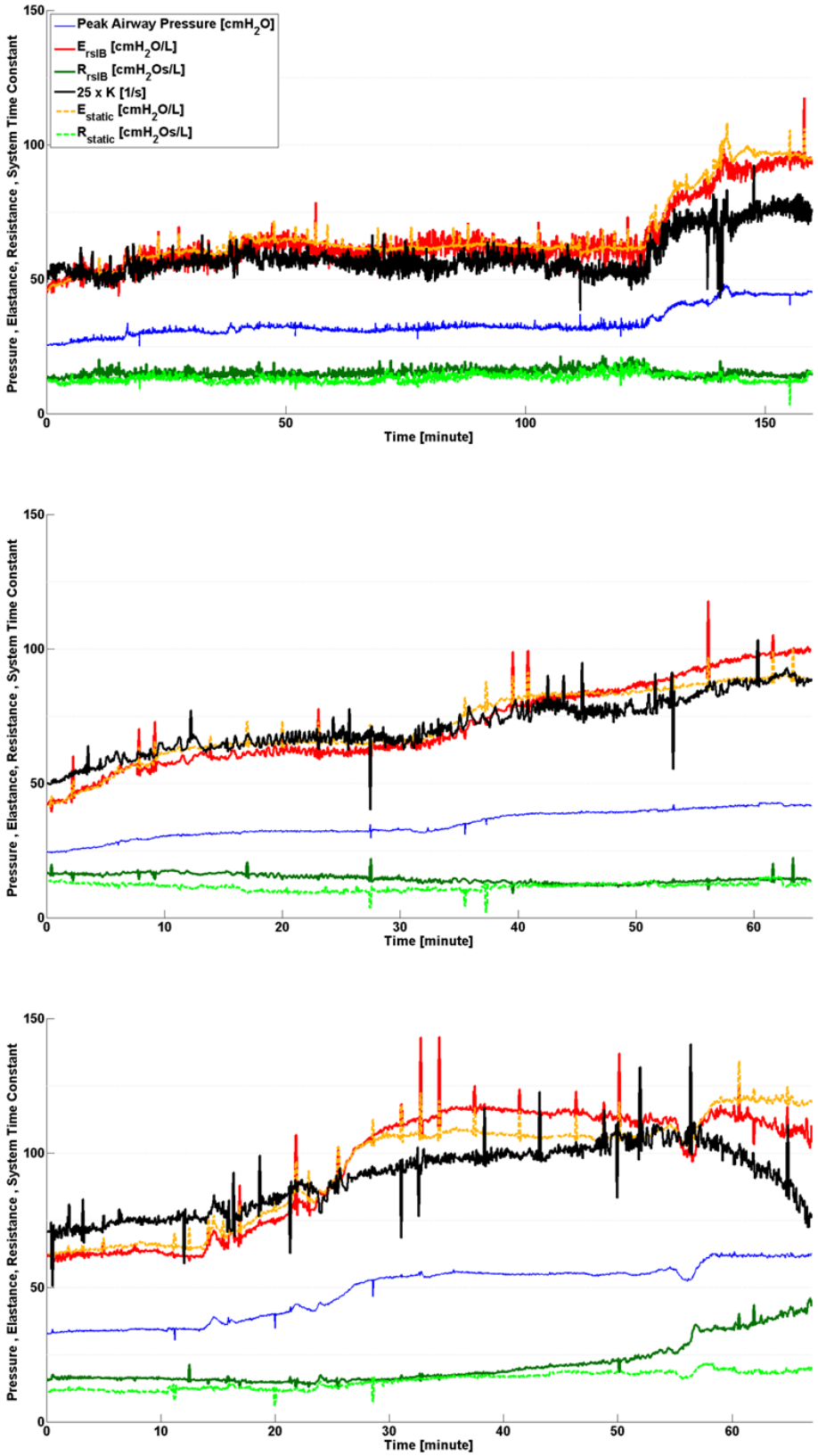

Figure 6.5 – Respiratory system mechanics monitoring during Phase 2, disease progression. (Top) Subject 1. (Middle) Subject 2. (Bottom) Subject 3. Values of *K* are scaled for clarity and serve only as an indication for trend comparison.

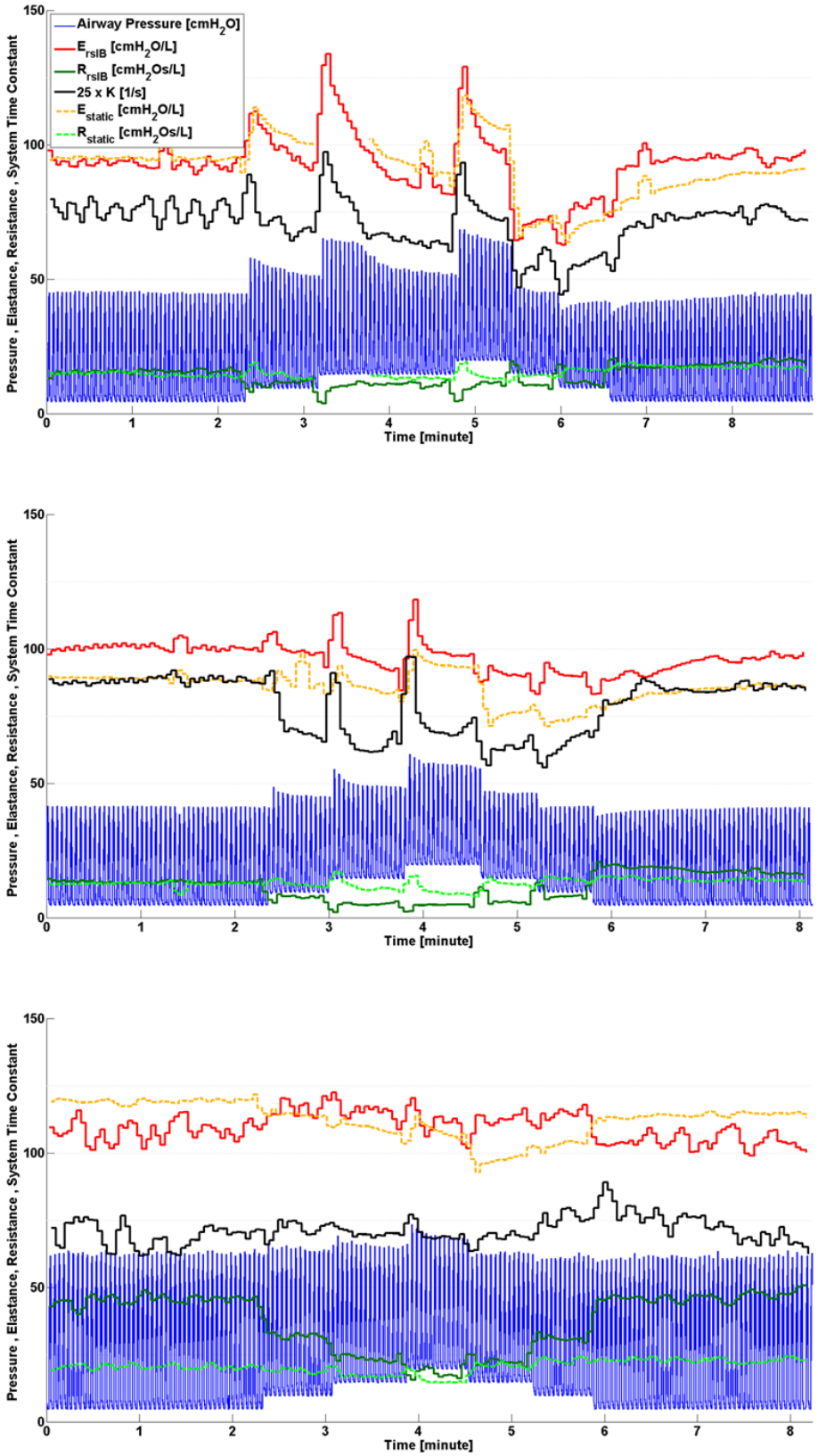

Figure 6.6 – Respiratory system mechanics monitoring during Phase 3, disease state RM. (Top) Subject 1. (Middle) Subject 2. (Bottom) Subject 3. Values of *K* are scaled for clarity and serve only as an indication for trend comparison.

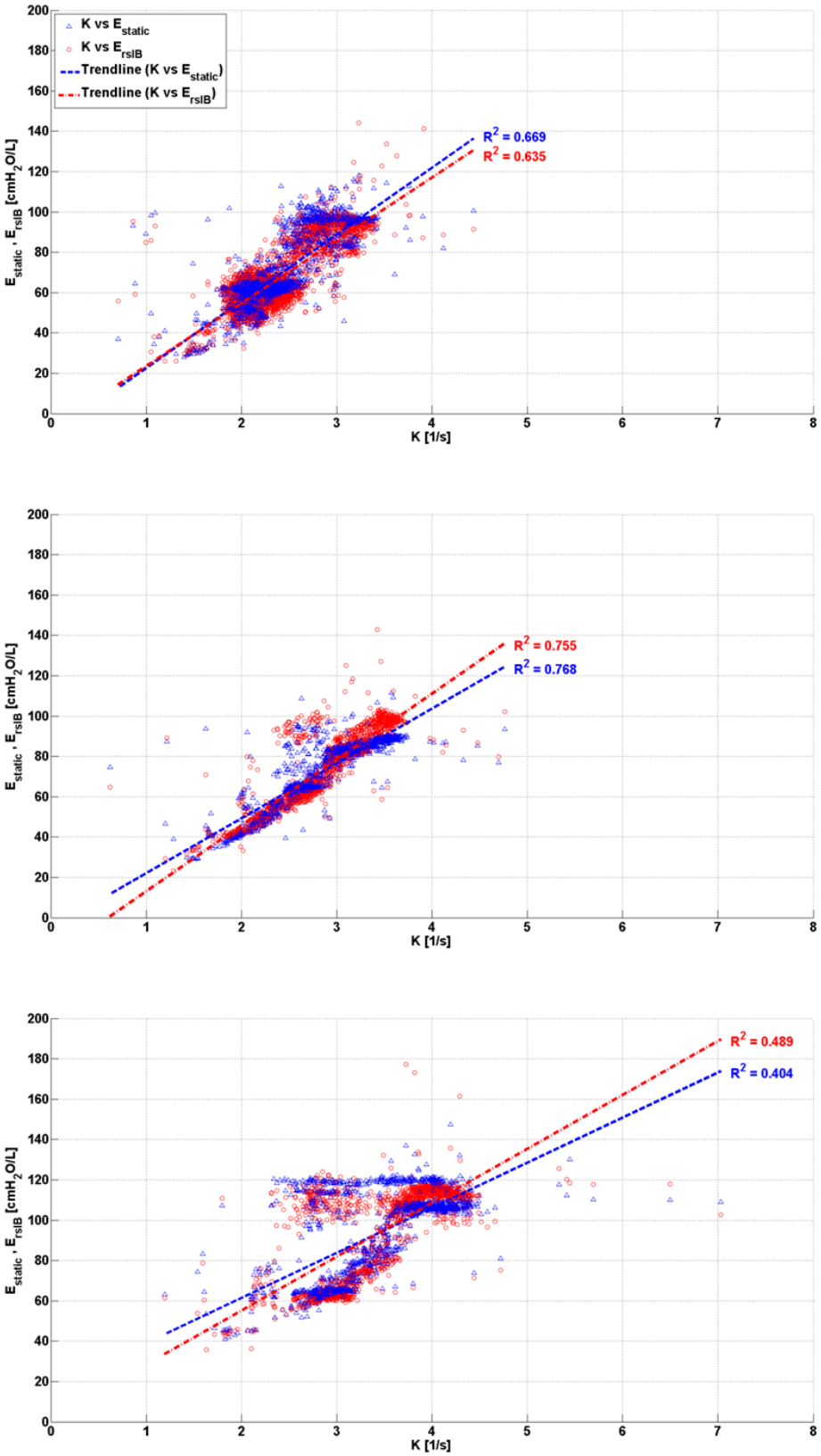

Figure 6.7 – Correlation between *K* and validation metrics E_{static} and E_{rsIB}. (Top) Subject 1. (Middle) Subject 2. (Bottom) Subject 3.

6.5 DISCUSSION

6.5.1 Phase 1 – Healthy State Recruitment Manoeuvre

K closely follows the trends of both E_{rsIB} and E_{static} for all three subjects, as shown in Figure 6.4. Both R_{rsIB} and R_{static} remain relatively constant across the RM, justifying the use of the lumped parameter, *K*, during this phase.

6.5.2 Phase 2 – Disease Progression

Inter-subject differences in ARDS progression over time can be seen in Figure 6.5, and indicate a variable response to oleic acid to induce ARDS, as well as a variable response to MV for each subject (Schuster, 1994, Ware, 2008, Bastarache and Blackwell, 2009, Ballard-Croft et al., 2012). After oleic acid injection, E_{rsIB}, E_{static}, and *K* in Subjects 1 and 2 all follow similar trends. Each parameter shows a slow increase, followed by a rapid increase as ARDS develops and the lungs become stiffer (Gattinoni and Pesenti, 2005, Chiew et al., 2012a). However, in Subject 3, the trend of *K* does not follow either E_{rsIB} or E_{static}. This lack of correlation may be a subject-specific response due to the increasing severity of ARDS collapsing airways within the lungs, thereby increasing the resistance of the conducting airways (Gattinoni and Pesenti, 2005). Since $K = E_{rs}/R_{rs}$, an increasing airway resistance would result in a decreasing *K*, consistent with that shown in Figure 6.5. In addition, because R_{rs} is found to vary for Subject 3, no information about E_{rs} can be directly gained from *K* during this phase. This result highlights the importance of the assumption of constant airway resistance for accurate tracking of disease progression when using this method.

6.5.3 Phase 3 – ARDS State Recruitment Manoeuvre

Subject-specific responses during Phase 3 vary significantly as shown in Figure 6.6. Subject 1 has the highest variation in E_{rsIB}, E_{static}, and *K*, while Subject 3 does not show any significant change in either E_{rsIB} or *K*. Trends of E_{rsIB}, E_{static}, and *K* for both Subject 1 and Subject 2 agree, and show a definite response to the RM. Subject 3, and to a lesser extent Subject 2, show a decrease in R_{rsIB} during increasing PEEP titration and an increase in R_{rsIB} during decreasing PEEP titration, suggesting that increasing PEEP is responsible for opening airways (Mols et al., 2001, Carvalho et al., 2007, Suarez-Sipmann et al., 2007). This change of airway resistance indirectly affects the estimated parameters determined by the integral-based method. Furthermore, Subject 3 has the highest PIP across all three phases. This is because a higher inspiratory pressure is required to counter the effect of a larger body mass. However, Subject 3 also has the highest severity of ARDS, as presented in Table 6.2 by a lower PaO_2/FiO_2 (PF ratio). Thus, it is possible that factors aside from variations in R_{rs} may influence the response. This significant inter-subject variability highlights the need for a patient-specific model-based approach.

Table 6.2 – Body mass and PF ratio (Phase 3) for each subject.

Subject	Mass [kg]	PaO_2/FiO_2 (Phase 3) [mmHg]
1	24.0	126.6
2	20.3	183.6
3	29.6	113.6

During PEEP titration in Phase 3, E_{rsIB}, E_{static}, and *K* drop to an overall minimum at a specific PEEP for each subject (PEEP = 15 cmH_2O for Subject 1, PEEP = 10-15 cmH_2O for Subject 2 and PEEP = 15-20 cmH_2O for Subject 3). Because recruitment is a function of

PEEP and time (Albert et al., 2009, Barbas et al., 2005), true minimum E_{rsIB}, E_{static}, and K can only be determined after a stabilisation period at each PEEP level. Decrease of elastance over time to a specific minimum can be described by increasing recruitment and/or the lung's viscoelastic properties, causing hysteresis (Ganzert et al., 2009, Andreassen et al., 2010). Setting PEEP at minimum elastance theoretically benefits ventilation by maximising recruitment, reducing Work of Breathing (WoB) and avoiding overdistension (Carvalho et al., 2007, Suarez-Sipmann et al., 2007, Lambermont et al., 2008, Zhao et al., 2010a). Furthermore, decreasing PEEP titration results in lower overall E_{rsIB}, E_{static}, and K compared to increasing PEEP titration, as shown in Figure 6.6. When PEEP is increased to a higher level, recruitment, as well as potential lung overstretching, occurs. However, after PEEP is reduced, the lung remains more compliant, as expected clinically after such a RM.

6.5.4 Trend Comparison

From Figure 6.7, it can be seen that Subject 3 has the lowest correlation coefficients across both validation metrics, while Subject 2 has the highest correlation coefficients as expected from observation of Figure 6.4-Figure 6.6. In this study, Subject 3 had the largest body mass and reached the highest severity of ARDS while Subject 2 had the lowest body mass and reached the lowest severity of ARDS. Thus, it is possible that increased body mass and/or severity of ARDS may influence the physiological process of expiration, leading to a lower observed correlation between K and the elastance validation metrics. However, due to the small number of subjects in this study, this conclusion is limited in its impact and thus warrants further investigation.

6.5.5 Outcomes

The overall median fitting error of the expiratory time-constant model is comparable to that obtained using the EIP method. However, variations in R_{rs} may lead to a lower correlation between K and E_{rs}. Based on the results of the integral-based method, it was found that airway resistance varies in Subject 3 during Phase 2 and Subjects 2 and 3 during Phase 3. Thus, a larger study cohort is required to further validate this method. However, it should be noted that if airway resistance is varying, it can be identified and accounted for. In general, the expiratory time-constant model was able to provide clinically relevant physiological insight not readily available at the bedside to guide MV therapy.

Spontaneously breathing patients have individual breathing efforts aside from ventilator support (Grinnan and Truwit, 2005), significantly altering the lung mechanics. In this case, oesophageal pressure measurements are required to determine patient-specific lung mechanics during inspiration (Bates, 2009). However, this technique is considered uncomfortable for the patient and its application is limited in daily monitoring, despite its potential to guide MV (Talmor et al., 2008, Khirani et al., 2010). Expiration is hypothesised to be primarily or completely passive, regardless of whether the patient is sedated or spontaneously breathing. Thus, muscle activity is assumed to be absent or relatively minimal (Grinnan and Truwit, 2005, Al-Rawas et al., 2013). Therefore, one potential application of the expiratory time-constant model is to determine real-time lung parameters for spontaneously breathing patients without additional measuring tools, expanding the clinical applicability of a model-based approach to guiding PEEP selection. Thus, application of the

expiratory time-constant model in tracking lung mechanics in spontaneously breathing patients warrants further investigation.

6.5.6 Limitations

The EIP method may be erroneous when the automated EIP is too short and does not allow the PIP to drop to the true P_{plat} (Barberis et al., 2003). In addition, this simple two-point, static approach may be too simplistic to capture some finer aspects of lung mechanics. Hence, no elastance metric is necessarily a gold standard. This study is predominantly based on the comparison of trends where each subject is their own reference. Thus, the best validation of a model is the ability to track clinically expected trends.

The estimation of airway resistance and the effect of ARDS on this parameter may be limited. Airway collapse alters airway resistance (Mols et al., 2001, Carvalho et al., 2007, Suarez-Sipmann et al., 2007, Chiew et al., 2011). However, this change is less significant compared to changes in lung elastance due to alveolar collapse. A collapsed airway will not have air entering and thus, airway resistance on expiration will not exist. Equally, a nearly closed airway will have higher airway resistance. Both hypotheses are potential effects from ARDS, but result in contradiction.

The clinical merit of *K* relies on the assumption that R_{rs} remains constant throughout therapy. Significant variation in R_{rs} will result in a poor correlation between *K* and E_{rs}. However, the

degree to which R_{rs} varies with PEEP and disease state was different for each subject in this study. A larger cohort may provide more consistency.

The expiratory time-constant model may not accurately capture regional differences in mechanical properties (Bates, 2009). Passive expiration could be more accurately modelled using a bi-exponential function, combining the effects of a slower and a faster time-constant, to effectively model each lung separately (Chelucci et al., 1993, Chelucci et al., 2005, Bates, 2009). However, each time-constant cannot be uniquely distinguished. Thus, this method cannot track disease progression within each lung separately, limiting its potential for use in the ICU.

6.6 SUMMARY

Expiratory data is normally neglected when determining conventional metrics of lung mechanics. However, the expiratory time-constant model parameter (*K*) provides an alternative means to track changes in disease state throughout therapy. Setting PEEP at minimum elastance, i.e. minimum *K*, theoretically provides optimal patient-specific PEEP. The expiratory time-constant model demonstrates potential for continuous monitoring of lung mechanics as disease state progresses. In particular, the trends obtained using the expiratory time-constant model generally match those obtained using the EIP method and the integral-based method. However, the assumption of constant R_{rs} leads to less physiological insight.

These are the first results to track and identify clinically relevant and expected breath-to-breath pulmonary mechanics throughout a clinical RM. Such tracking offers insight beyond the metrics and methods presented. Overall, further research is required to confirm the use of such real-time methods in actual ARDS patients, both sedated and spontaneously breathing. However, the ability to identify and track clinically relevant responses to disease progression and MV in real-time shows significant new potential.

Chapter 7 – Model-Based dFRC

7.1 INTRODUCTION

This chapter presents and evaluates four model-based methods of estimating the level of PEEP induced Functional Residual Capacity (FRC) change, known as dynamic FRC (dFRC). Recruitment models provide insight into the recruitment status of the lungs. Thus, determining when maximum recruitment occurs provides an alternative metric for use in guiding optimal PEEP selection. All four methods are assessed based on their predictive capability using three separate clinical and experimental data cohorts. The bulk of this work has been published as a journal article (van Drunen et al., 2013a).

7.2 BACKGROUND

PEEP improves gas exchange and ensures pulmonary volume above FRC, the pulmonary gas volume of the lungs at Zero End Expiratory Pressure (ZEEP), i.e. after normal expiration. Figure 7.1 shows a schematic of the lungs. An absolute value of FRC gives no information on the number of potentially recruitable lung units that are available. A lung with an FRC of 1.4 L could be the result of a lung with 1.4 L of fully recruited healthy lung units or 1.0 L of recruited lung plus an additional amount of recruited lung volume due to additional PEEP. Knowing this difference would allow PEEP to be optimised to maximise recruitment and ensure any increase in PEEP added recruited lung volume.

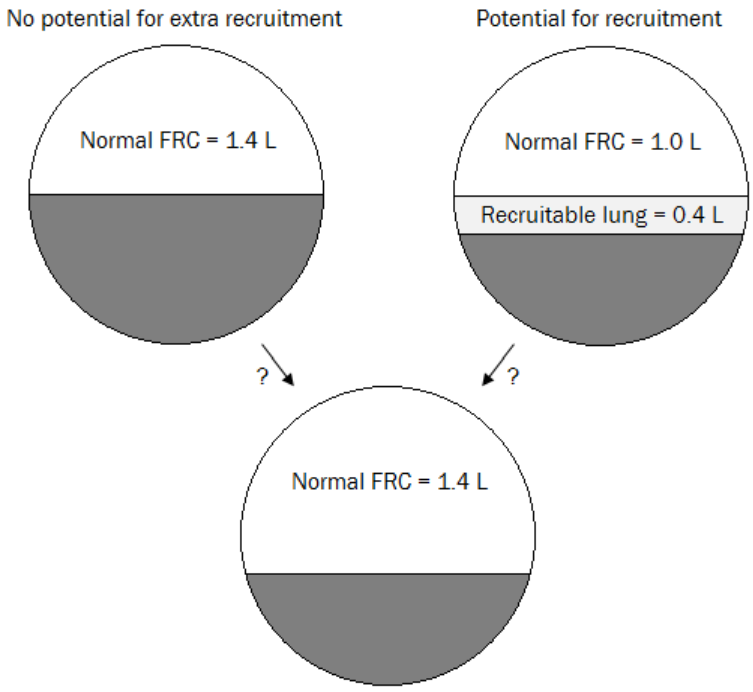

Figure 7.1 – Schematic showing the limitation of an absolute FRC value.

Currently, there are few methods of measuring FRC at the bedside. Gas washout/washin techniques are one method (Heinze et al., 2007), but are not necessarily available on most ventilators. FRC can also be measured by using chest imaging methods, such as Computed Tomography (CT) scans (Malbouisson et al., 2001) and Electrical Impedance Tomography (EIT) (Zhao et al., 2009, Zhao et al., 2010b). Timed at the end of expiration, the lung volume can be assessed at each CT or EIT slice and summed across all the slices to evaluate true lung FRC. However, this type of measurement is clinically and ethically unrealistic for regular use in guiding MV, or continuous monitoring in the ICU. Although specialised ventilators can measure FRC and re-estimate FRC following changes in PEEP (GE, Engstrom, Carestation ventilators), most standard ventilators cannot. Thus, there is motivation to estimate the PEEP induced FRC change to avoid further lung injury.

The level of additional lung volume due to additional PEEP is known as dynamic FRC (dFRC) (Sundaresan et al., 2011b) and is shown schematically in Figure 7.2. The ability to use standard ventilator data to simply and non-invasively estimate dFRC without interrupting MV therapy would be a significant potential enhancement in ventilation management. Although dFRC cannot by itself estimate the potential of lung recruitment, used with Arterial Blood Gas (ABG) measurements it can provide the clinician with useful information on lung recruitability as PEEP or other MV settings are modified. Thus, dFRC represents an aspect of the primary clinical endpoint in ventilation management, with the potential to be continuously tracked with changes in patient condition.

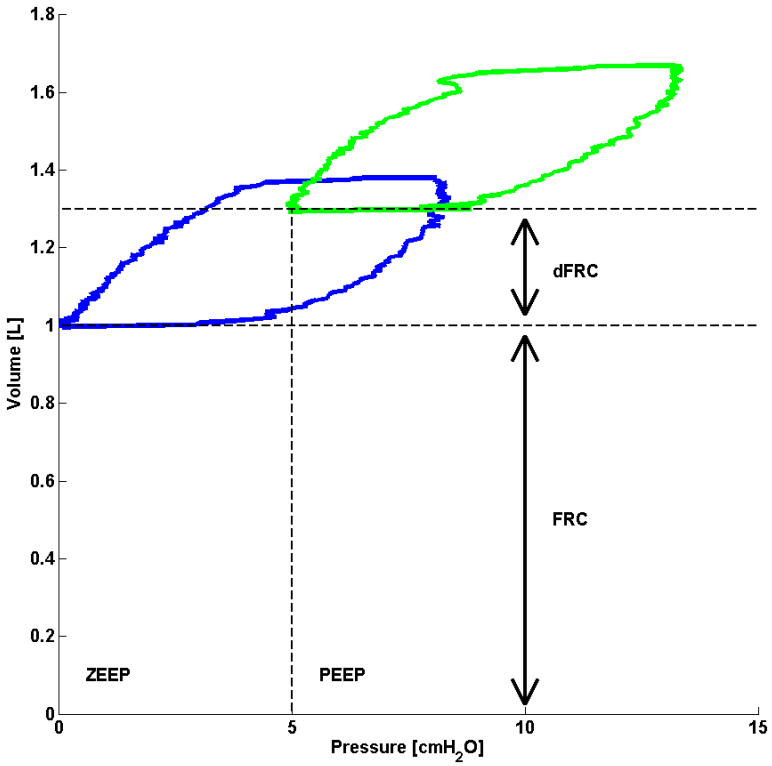

Figure 7.2 – Schematic showing the difference between FRC and dFRC.

7.3 MODEL SUMMARY

7.3.1 Stress-Strain Multiple Breath Method (SSMB)

Chiumello et al. (Chiumello et al., 2008) proposed a stress-strain theory of lung dynamics where transpulmonary pressure, ΔP_L, is defined as the clinical equivalent of stress. The clinical equivalent of strain is defined as the ratio of the change in volume, ΔV, to the FRC, yielding a stress-strain definition:

$$\Delta P_L(stress) = E_{L,spec} \times \frac{\Delta V}{FRC}(strain) \quad \textbf{Equation 7.1}$$

where the specific lung elastance, $E_{L,spec}$, can be defined as the transpulmonary pressure at which FRC doubles.

The relationship between the change in plateau airway pressure, ΔP_{aw}, and the corresponding ΔP_L is defined (Chiumello et al., 2008):

$$\Delta P_L = \Delta P_{aw} \times \alpha \quad \textbf{Equation 7.2}$$

$$\alpha = \frac{E_{lung}}{E_{lung} + E_{cw}} \quad \textbf{Equation 7.3}$$

where α represents the ratio of the lung elastance, E_{lung}, to the chest wall elastance, E_{cw}. The value of α indicates the severity of ARDS, where a larger value of α indicates a higher severity of ARDS (Gattinoni et al., 2004, Sundaresan et al., 2011b). Transpulmonary pressure is not typically measured at the bedside. Thus, it is estimated using the airway pressure, based on Equation 7.2.

At the beginning of inspiration, when airflow is zero, the airway pressure (i.e. PEEP) is equal to the plateau airway pressure. Thus, at this point, Sundaresan et al. (Sundaresan et al., 2011b) proposed that ΔP_{aw} = ΔPEEP, and ΔV = ΔdFRC. Combining Equation 7.1 and Equation 7.2, and substituting for ΔP_{aw} and ΔV, yields a formula for FRC:

$$FRC = \frac{\Delta dFRC}{\Delta PEEP} \times \frac{E_{L,spec}}{\alpha} \quad \textbf{Equation 7.4}$$

Equation 7.4 defines FRC as a function of the volume responsiveness of the patient to the specified change in PEEP, $E_{L,spec}$, and α of the patient. Sundaresan et al. hypothesised that dFRC follows a similar mathematical form to Equation 7.4:

$$FRC + dFRC = \frac{\Delta dFRC}{\Delta PEEP} \times \frac{E_{L,spec}}{\alpha}(1 + x) \quad \textbf{Equation 7.5}$$

Therefore, dFRC takes the form:

$$dFRC = \frac{\Delta dFRC}{\Delta PEEP} \times \frac{E_{L,spec}}{\alpha} x \quad \textbf{Equation 7.6}$$

where x is a function of the PEEP at which dFRC is estimated. $E_{L,spec}$, and α are relatively constant parameters (Chiumello et al., 2008) so can be combined into one unknown parameter, β, yielding:

$$dFRC = \frac{\Delta dFRC}{\Delta PEEP} \times \beta \quad \textbf{Equation 7.7}$$

The assumption that α is constant is true only for the linear portion of the static Pressure-Volume (PV) curve (Sundaresan et al., 2011b). The value of β for a single value of PEEP is

assumed constant across all patients. Because FRC is not known for any patient, β is analytically solved based on Equation 7.7 using measured dFRC values from the data. Once β values are evaluated for all patients at each PEEP, a median β is then evaluated at each PEEP to serve as a population constant for that PEEP. The dFRC is then estimated using Equation 7.7 and the median β value. The process can be summarised as follows:

1. Analytically solve Equation 7.7 to find β for all patients at each PEEP.
2. Evaluate the population based median β at each PEEP.
3. Estimate the dFRC using Equation 7.7 and the population based median β.

This method requires the patient to undergo a stepwise increase in PEEP to obtain multiple PV loops at different PEEPs prior to analysis.

7.3.2 Stress-Strain Single Breath Method (SSSB)

Mishra et al. (Mishra et al., 2012) proposed a model to estimate ΔdFRC using only PV data from a single PEEP. Once again, combining Equation 7.1 and Equation 7.2, and substituting $\Delta V = V_t$, yields a formula for FRC:

$$FRC = \frac{V_t}{\Delta P_{aw}} \times \frac{E_{L,spec}}{\alpha} \qquad \textbf{Equation 7.8}$$

where V_t is the tidal volume. Equation 7.8 defines FRC as a function of the volume responsiveness of the patient to the specified change in airway pressure observed during

inspiration, $E_{L,spec}$, and α of the patient. Mishra et al. hypothesised that ΔdFRC follows a similar mathematical form to Equation 7.8:

$$FRC + \Delta dFRC = \frac{V_t}{\Delta P_{aw}} \times \frac{E_{Lspec}}{\alpha}(1 + x) \quad \textbf{Equation 7.9}$$

Therefore, ΔdFRC takes the form:

$$\Delta dFRC = \frac{V_t}{\Delta P_{aw}} \times \frac{E_{Lspec}}{\alpha} x \quad \textbf{Equation 7.10}$$

Once again, combining x, $E_{L,spec}$, and α into one unknown parameter, β, yields:

$$\Delta dFRC = \frac{V_t}{\Delta P_{aw}} \times \beta \quad \textbf{Equation 7.11}$$

As with the SSMB method, the assumption that α is constant is true only for the linear portion of the static PV curve (Sundaresan et al., 2011b). The value of β for a single value of PEEP is assumed constant across all patients. Calculated β values are normalised by V_t as dFRC can vary with the applied V_t (Mishra et al., 2012).

$$\beta_1 = \frac{\beta}{V_t} \quad \textbf{Equation 7.12}$$

Values of β and ΔdFRC are calculated through the same approach outlined for the SSMB method.

7.3.3 Single Compartment Single Breath Method (SCSB)

The single compartment equation of motion describing the airway pressure as a function of the resistive and elastic components of the respiratory system for a fully sedated patient is defined (Bates, 2009):

$$P_{aw}(t) = R_{rs} \times Q(t) + E_{rs} \times V(t) + P_0 \quad \textbf{Equation 7.13}$$

where t is time, R_{rs} is the overall respiratory system resistance consisting of the series resistance of the conducting airways, Q is the volumetric flow rate, E_{rs} is the overall respiratory system elastance, V is the lung volume, and P_0 is the offset pressure.

An alternative method of estimating dFRC without the use of a population constant assumes P_0 is also the pressure to increase baseline FRC, as described in Chapter 4:

$$P_{aw}(t) = R_{rs} \times Q(t) + E_{rs} \times (V(t) + V_{P_0}) \quad \textbf{Equation 7.14}$$

where, V_{P_0} is the additional lung volume increase due to PEEP. Thus:

$$P_0 = PEEP = E_{rs} \times V_{P_0} \quad \textbf{Equation 7.15}$$

From Equation 7.14, V_{P_0} is expected to capture the change in FRC due to a change in PEEP. Thus, $V_{P_0} \propto$ dFRC and Equation 7.15 can be rearranged for V_{P_0}:

$$V_{P_0} = \frac{PEEP}{E_{rs}}$$ **Equation 7.16**

Equation 7.16 provides an alternative method of estimating dFRC using E_{rs} (Stenqvist et al., 2012).

The integral-based method (Hann et al., 2005) is used to estimate breath-specific values of respiratory system elastance (E_{rsIB}) and respiratory system resistance (R_{rsIB}) that best fit Equation 7.13:

$$\int P_{aw}(t) = R_{rsIB} \times \int Q(t) + E_{rsIB} \times \int V(t) + \int P_0$$ **Equation 7.17**

7.3.4 Combined Method (CM)

This model-based approach is intended for real-time use in the ICU. Initially, when data at only one PEEP is available, the model relies on the SSSB analysis (Mishra et al., 2012). As additional higher PEEPs are introduced throughout the course of care, the model converts from SSSB to SSMB analysis (Sundaresan et al., 2011b). Therefore, the model can predict dFRC at any PEEP with the potential advantage of increasing accuracy as different PEEPs are progressively introduced throughout the course of care. This approach presents a non-invasive method that utilises all available and prior data, and aims to combine the higher accuracy of the SSMB method with the higher clinical feasibility of the SSSB method.

7.4 MODEL VALIDATION

7.4.1 Clinical and Experimental Data:

The models are assessed using retrospective clinical and experimental data. In this chapter:

1. **Cohort 1**: Clinical data from 10 patients (Sundaresan et al., 2011a).
2. **Cohort 2**: Clinical data from 10 patients (Bersten, 1998).
3. **Cohort 3**: Experimental data from 9 animal subjects (Chiew et al., 2012a).

The demographics and cause of ARDS for all patients and subjects, and the associated protocols, are described in detail in Chapter 3. For Cohorts 1 and 3, the dFRC was measured during post-processing of the volumetric flow rate data obtained by a pneumotachometer. The difference in volumetric flow rate across a PEEP change was used to determine dFRC. For Cohort 2, the dFRC was measured directly by deflation to ZEEP at the end of a breathing cycle for each PEEP.

7.4.2 Analysis

The estimated dFRC is compared with the clinically measured dFRC to determine the estimation error over each method and cohort. Performance is assessed by trend correlation coefficient (R^2), where comparisons between measured and estimated values are made. The maximum, minimum, median and Inter-Quartile Range (IQR) are used as summary statistics. The accuracy of each method is compared and evaluated in relation to the other methods.

7.4.3 Stress-Strain Multiple Breath Method (SSMB)

The β values determined for each data cohort are presented in Table 7.1.

Table 7.1 – Median β values [cmH_2O].

PEEP [cmH_2O]	0	5	7	10	12	15	20	25	30
Cohort 1	-0.0026	3.0287	-	7.4455	-	12.613	18.169	23.821	28.731
Cohort 2	0.4825	4.4890	6.5108	9.3080	11.790	13.797	-	-	-
Cohort 3	-	0.0301	-	3.7004	-	8.7759	14.961	-	-

The linear trend in measured dFRC versus estimated dFRC across all PEEPs, and the associated error for each cohort, is shown in Figure 7.3. Values of R^2 are given, $R^2(i)$, for all three cohorts i = 1, 2, 3 separately and combined.

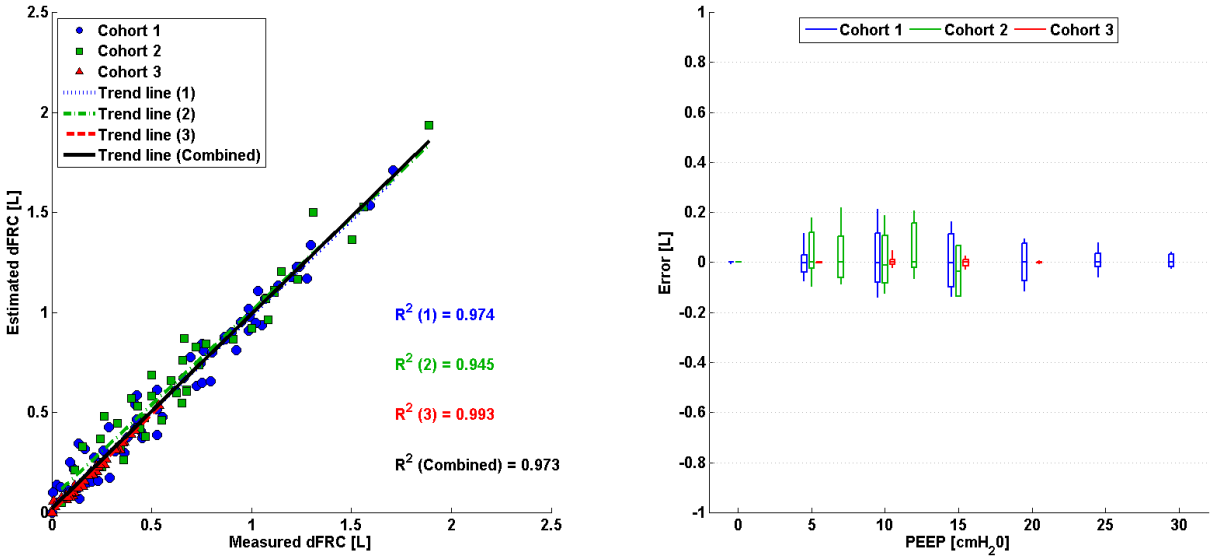

Figure 7.3 – SSMB: (Left) Plot of measured dFRC vs. estimated dFRC for each cohort. (Right) Box plot of errors between measured dFRC and estimated dFRC for each cohort.

7.4.4 Stress-Strain Single Breath Method (SSSB)

The β_1 values determined for each data cohort are presented in Table 7.2.

Table 7.2 – Median β_1 values [cmH$_2$O/mL].

PEEP [cmH$_2$O]	0	5	7	10	12	15	20	25	30
Cohort 1	0.0000	0.0081	-	0.0206	-	0.0348	0.0586	0.0802	0.0872
Cohort 2	0.0015	0.0140	0.0241	0.0362	0.0611	0.0796	-	-	-
Cohort 3	-	0.0000	-	0.0357	-	0.0829	0.1564	-	-

The linear trend in measured dFRC versus estimated dFRC across all PEEPs, and the associated error for each cohort, is shown in Figure 7.4. Values of R^2 are given, $R^2(i)$, for all three cohorts i = 1, 2, 3 separately and combined. Values of R^2 are also given for the cases where outlying patients have been excluded.

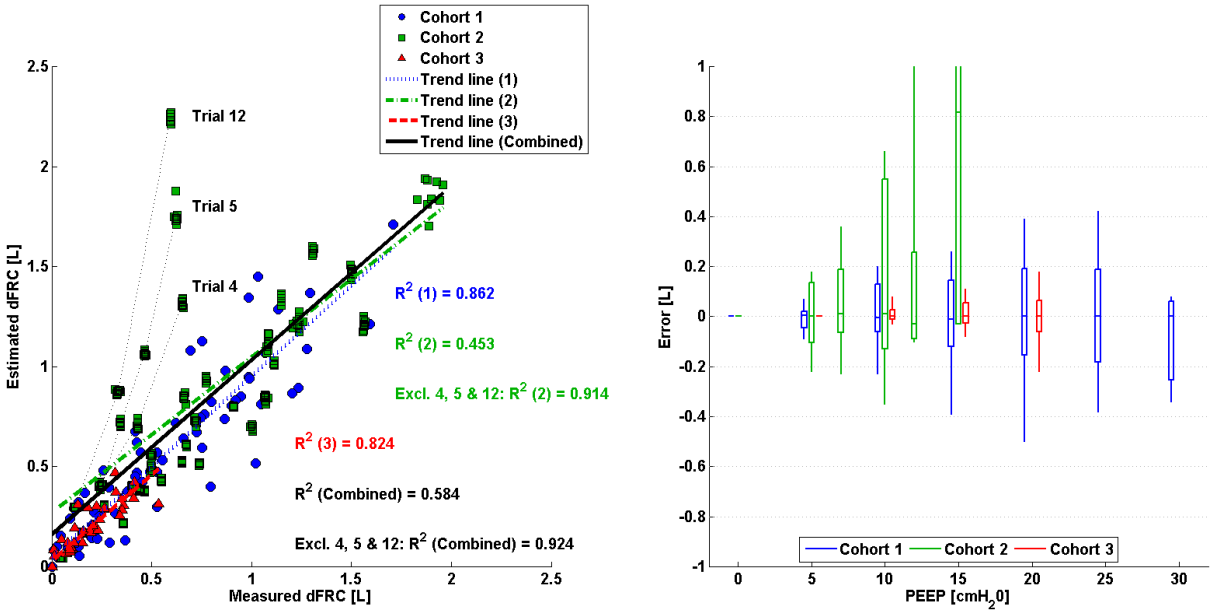

Figure 7.4 – SSSB: (Left) Plot of measured dFRC vs. estimated dFRC for each cohort. Patient specific trends are indicated for the cases of significant overestimation. (Right) Box plot of errors between measured dFRC and estimated dFRC for each cohort. Errors larger than ± 1 L are truncated for clarity.

7.4.5 *Single Compartment Single Breath Method (SCSB)*

The linear trend in measured dFRC versus estimated V_{P_0} across all PEEPs, and the associated error for each cohort, is shown in Figure 7.5. Values of R^2 are given, $R^2(i)$, for all three cohorts i = 1, 2, 3 separately and combined.

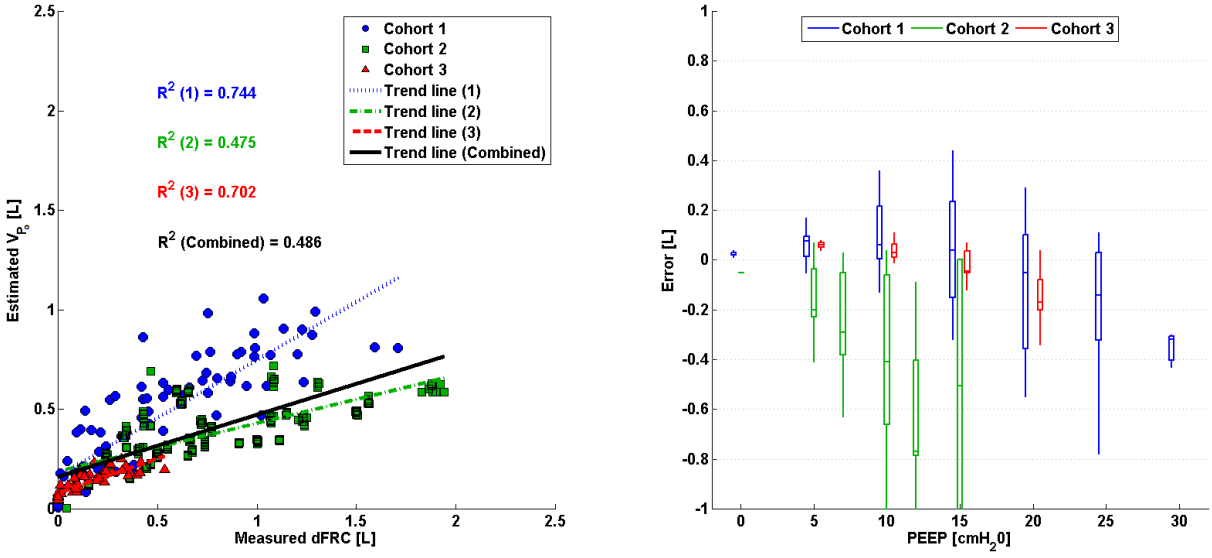

Figure 7.5 – SCSB: (Left) Plot of measured dFRC vs. estimated V_{P_0} for each cohort. (Right) Box plot of errors between measured dFRC and estimated V_{P_0} for each cohort. Errors larger than ± 1 L are truncated for clarity.

7.4.6 *Combined Method (CM)*

The linear trend in measured dFRC versus estimated dFRC across all PEEPs, and the associated error for each cohort, is shown in Figure 7.6. Values of R^2 are given, $R^2(i)$, for all three cohorts i = 1, 2, 3 separately and combined.

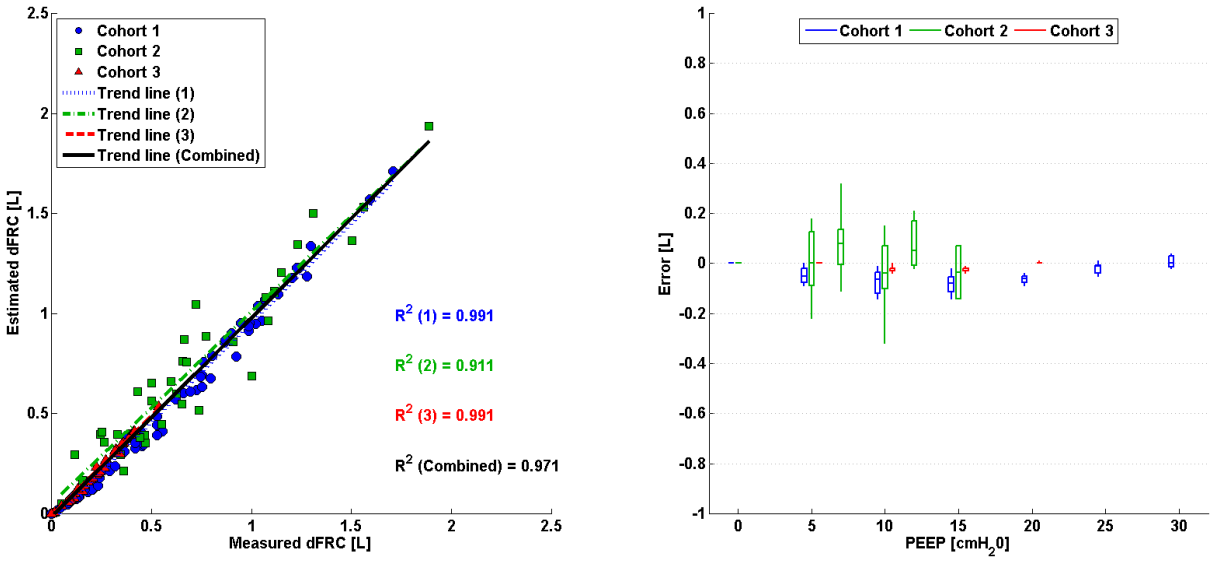

Figure 7.6 – CM: (Left) Plot of measured dFRC vs. estimated dFRC for each cohort. (Right) Box plot of errors between measured dFRC and estimated dFRC for each cohort.

7.4.7 Summary

Table 7.3 presents a summary of the correlation coefficients for each method and cohort.

Table 7.3 – Summary of trend correlation coefficients (R^2) for each method and cohort. Low R^2 values are shown in red while high R^2 values are shown in green.

	Cohort 1	Cohort 2	Cohort 3	Overall coefficient
SSMB	0.974	0.945	0.993	0.973
SSSB	0.862	0.453	0.824	0.584
SCSB	0.744	0.475	0.702	0.486
CM	0.991	0.911	0.991	0.971

7.5 DISCUSSION

7.5.1 Stress-Strain Multiple Breath Method (SSMB)

There exists a strong, sustained linear trend in measured dFRC versus estimated dFRC over all PEEPs and a wide range of dFRC for each cohort. Auto-PEEP, present in some patients from Cohort 1, may affect the correlation coefficient for that cohort. Auto-PEEP has the effect of a sudden change in the level of recruitment (ΔdFRC) once the PEEP becomes greater than the auto-PEEP, as shown in Figure 7.7 for an auto-PEEP of 7 cmH_2O. Although Cohort 1 contains patients with auto-PEEP, the median error, as shown in Figure 7.3, is consistently small across all PEEPs indicating no inherent tendency for overestimation or underestimation.

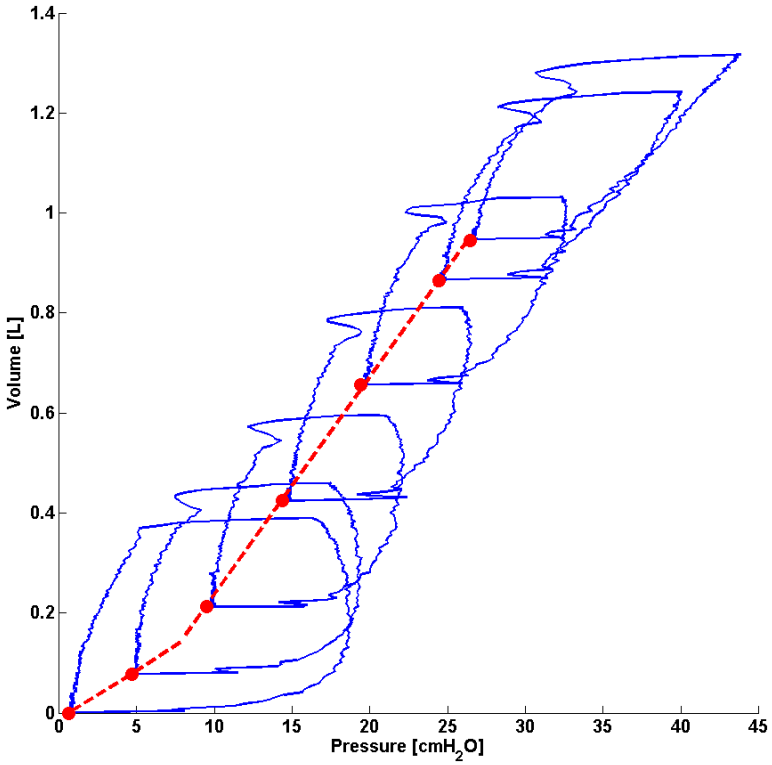

Figure 7.7 – PV loops for patient 1 (Cohort 1) indicating a change in the compliance (1/elastance) trend at an auto-PEEP of 7 cmH_2O.

A significant drawback with this method is that it assumes a linear compliance (1/elastance) trend across all PEEPs which may not hold true for cases where auto-PEEP is present, or at high PEEP where overdistension can occur. Another limitation with this model is that it requires PV data from at least two PEEPs so it cannot be used for continuous tracking of dFRC. Thus, its application in real-time dFRC measurement is limited without interrupting MV therapy.

7.5.2 Stress-Strain Single Breath Method (SSSB)

The SSSB method proposed by Mishra et al. (Mishra et al., 2012) and applied to Cohort 2 results in the lowest overall correlation coefficient in the study. This result is specifically due to the trends of Trials 4, 5 and 12, as shown in Figure 7.4, where the error reaches as high as 1.66 L. This large error is caused by two factors:

1. All three trials exhibit a relatively low compliance (high elastance) trend when compared to the majority of other trials in the cohort, resulting in a lower calculated β_1 value. The population constant β_1 value is calculated as the median of all β_1 values at a given PEEP. Hence, a significantly higher median β_1 value is, in turn, applied to these patients, resulting in error.
2. Several other trials also exhibit reasonably low compliance (high elastance) trends, but did not result in overestimation. This difference in outcome occurs because values of β_1 are normalised by V_t. Generally, Trials 4, 5 and 12 have a

higher V_t compared to other trials exhibiting the same trend in compliance (1/elastance).

Combined, these two factors result in considerable overestimation of dFRC for these three trials, potentially highlighting a significant limitation with this method. No patient-specific or case-specific factor could be identified as the root cause of this difference. However, it should be noted that measurements for patients in Cohort 1 and subjects in Cohort 3 were obtained with no prior recruitment manoeuvre or stabilisation and had a far higher R^2 value of 0.862 and 0.824 respectively, as presented in Table 7.3. In contrast, patients in Cohort 2 were recruited and stabilised at each PEEP for 30 min. Thus, as a result, patients in Cohort 2 may see a higher V_t despite low compliance (high elastance), which is a scenario not typically seen clinically.

An advantage of the SSSB method over the SSMB method is that a unique value of β_1 is determined at each PEEP, which is independent of lung behaviour at other PEEPs. Thus, values of β_1 can account for the natural sigmoid shape of a patients' volume responsiveness to PEEP. This outcome is important for cases where auto-PEEP is present, or at high PEEP, where unintended overdistension can occur.

A disadvantage of the SSSB method is that the calculated values of β_1 are dependent on the method of data measurement. As previously mentioned, patients in Cohort 2 were stabilised prior to measurement while those in Cohort 1 were not. Thus, the β_1 values obtained from

Cohorts 1 and 2 diverge as PEEP increases, as shown in Figure 7.8. Thus, combining both human cohorts and determining new values of median β_1 would result in poorer dFRC estimation.

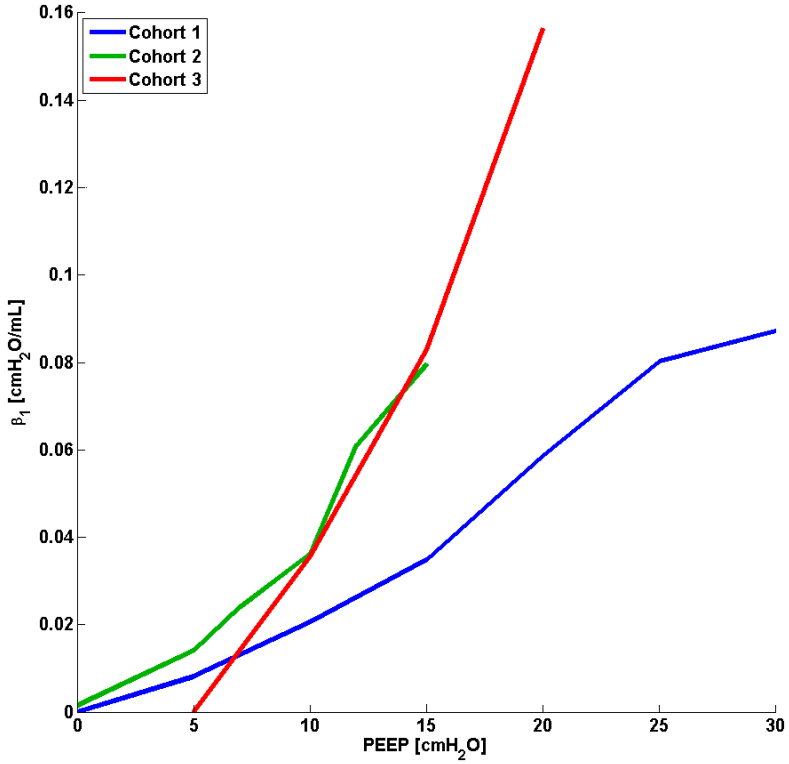

Figure 7.8 – Values of β_1 for each cohort. The lowest available PEEP in each cohort provides the reference PEEP for that cohort.

7.5.3 Single Compartment Single Breath Method (SCSB)

The correlation coefficients observed in Figure 7.5 and Table 7.3 for the SCSB method indicate a possible linear relationship between measured dFRC and estimated V_{P_0}, indicating that V_{P_0} may be linearly related to dFRC. This relationship is based on the assumption that E_{rs} is the same in both Equation 7.13 and Equation 7.14. If this assumption is valid, it would be expected that for each patient/subject, a strong correlation would result between the E_{rs} calculated using Equation 7.13, and the E_{rs} calculated using Equation 7.14, where the

measured dFRC is substituted for V_{P_0}. For both cases, the integral-based method is used to estimate breath-specific values of respiratory system elastance (E_{rsIB}) and respiratory system resistance (R_{rsIB}) that that best fit each equation. The scatter in Figure 7.9, for patients in Cohort 1, suggests that the assumption of identical E_{rs} may not be fully justified, leading to estimation errors in the calculation of V_{P_0}.

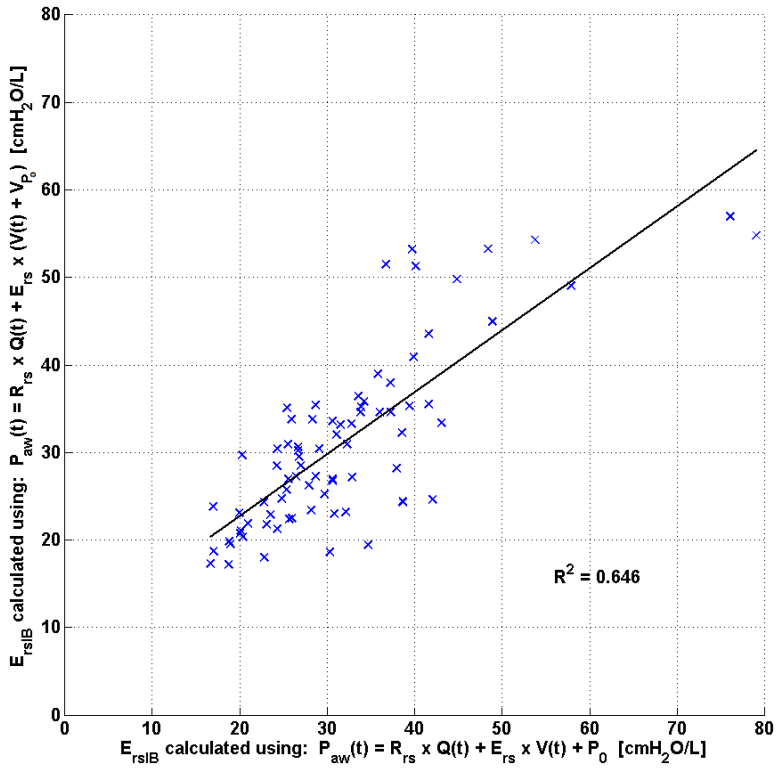

Figure 7.9 – Comparison between E_{rsIB} when calculated using Equation 7.13 and Equation 7.14 for all patients in Cohort 1.

The error in V_{P_0} across a range of PEEPs can be seen in Figure 7.10 where the individual patient specific trends between measured dFRC and estimated V_{P_0} from Cohort 1 in Figure 7.5 have been highlighted. The relationship is seen to be non-linear with a concave response as PEEP, and consequently dFRC, increase. However, it is possible that some normalisation of the data may correct for this effect.

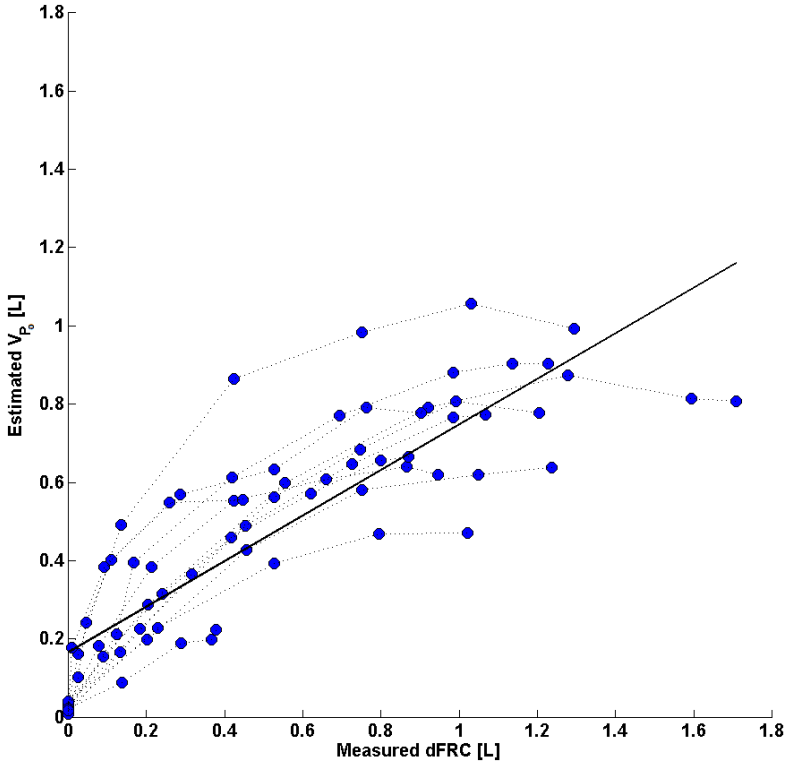

Figure 7.10 – Patient specific trends in Cohort 1 between measured dFRC and estimated V_{P_0} for all patients and PEEPs. Patient specific trends are indicated to show general non-linearity.

7.5.4 Combined Method (CM)

The CM incorporates the higher linear correlation coefficient observed with the SSMB method with the clinical applicability of the SSSB method. Because the combined method considers a progressive increase in the number of available PEEPs, it can manage changes in compliance (1/elastance) with less error than the SSMB method alone, which assumes linear compliance (linear elastance) across all PEEPs, as well as versus the single breath methods. Overall, this approach is clinically feasible, practical and accurate for the range of clinically acceptable PEEPs seen in application.

7.6 SUMMARY

Four model-based methods are evaluated based on their capability of estimating dynamic FRC (dFRC) for mechanically ventilated ARDS patients and experimental ARDS subjects. By using non-invasive model-based approaches, dFRC can be tracked continuously as it changes with the evolution of the disease. Evaluating the potential of recruitable lung volume may help to determine the optimal PEEP required during MV. The models can be implemented in the ICU without the need for clinically and ethically unrealistic methods such as CT scans.

The proposed methods have limitations in their predictive capability, since in some cases the error observed between the measured and estimated values is exceptionally large. In particular, auto-PEEP has the potential to affect the accuracy of the models. However, it can be detected directly from PV loop responses and thus managed. The CM is found to be the optimal method to estimate dFRC for real-time application.

Chapter 8 – Conclusions and Clinical Potential

8.1 INTRODUCTION

MV is one of the most common treatments in the ICU, with significant implications for both patient mortality and cost of treatment. However, the major problem with MV lies with the lack of standardised protocols, resulting in variable ventilator settings that are strongly dependent on the experience and intuition of the clinicians. Therefore, there is a clear need to determine optimal patient-specific MV therapy that can provide the greatest benefit to the patient at the lowest risk.

This thesis presented several unique and physiologically relevant models and model-based methods to provide clinically useful information that captures patient-specific lung condition and response to PEEP. The models provided rapid parameter identification, while retaining important physiological information, and were validated using data from clinical ICU patients and experimental ARDS animal models. These model-based approaches show potential to be used as a diagnostic tool at the bedside in the ICU.

Chapter 4 presented a single compartment lung model and investigated its ability to capture parameters of respiratory mechanics. This fundamental model provided the basis for several of the models and model-based methods presented throughout this thesis, allowing in-depth understanding of patient-specific response to PEEP, and disease state evolution over time.

Chapter 5 presented a novel method of mapping and visualising dynamic respiratory system elastance (E_{drs}), providing significantly more insight into dynamic lung behaviour than can be provided by a single average value of respiratory system elastance (E_{rs}). Simultaneous mapping of elastance, both within a breath and throughout the course of care, provides a new perspective to guide therapy. The clinical potential of E_{drs} mapping requires a compromise between physiological accuracy and clarity. However, the trends obtained in this study matched clinical expectations, providing unique insight into the heterogeneous response of the ARDS affected lungs to PEEP.

Chapter 6 presented a method of using only the expiratory portion of the breathing cycle to estimate a parameter (*K*) hypothesised to be a proxy for lung elastance. *K* provides an alternative means to track changes in respiratory mechanics throughout therapy and showed a high correlation with estimates of lung elastance obtained using alternative methods. Thus, the expiratory time-constant model shows potential for continuous, real-time monitoring of breath-to-breath pulmonary mechanics as disease state progresses. Furthermore, the model shows potential to be used on spontaneously breathing patients.

Chapter 7 evaluated four model-based methods on their capability of estimating dynamic Functional Residual Capacity (dFRC). Evaluating the potential of recruitable lung volume aids optimal PEEP selection. The models enable dFRC to be tracked continuously as it changes with the evolution of the disease. Based on a variety of clinical and experimental datasets, the Combined Method (CM) was found to provide the optimal balance between predictive capability and real-time bedside application in the ICU.

8.2 CLINICAL POTENTIAL

The models presented in this thesis represent the first steps into a potential future clinical practice. Results indicate that these models have the potential to be used to guide MV decision making in the ICU, providing a consistent path to standardise PEEP selection. In particular, this type of "next-generation" care would provide a quantitative, patient-specific foundation for much more consistent clinical decision making.

A model-based approach to guiding MV therapy is not necessarily intended to override the human component of clinical decision making in the ICU. Rather, models aim to provide an alternative perspective, or second opinion, to reassure a clinician's decision. Thus, a model-based approach to MV therapy is intended to support clinical decision making as there may be many other factors involved with such decisions. Clinicians will always have the ability to ignore a model-based recommendation if it is deemed necessary, but equally, typical cases may become far more automated.

Each lung model uses different physiological principles to determine metrics to guide PEEP selection. However, fundamentally, all of these models essentially monitor trends in patient condition throughout the course of care. Thus, simultaneous application of all available models will provide a more robust system, where the recommendation of each model can be validated against the recommendations of the other models. Equally, since each model provides a slightly different perspective, the range of recommendations, while narrow, would provide clinicians with an acceptable foundation range within which to set PEEP.

Chapter 9 – Future Work

9.1 INTRODUCTION

The models presented in this thesis have shown potential in guiding patient-specific PEEP selection. However, there is a significant amount of additional research to be performed before these models can become a regular clinical feature in the ICU. In particular, the use of broader patient cohorts and Randomised Controlled Trials (RCTs) are required to further validate the effectiveness of the models, particularly on patient outcomes such as mortality rate and duration of MV. This chapter describes these validation processes in detail, as well as describing additional work required to expand the capability of the models.

9.2 CLINICAL DATA

Pathogenesis of experimental ARDS animal models is more consistent where the methods of developing ARDS are known and controlled. In contrast, ICU patients are more variable as the causes of disease are different, and there is a greater inter-patient variability in response to therapy. Thus, application of time-varying elastance mapping and the expiratory time-constant model to clinical data warrants further investigation in ICU patients. Robust validation requires additional clinical data from a variety of different patients with different disease conditions.

A Randomised Controlled Trial (RCT), consisting of two matched clinical cohorts, is required to evaluate the impact of a model-based approach on patient outcome. In particular, one cohort acts as a control group, while the second patient cohort undergoes a clinical protocol where PEEP is selected based on model derived metrics. Comparing the length of stay and the mortality rates of the patients in each cohort provides a fair comparison between standard MV therapy and a model-based approach in a clinical setting.

9.3 DIRECT IMAGING FOR MODEL VALIDATION

The models and metrics developed in this thesis have demonstrated clinical potential to guide optimal PEEP selection. Model-based approaches guide MV therapy using patient-specific parameters derived from measured data. However, validation of the clinical relevance and physiological insight of a model-based approach is currently limited. In particular, some of the findings of this research are based solely on observation of clinically expected trends. Thus, model recommendations must be further investigated by additional monitoring tools such as in-vivo microscopy, Computed Tomography (CT) scans (Lu et al., 2001, Malbouisson et al., 2001, Gattinoni et al., 2006b) and/or Electrical Impedance Tomography (EIT) (Denai et al., 2010, Luecke et al., 2012). These monitoring tools enable the recruitment of collapsed lung regions to be observed in real-time, validating the predictive capability and clinical potential of the models.

9.4 EXTENSION OF THE MODELS

9.4.1 Time-Varying Elastance Mapping

Directly following a PEEP step increase, some subjects showed a decreasing dynamic respiratory system elastance (E_{drs}) trajectory, followed by an increasing E_{drs} trajectory towards the end of inspiration. Therefore, PEEP increments of 1 cmH_2O, rather than the more typical and much larger increments of 5 cmH_2O, may avoid any damage due to the raised elastance in the early breaths and adaptation period following a PEEP increase. Smaller PEEP increments, each followed by a short period of stabilisation, may substantially reduce the peak of the E_{drs} spikes at the end of inspiration. This finding warrants further investigation where staircase recruitment is performed using smaller PEEP increments. The added clinical effect could be readily offset by automation. Changes in ventilator pattern or mode also have the potential to modify the E_{drs} trajectory, thus requiring further investigation.

9.4.2 Expiratory Time-Constant Model

The clinical merit of the expiratory time-constant model parameter (K) relies on the assumption that the respiratory system resistance, R_{rs}, remains constant throughout therapy. Significant variation in R_{rs} will result in a poor correlation between K and the respiratory system elastance, E_{rs}. However, the degree to which R_{rs} varies with PEEP and disease state was different for each subject in this study. A larger cohort may provide more consistency. In addition, the relationship between airway resistance and PEEP could be determined by designing a clinical protocol where the tidal volume, V_t, is varied between low and high values at a constant PEEP, as shown in Figure 9.1. An associated End-Inspiratory Pause

(EIP) would allow the static resistance, R_{static}, to be determined at a corresponding plateau airway pressure, P_{plat}. Thus, P_{plat} is used as a proxy for PEEP, and the relationship between R_{rs} and airway pressure can be established. Alternatively, developing and integrating a database of the resistance characteristics of common breathing circuit tubes, under a variety of different flow patterns, would increase the accuracy of bedside diagnosis.

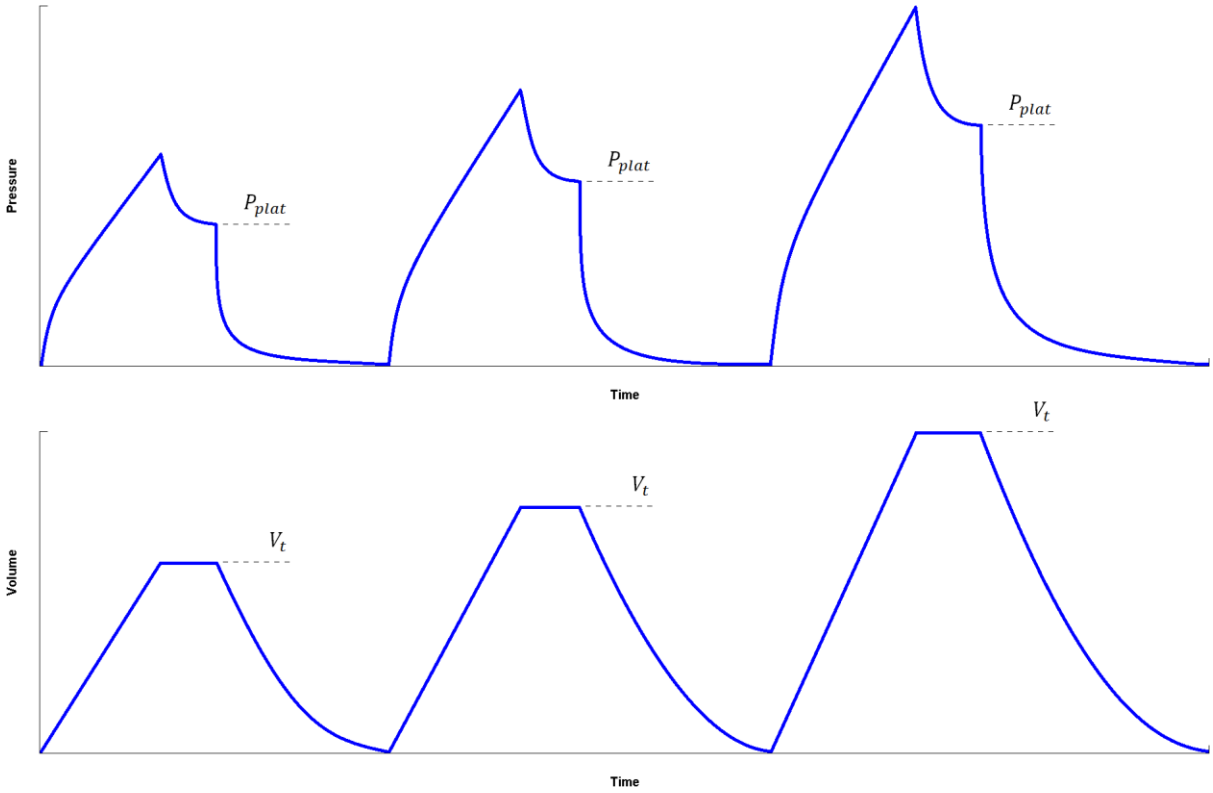

Figure 9.1 – Outline of a clinical protocol to determine the relationship between airway resistance and PEEP.

The effect of body mass and/or severity of ARDS may influence the physiological process of expiration, leading to a lower observed correlation between K and E_{rs}. However, due to the small number of subjects in this study, this conclusion is limited in its impact and thus warrants further investigation.

For patients with impaired lung function, MV is used as a supportive means, rather than completely taking over the breathing process. Thus, one potential application of the expiratory time-constant model is to estimate real-time lung parameters of spontaneously breathing patients, without additional measuring tools, opening up the clinical applicability of a model-based approach to guiding MV therapy. However, further investigation is required. In particular, continuous data from patients who transition between a fully sedated state and a spontaneously breathing state, where the state of breathing is known throughout, must be obtained. Continuous monitoring of *K* will allow for differences in trend to be observed between the two breathing states. Minimal differences in trend would suggest that the model can be extended to spontaneously breathing patients.

9.4.3 Model-Based dFRC

Ultimately, validation of the use of β and β_1 as population constants in the ICU requires the size of the sampled dataset to be large enough to warrant their applicability. The research presented in this thesis suggests that β and β_1 are appropriate as population constants. However, there is some variation in β and β_1 across different patient cohorts. Although this variation is minimal across the majority of patients studied, some β_1 values varied significantly. Further clinical trials may indicate that more accurate prediction of dynamic Functional Residual Capacity (dFRC) is achieved using different ARDS patient cohorts, each with their own unique β and β_1 values, unique to a specific disease condition or type of ventilation history.

9.5 CLINICAL APPLICATION AND AUTOMATION

Real-time application of the models presented in this thesis requires a full or semi-automated system that features data acquisition, data processing, and analysis. Furthermore, the entire system must be arranged such that it requires minimal effort from the ICU staff to operate. The model recommendations and associated information must also be presented in an intuitively clear manner. Hence, automation of the system provides further technical research avenues based on clinical implementation.

References

AGARWAL, R. & NATH, A. 2007. Peak pressures or plateau pressures in acute asthma. *Intensive Care Medicine,* 33**,** 203-203.

AL-RAWAS, N., BANNER, M., EULIANO, N., TAMS, C., BROWN, J., MARTIN, A. D. & GABRIELLI, A. 2013. Expiratory time constant for determinations of plateau pressure, respiratory system compliance, and total resistance. *Critical Care,* 17**,** R23.

ALBAICETA, G., GARCIA, E. & TABOADA, F. 2007. Comparative study of four sigmoid models of pressure-volume curve in acute lung injury. *BioMedical Engineering OnLine,* 6**,** 7.

ALBAICETA, G. M., BLANCH, L. & LUCANGELO, U. 2008. Static pressure-volume curves of the respiratory system: were they just a passing fad? *Current Opinion in Critical Care,* 14**,** 80-86.

ALBERT, S. P., DIROCCO, J., ALLEN, G. B., BATES, J. H. T., LAFOLLETTE, R., KUBIAK, B. D., FISCHER, J., MARONEY, S. & NIEMAN, G. F. 2009. The role of time and pressure on alveolar recruitment. *Journal of Applied Physiology,* 106**,** 757-765.

ALLARDET-SERVENT, J., FOREL, J.-M., ROCH, A., GUERVILLY, C., CHICHE, L., CASTANIER, M., EMBRIACO, N., GAINNIER, M. & PAPAZIAN, L. 2009. FIO2 and acute respiratory distress syndrome definition during lung protective ventilation. *Critical Care Medicine,* 37**,** 202-207.

AMATO, M. B. P., BARBAS, C. S. V., MEDEIROS, D. M., MAGALDI, R. B., SCHETTINO, G. P., LORENZI-FILHO, G., KAIRALLA, R. A., DEHEINZELIN, D., MUNOZ, C., OLIVEIRA, R., TAKAGAKI, T. Y. & CARVALHO, C. R. R. 1998. Effect of a Protective-Ventilation Strategy on Mortality in the Acute Respiratory Distress Syndrome. *New England Journal of Medicine,* 338**,** 347-354.

ANDREASSEN, S., STEIMLE, K. L., MOGENSEN, M. L., SERNA, J. B. D. L., REES, S. & KARBING, D. S. 2010. The effect of tissue elastic properties and surfactant on alveolar stability. *Journal of Applied Physiology,* 109**,** 1369-1377.

ANZUETO, A., PETERS, J. I., TOBIN, M. J., DE LOS SANTOS, R., SEIDENFELD, J. J., MOORE, G., COX, W. J. & COALSON, J. J. 1997. Effects of prolonged controlled mechanical ventilation on diaphragmatic function in healthy adult baboons. *Critical Care Medicine,* 25**,** 1187-90.

ARTIGAS, A., BERNARD, G. R., CARLET, J., DREYFUSS, D., GATTINONI, L., HUDSON, L., LAMY, M., MARINI, J. J., MATTHAY, M. A., PINSKY, M. R., SPRAGG, R., SUTER, P. M. & THE CONSENSUS COMMITTEE 1998. The American-European Consensus Conference on ARDS, Part 2. Ventilatory, Pharmacologic, Supportive Therapy, Study Design Strategies, and Issues Related to

Recovery and Remodeling. *American Journal of Respiratory and Critical Care Medicine,* 157**,** 1332-1347.

BALLARD-CROFT, C., WANG, D., SUMPTER, L. R., ZHOU, X. & ZWISCHENBERGER, J. B. 2012. Large-Animal Models of Acute Respiratory Distress Syndrome. *The Annals of Thoracic Surgery,* 93**,** 1331-1339.

BARBAS, C. S. L. V., DE MATOS, G. F. J., PINCELLI, M. P., DA ROSA BORGES, E., ANTUNES, T., DE BARROS, J. M., OKAMOTO, V., BORGES, J. O. B., AMATO, M. B. P. & RIBEIRO DE CARVALHO, C. R. 2005. Mechanical ventilation in acute respiratory failure: recruitment and high positive end-expiratory pressure are necessary. *Current Opinion in Critical Care,* 11**,** 18-28.

BARBERIS, L., MANNO, E. & GUÉRIN, C. 2003. Effect of end-inspiratory pause duration on plateau pressure in mechanically ventilated patients. *Intensive Care Medicine,* 29**,** 130-134.

BASTARACHE, J. A. & BLACKWELL, T. S. 2009. Development of animal models for the acute respiratory distress syndrome. *Disease Models & Mechanisms,* 2**,** 218-223.

BATES, J. 2007. A Recruitment Model of Quasi-Linear Power-Law Stress Adaptation in Lung Tissue. *Annals of Biomedical Engineering,* 35**,** 1165-1174.

BATES, J. H. T. 2009. *Lung Mechanics: An Inverse Modeling Approach,* New York, Cambridge University Press.

BATES, J. H. T. & IRVIN, C. G. 2002. Time dependence of recruitment and derecruitment in the lung: a theoretical model. *Journal of Applied Physiology,* 93**,** 705-713.

BERNSTEIN, D. B., NGUYEN, B., ALLEN, G. B. & BATES, J. H. 2013. Elucidating the fuzziness in physician decision making in ARDS. *Journal of Clinical Monitoring and Computing,* 27**,** 357-63.

BERSTEN, A. D. 1998. Measurement of overinflation by multiple linear regression analysis in patients with acute lung injury. *European Respiratory Journal,* 12**,** 526-532.

BERSTEN, A. D., EDIBAM, C., HUNT, T., MORAN, J., GROUP, T. A. & NEW ZEALAND INTENSIVE CARE SOCIETY CLINICAL, T. 2002. Incidence and Mortality of Acute Lung Injury and the Acute Respiratory Distress Syndrome in Three Australian States. *American Journal of Respiratory and Critical Care Medicine,* 165**,** 443-448.

BORGES, J. B., OKAMOTO, V. N., MATOS, G. F., CARAMEZ, M. P., ARANTES, P. R., BARROS, F., SOUZA, C. E., VICTORINO, J. A., KACMAREK, R. M., BARBAS, C. S., CARVALHO, C. R. & AMATO, M. B. 2006. Reversibility of lung collapse and hypoxemia in early acute respiratory distress syndrome. *American Journal of Respiratory and Critical Care Medicine,* 174**,** 268 - 278.

BORGES SOBRINHO, J. B., DE CARVALHO, C. R. R. & AMATO, M. B. P. 2006. Is Maximal Lung Recruitment Worth It? *American Journal of Respiratory and Critical Care Medicine,* 174**,** 1159a.

BRIEL, M., MEADE, M., MERCAT, A., BROWER, R. G., TALMOR, D., WALTER, S. D., SLUTSKY, A. S., PULLENAYEGUM, E., ZHOU, Q., COOK, D., BROCHARD, L., RICHARD, J. C., LAMONTAGNE, F., BHATNAGAR, N., STEWART, T. E. &

GUYATT, G. 2010. Higher vs lower positive end-expiratory pressure in patients with acute lung injury and acute respiratory distress syndrome: systematic review and meta-analysis. *JAMA: The Journal of the American Medical Association,* 303**,** 865-73.

BROCHARD, L., ROUDOT-THORAVAL, F., ROUPIE, E., DELCLAUX, C., CHASTRE, J., FERNANDEX-MONDEJAR, E., CLEMENTI, E., MANCEBO, J., FACTOR, P., MATAMIS, D., RANIERI, M., BLANCH, L., RODI, G., MENTEC, H., DREYFUSS, D., FERRER, M., BRUN-BUISSON, C., TOBIN, M. & LEMAIRE, F. 1998. Tidal Volume Reduction for Prevention of Ventilator-induced Lung Injury in Acute Respiratory Distress Syndrome. *American Journal of Respiratory and Critical Care Medicine,* 158**,** 1831-1838.

BROWER, R. G., LANKEN, P. N., MACINTYRE, N., MATTHAY, M. A., MORRIS, A., ANCUKIEWICZ, M., SCHOENFELD, D. & THOMPSON, B. T. 2004. Higher versus Lower Positive End-Expiratory Pressures in Patients with the Acute Respiratory Distress Syndrome. *New England Journal of Medicine,* 351**,** 327-336.

BROWER, R. G., SHANHOLTZ, C. B., FESSLER, H. E., SHADE, D. M., WHITE, P. J., WIENER, C. M., TEETER, J. G., DODD-O, J. M., ALMOG, Y. & PIANTADOSI, S. 1999. Prospective, randomized, controlled clinical trial comparing traditional versus reduced tidal volume ventilation in acute respiratory distress syndrome patients. *Critical Care Medicine,* 27**,** 1492-1498.

BURLESON, B. S. & MAKI, E. D. 2005. Acute Respiratory Distress Syndrome. *Journal of Pharmacy Practice,* 18**,** 118-131.

BURROWES, K. S., HUNTER, P. J. & TAWHAI, M. H. 2005. Anatomically based finite element models of the human pulmonary arterial and venous trees including supernumerary vessels. *Journal of Applied Physiology,* 99**,** 731-738.

CAGIDO, V. R. & ZIN, W. A. 2007. The pressure-volume curve. *In:* GULLO, A. (ed.) *Anaesthesia, Pain, Intensive Care and Emergency A.P.I.C.E.* Springer Milan.

CARNEY, D., DIROCCO, J. & NIEMAN, G. 2005. Dynamic alveolar mechanics and ventilator-induced lung injury. *Critical Care Medicine,* 33**,** S122-S128.

CARNEY, D. E., BREDENBERG, C. E., SCHILLER, H. J., PICONE, A. L., MCCANN, U. G., GATTO, L. A., BAILEY, G., FILLINGER, M. & NIEMAN, G. F. 1999. The Mechanism of Lung Volume Change during Mechanical Ventilation. *American Journal of Respiratory and Critical Care Medicine,* 160**,** 1697-1702.

CARVALHO, A., JANDRE, F., PINO, A., BOZZA, F., SALLUH, J., RODRIGUES, R., ASCOLI, F. & GIANNELLA-NETO, A. 2007. Positive end-expiratory pressure at minimal respiratory elastance represents the best compromise between mechanical stress and lung aeration in oleic acid induced lung injury. *Critical Care,* 11**,** R86.

CARVALHO, A., JANDRE, F., PINO, A., BOZZA, F., SALLUH, J., RODRIGUES, R., SOARES, J. & GIANNELLA-NETO, A. 2006. Effects of descending positive end-expiratory pressure on lung mechanics and aeration in healthy anaesthetized piglets. *Critical Care,* 10**,** R122.

CHASE, J. G., YUTA, T., MULLIGAN, K., SHAW, G. & HORN, B. 2006. A novel mechanical lung model of pulmonary diseases to assist with teaching and training. *BMC Pulmonary Medicine,* 6**,** 21.

CHELUCCI, G.-L., LOCCHI, F. & ZIN, W. A. 2005. On the interaction between respiratory compartments during passive expiration in ARDS patients. *Respiratory Physiology & Neurobiology,* 145**,** 53-63.

CHELUCCI, G. L., DALL' AVA-SANTUCCI, J., DHAINAUT, J. F., CHELUCCI, A., ALLEGRA, A., PACCALY, D., BRUNET, F., MILIC-EMILI, J. & LOCKHART, A. 1993. Modelling of passive expiration in patients with adult respiratory distress syndrome. *European Respiratory Journal,* 6**,** 785-90.

CHENEY, M., ISAACSON, D. & NEWELL, J. C. 1999. Electrical impedance tomography. *Society for Industrial and Applied Mathematics Review,* 41**,** 85.

CHEW, M., IHRMAN, L., DURING, J., BERGENZAUN, L., ERSSON, A., UNDEN, J., RYDEN, J., AKERMAN, E. & LARSSON, M. 2012. Extravascular lung water index improves the diagnostic accuracy of lung injury in patients with shock. *Critical Care,* 16**,** R1.

CHIEW, Y. S., CHASE, J. G., LAMBERMONT, B., JANSSEN, N., SCHRANZ, C., MOELLER, K., SHAW, G. & DESAIVE, T. 2012a. Physiological relevance and performance of a minimal lung model - an experimental study in healthy and acute respiratory distress syndrome model piglets. *BMC Pulmonary Medicine,* 12**,** 59.

CHIEW, Y. S., CHASE, J. G., SHAW, G., SUNDARESAN, A. & DESAIVE, T. 2011. Model-based PEEP Optimisation in Mechanical Ventilation. *BioMedical Engineering OnLine,* 10**,** 111.

CHIEW, Y. S., CHASE, J. G., SHAW, G. M. & DESAIVE, T. 2012b. Respiratory system elastance monitoring during PEEP titration. *Critical Care,* 16**,** P103.

CHIUMELLO, D., CARLESSO, E., CADRINGHER, P., CAIRONI, P., VALENZA, F., POLLI, F., TALLARINI, F., COZZI, P., CRESSONI, M., COLOMBO, A., MARINI, J. J. & GATTINONI, L. 2008. Lung Stress and Strain during Mechanical Ventilation for Acute Respiratory Distress Syndrome. *American Journal of Respiratory and Critical Care Medicine,* 178**,** 346-355.

CINEL, I., JEAN, S. & TAY, C. 2006. Effect of end inspiratory flow on configuration of vibration response imaging (VRI) waveform. *Intensive Care Medicine,* Suppl 1**,** S91.

CROTTI, S., MASCHERONI, D., CAIRONI, P., PELOSI, P., RONZONI, G., MONDINO, M., MARINI, J. J. & GATTINONI, L. 2001. Recruitment and Derecruitment during Acute Respiratory Failure. A Clinical Study. *American Journal of Respiratory and Critical Care Medicine,* 164**,** 131-140.

DASTA, J. F., MCLAUGHLIN, T. P., MODY, S. H. & PIECH, C. T. 2005. Daily cost of an intensive care unit day: The contribution of mechanical ventilation. *Critical Care Medicine,* 33**,** 1266-1271.

DE MATOS, G., STANZANI, F., PASSOS, R., FONTANA, M., ALBALADEJO, R., CASERTA, R., SANTOS, D., BORGES, J., AMATO, M. & BARBAS, C. 2012. How large is the lung recruitability in early acute respiratory distress syndrome: a prospective case series of patients monitored by computed tomography. *Critical Care,* 16**,** R4.

DENAI, M. A., MAHFOUF, M., MOHAMAD-SAMURI, S., PANOUTSOS, G., BROWN, B. H. & MILLS, G. H. 2010. Absolute Electrical Impedance Tomography (aEIT) Guided Ventilation Therapy in Critical Care Patients: Simulations and Future Trends. *Information Technology in Biomedicine, IEEE Transactions on,* 14**,** 641-649.

DREYFUSS, D. & SAUMON, G. 1998. Ventilator-induced Lung Injury. Lessons from Experimental Studies. *American Journal of Respiratory and Critical Care Medicine,* 157**,** 294 - 323.

DRIES, D. J. 1997. Weaning from Mechanical Ventilation. *The Journal of Trauma and Acute Care Surgery,* 43**,** 372-384.

DUNKEL, B. 2006. Acute Lung Injury and Acute Respiratory Distress Syndrome in Foals. *Clinical Techniques in Equine Practice,* 5**,** 127-133.

EBERHARD, L., GUTTMANN, J., WOLFF, G., BERTSCHMANN, W., MINZER, A., KOHL, H., ZERAVIK, J., ADOLPH, M. & ECKART, J. 1992. Intrinsic PEEP monitored in the ventilated ARDS patient with a mathematical method. *Journal of Applied Physiology,* 73**,** 479 - 485.

FERGUSON, N. D., FRUTOS-VIVAR, F., ESTEBAN, A., ANZUETO, A., ALIA, I., BROWER, R. G., STEWART, T. E., APEZTEGUIA, C., GONZALEZ, M., SOTO, L., ABROUG, F. & BROCHARD, L. 2005. Airway pressures, tidal volumes, and mortality in patients with acute respiratory distress syndrome. *Critical Care Medicine,* 33**,** 21-30.

FOREL, J.-M., VOILLET, F., PULINA, D., GACOUIN, A., PERRIN, G., BARRAU, K., JABER, S., ARNAL, J.-M., FATHALLAH, M., AUQUIER, P., ROCH, A., AZOULAY, E. & PAPAZIAN, L. 2012. Ventilator-associated pneumonia and ICU mortality in severe ARDS patients ventilated according to a lung-protective strategy. *Critical Care,* 16**,** R65.

FRERICHS, I. 2000. Electrical impedance tomography (EIT) in applications related to lung and ventilation: a review of experimental and clinical activities. *Physiological Measurement,* 21**,** R1.

FRERICHS, I., PULLETZ, S., ELKE, G., ZICK, G. & WEILER, N. 2010. Electrical Impedance Tomography in Acute Respiratory Distress Syndrome. *The Open Nuclear Medicine Journal,* 2**,** 110-118.

FULEIHAN, S. F., WILSON, R. S. & PONTOPPIDAN, H. 1976. Effect of Mechanical Ventilation with End-inspiratory Pause on Blood-Gas Exchange. *Anesthesia & Analgesia,* 55**,** 122-130.

GAJIC, O., DARA, S. I., MENDEZ, J. L., ADESANYA, A. O., FESTIC, E., CAPLES, S. M., RANA, R., ST. SAUVER, J. L., LYMP, J. F., AFESSA, B. & HUBMAYR, R. D. 2004. Ventilator-associated lung injury in patients without acute lung injury at the onset of mechanical ventilation *. *Critical Care Medicine,* 32**,** 1817-1824.

GANZERT, S., MOLLER, K., STEINMANN, D., SCHUMANN, S. & GUTTMANN, J. 2009. Pressure-dependent stress relaxation in acute respiratory distress syndrome and healthy lungs: an investigation based on a viscoelastic model. *Critical Care,* 13**,** R199.

GATTINONI, L., CAIRONI, P., CRESSONI, M., CHIUMELLO, D., RANIERI, V. M., QUINTEL, M., RUSSO, S., PATRONITI, N., CORNEJO, R. & BUGEDO, G. 2006a. Lung Recruitment in Patients with the Acute Respiratory Distress Syndrome. *New England Journal of Medicine,* 354**,** 1775-1786.

GATTINONI, L., CAIRONI, P., PELOSI, P. & GOODMAN, L. R. 2001. What Has Computed Tomography Taught Us about the Acute Respiratory Distress Syndrome? *American Journal of Respiratory and Critical Care Medicine,* 164**,** 1701-1711.

GATTINONI, L., CAIRONI, P., VALENZA, F. & CARLESSO, E. 2006b. The role of CT-scan studies for the diagnosis and therapy of acute respiratory distress syndrome. *Clinics in Chest Medicine,* 27**,** 559 - 570.

GATTINONI, L., CARLESSO, E., CADRINGHER, P., VALENZA, F., VAGGINELLI, F. & CHIUMELLO, D. 2003. Physical and biological triggers of ventilator-induced lung injury and its prevention. *European Respiratory Journal,* 22**,** 15s-25.

GATTINONI, L., CHIUMELLO, D., CARLESSO, E. & VALENZA, F. 2004. Bench-to-bedside review: Chest wall elastance in acute lung injury/acute respiratory distress syndrome patients. *Critical Care,* 8**,** 350 - 355.

GATTINONI, L. & PESENTI, A. 2005. The concept of "baby lung". *Intensive Care Medicine,* 31**,** 776 - 784.

GIRGIS, K., HAMED, H., KHATER, Y. & KACMAREK, R. M. 2006. A decremental PEEP trial identifies the PEEP level that maintains oxygenation after lung recruitment. *Respiratory Care,* 51**,** 1132 - 1139.

GRASSO, S., STRIPOLI, T., DE MICHELE, M., BRUNO, F., MOSCHETTA, M., ANGELELLI, G., MUNNO, I., RUGGIERO, V., ANACLERIO, R., CAFARELLI, A., DRIESSEN, B. & FIORE, T. 2007. ARDSnet Ventilatory Protocol and Alveolar Hyperinflation: Role of Positive End-Expiratory Pressure. *American Journal of Respiratory and Critical Care Medicine,* 176**,** 761-767.

GRINNAN, D. & TRUWIT, J. 2005. Clinical review: Respiratory mechanics in spontaneous and assisted ventilation. *Critical Care,* 9**,** 472 - 484.

GUTTMANN, J., EBERHARD, L., FABRY, B., ZAPPE, D., BERNHARD, H., LICHTWARCK-ASCHOFF, M., ADOLPH, M. & WOLFF, G. 1994. Determination of volume-dependent respiratory system mechanics in mechanically ventilated patients using the new SLICE method. *Technology Assessment in Health Care,* 2**,** 175 - 191.

HABERTHUR, C., MEHLIG, A., STOVER, J., SCHUMANN, S., MOLLER, K., PRIEBE, H.-J. & GUTTMANN, J. 2009. Expiratory automatic endotracheal tube compensation reduces dynamic hyperinflation in a physical lung model. *Critical Care,* 13**,** R4.

HAHN, G., JUST, A., HELLIGE, G., SCHARFETTER, H. & MERWA, R. 2007. Determination of the dynamic measurement error of EIT systems. 13th International Conference on Electrical Bioimpedance and the 8th Conference on Electrical Impedance Tomography. *In:* MAGJAREVIC, R. (ed.). Springer Berlin Heidelberg.

HALTER, J. M., STEINBERG, J. M., SCHILLER, H. J., DASILVA, M., GATTO, L. A., LANDAS, S. & NIEMAN, G. F. 2003. Positive End-Expiratory Pressure after a

Recruitment Maneuver Prevents Both Alveolar Collapse and Recruitment/Derecruitment. *American Journal of Respiratory and Critical Care Medicine,* 167**,** 1620-1626.

HANN, C. E., CHASE, J. G., LIN, J., LOTZ, T., DORAN, C. V. & SHAW, G. M. 2005. Integral-based parameter identification for long-term dynamic verification of a glucose-insulin system model. *Computer Methods and Programs in Biomedicine,* 77**,** 259-270.

HARRIS, R. S. 2005. Pressure-volume curves of the respiratory system. *Respiratory Care,* 50**,** 78-98.

HEDENSTIERNA, G. & ROTHEN, H. U. 2000. Atelectasis formation during anesthesia: causes and measures to prevent it. *Journal of Clinical Monitoring and Computing,* 16**,** 329 - 335.

HEINZE, H., SCHAAF, B., GREFER, J., KLOTZ, K. & EICHLER, W. 2007. The Accuracy of the Oxygen Washout Technique for Functional Residual Capacity Assessment During Spontaneous Breathing. *Anesthesia & Analgesia,* 104**,** 598-604.

HENDERSON, W. R. & SHEEL, A. W. 2012. Pulmonary mechanics during mechanical ventilation. *Respiratory Physiology & Neurobiology,* 180**,** 162-172.

HICKLING, K. G. 2001. Best compliance during a decremental, but not incremental, positive end-expiratory pressure trial is related to open-lung positive end-expiratory pressure: a mathematical model of acute respiratory distress syndrome lungs. *American Journal of Respiratory and Critical Care Medicine,* 163**,** 69 - 78.

HODGSON, C., TUXEN, D., DAVIES, A., BAILEY, M., HIGGINS, A., HOLLAND, A., KEATING, J., PILCHER, D., WESTBROOK, A., COOPER, D. & NICHOL, A. 2011a. A randomised controlled trial of an open lung strategy with staircase recruitment, titrated PEEP and targeted low airway pressures in patients with acute respiratory distress syndrome. *Critical Care,* 15**,** R133.

HODGSON, C. L., TUXEN, D. V., BAILEY, M. J., HOLLAND, A. E., KEATING, J. L., PILCHER, D., THOMSON, K. R. & VARMA, D. 2011b. A Positive Response to a Recruitment Maneuver With PEEP Titration in Patients With ARDS, Regardless of Transient Oxygen Desaturation During the Maneuver. *Journal of Intensive Care Medicine,* 26**,** 41-49.

INGELSTEDT, S., JONSON, B., NORDSTRÖM, L. & OLSSON, S.-G. 1972. A Servo-Controlled Ventilator Measuring Expired Minute Volume, Airway Flow and Pressure. *Acta Anaesthesiologica Scandinavica,* 16**,** 7-27.

JEAN, S., DELLINGER, R., CINEL, I., RAO, S., KUSHNIR, I. & PARRILLO, J. 2006. Increased spatial distribution of airflow in lungs with low-level pressure support ventilation compared with maintenance ventilation. *Critical Care,* 10**,** P33.

JONSON, B., RICHARD, J. C., STRAUS, C., MANCEBO, J., LEMAIRE, F. & BROCHARD, L. 1999. Pressure-Volume Curves and Compliance in Acute Lung Injury. Evidence of Recruitment Above the Lower Inflection Point. *American Journal of Respiratory and Critical Care Medicine,* 159**,** 1172-1178.

JONSON, B. & UTTMAN, L. 2007. Efficient gas exchange with low tidal volume ventilation in acute respiratory distress syndrome. *Journal of Organ Dysfunction,* 3**,** 82-89.

KALLET, R. H., CAMPBELL, A. R., DICKER, R. A., KATZ, J. A. & MACKERSIE, R. C. 2006. Effects of tidal volume on work of breathing during lung-protective ventilation in patients with acute lung injury and acute respiratory distress syndrome *. *Critical Care Medicine,* 34**,** 8-14.

KARASON, S., KARLSEN, K. L., LUNDIN, S. & STENQVIST, O. 1999. A simplified method for separate measurements of lung and chest wall mechanics in ventilator-treated patients. *Acta Anaesthesiologica Scandinavica,* 43**,** 308-315.

KARASON, S., SONDERGAARD, S., LUNDIN, S. & STENQVIST, O. 2001. Continuous on-line measurements of respiratory system, lung and chest wall mechanics during mechanic ventilation. *Intensive Care Medicine,* 27**,** 1328-1339.

KARASON, S., SONDERGAARD, S., LUNDIN, S., WIKLUND, J. & STENQVIST, O. 2000. Evaluation of pressure/volume loops based on intratracheal pressure measurements during dynamic conditions. *Acta Anaesthesiologica Scandinavica,* 44**,** 571-577.

KHIRANI, S., POLESE, G., ALIVERTI, A., APPENDINI, L., NUCCI, G., PEDOTTI, A., COLLEDAN, M., LUCIANETTI, A., BACONNIER, P. & ROSSI, A. 2010. On-line monitoring of lung mechanics during spontaneous breathing: a physiological study. *Respiratory Medicine,* 104**,** 463-471.

LAMBERMONT, B., GHUYSEN, A., JANSSEN, N., MORIMONT, P., HARTSTEIN, G., GERARD, P. & D'ORIO, V. 2008. Comparison of functional residual capacity and static compliance of the respiratory system during a positive end-expiratory pressure (PEEP) ramp procedure in an experimental model of acute respiratory distress syndrome. *Critical Care,* 12**,** R91.

LAUZON, A. M. & BATES, J. H. 1991. Estimation of time-varying respiratory mechanical parameters by recursive least squares. *Journal of Applied Physiology,* 71**,** 1159-1165.

LEE, C. I., HAIMS, A. H., MONICO, E. P., BRINK, J. A. & FORMAN, H. P. 2004. Diagnostic CT Scans: Assessment of Patient, Physician, and Radiologist Awareness of Radiation Dose and Possible Risks1. *Radiology,* 231**,** 393-398.

LEVINE, S., NGUYEN, T., TAYLOR, N., FRISCIA, M. E., BUDAK, M. T., ROTHENBERG, P., ZHU, J., SACHDEVA, R., SONNAD, S., KAISER, L. R., RUBINSTEIN, N. A., POWERS, S. K. & SHRAGER, J. B. 2008. Rapid Disuse Atrophy of Diaphragm Fibers in Mechanically Ventilated Humans. *New England Journal of Medicine,* 358**,** 1327-1335.

LICHTWARCK-ASCHOFF, M., KESSLER, V., SJOSTRAND, U. H., HEDLUND, A., MOLS, G., RUBERTSSON, S., MARKSTROM, A. M. & GUTTMANN, J. 2000. Static versus dynamic respiratory mechanics for setting the ventilator. *British Journal of Anaesthesia,* 85**,** 577-586.

LIONHEART, W. R. B. 2004. Review: developments in EIT reconstruction algorithms: pitfalls, challenges and recent developments. *Physiological Measurement,* 25**,** 125.

LU, Q., MALBOUISSON, L. M., MOURGEON, E., GOLDSTEIN, I., CORIAT, P. & ROUBY, J. J. 2001. Assessment of PEEP-induced reopening of collapsed lung regions in acute lung injury: are one or three CT sections representative of the entire lung? *Intensive Care Medicine,* 27**,** 1504-1510.

LUCANGELO, U., BERNABÈ, F. & BLANCH, L. 2007. Lung mechanics at the bedside: make it simple. *Current Opinion in Critical Care,* 13**,** 64-72

LUECKE, T., CORRADI, F. & PELOSI, P. 2012. Lung imaging for titration of mechanical ventilation. *Current Opinion in Anesthesiology,* 25**,** 131-140.

LUHR, O. R., ANTONSEN, K. & KARLSSON, M. 1999. Incidence and mortality after acute respiratory failure and acute respiratory distress syndrome in Sweden, Denmark, and Iceland. *American Journal of Respiratory and Critical Care Medicine,* 159**,** 1849.

MAGGIORE, S. M., RICHARD, J. C. & BROCHARD, L. 2003. What has been learnt from P/V curves in patients with acute lung injury/acute respiratory distress syndrome. *European Respiratory Journal,* 22**,** 22s-26s.

MALBOUISSON, L. M., MULLER, J.-C., CONSTANTIN, J.-M., LU, Q. I. N., PUYBASSET, L., ROUBY, J.-J. & THE, C. T. S. A. S. G. 2001. Computed Tomography Assessment of Positive End-expiratory Pressure-induced Alveolar Recruitment in Patients with Acute Respiratory Distress Syndrome. *American Journal of Respiratory and Critical Care Medicine,* 163**,** 1444-1450.

MALHOTRA, A. 2007. Low-Tidal-Volume Ventilation in the Acute Respiratory Distress Syndrome. *The New England Journal of Medicine,* 357**,** 1113-1120.

MANZANO, F., YUSTE, E., COLMENERO, M., ARANDA, A., GARCIA-HORCAJADAS, A., RIVERA, R. & FERNANDEZ-MONDEJAR, E. 2005. Incidence of acute respiratory distress syndrome and its relation to age. *Journal of Critical Care,* 20**,** 274-280.

MARINI, J., CAPPS, J. & CULVER, B. 1985. The inspiratory work of breathing during assisted mechanical ventilation. *Chest,* 87**,** 612 - 618.

MCCANN, U. G., SCHILLER, H. J., CARNEY, D. E., GATTO, L. A., STEINBERG, J. M. & NIEMAN, G. F. 2001. Visual validation of the mechanical stabilizing effects of positive end-expiratory pressure at the alveolar level. *Journal of Surgical Research,* 99**,** 335-342.

MEAD, J. & WHITTENBERGER, J. L. 1953. Physical Properties of Human Lungs Measured During Spontaneous Respiration. *Journal of Applied Physiology,* 5**,** 779-796.

MEADE, M. O., COOK, D. J., GUYATT, G. H., SLUTSKY, A. S., ARABI, Y. M., COOPER, D. J., DAVIES, A. R., HAND, L. E., ZHOU, Q., THABANE, L., AUSTIN, P., LAPINSKY, S., BAXTER, A., RUSSELL, J., SKROBIK, Y., RONCO, J. J., STEWART, T. E. & INVESTIGATORS FOR THE LUNG OPEN VENTILATION STUDY 2008. Ventilation Strategy Using Low Tidal Volumes, Recruitment Maneuvers, and High Positive End-Expiratory Pressure for Acute Lung Injury and Acute Respiratory Distress Syndrome: A Randomized Controlled Trial. *JAMA: The Journal of the American Medical Association,* 299**,** 637-645.

MERCAT, A., RICHARD, J.-C. M., VIELLE, B., JABER, S., OSMAN, D., DIEHL, J.-L., LEFRANT, J.-Y., PRAT, G., RICHECOEUR, J., NIESZKOWSKA, A., GERVAIS, C., BAUDOT, J., BOUADMA, L., BROCHARD, L. & FOR THE EXPIRATORY PRESSURE STUDY, G. 2008. Positive End-Expiratory Pressure Setting in Adults With Acute Lung Injury and Acute Respiratory Distress Syndrome: A Randomized Controlled Trial. *JAMA: The Journal of the American Medical Association,* 299**,** 646-655.

MIRELES-CABODEVILA, E., DIAZ-GUZMAN, E., HERESI, G. A. & CHATBURN, R. L. 2009. Alternative modes of mechanical ventilation: A review for the hospitalist. *Cleveland Clinic Journal of Medicine,* 76**,** 417-430.

MISHRA, A., CHIEW, Y., SHAW, G. & CHASE, J. 2012. Model-based Approach to Estimate dFRC in the ICU Using Measured Lung Dynamics. 8th IFAC Symposium on Biological and Medical Systems.

MOLLER, K., ZHAO, Z., STAHL, C. A. & GUTTMANN, J. On the analysis of dynamic lung mechanics separately in ins- and expiration. *In:* BAMIDIS, P. D. & PALLIKARAKIS, N., eds. MEDICON 2010, IFMBE Proceedings, 2010a Chalkidiki, Greece. Springer, 164-7.

MOLLER, K., ZHAO, Z., STAHL, C. A. & GUTTMANN, J. Seperate analysis of respiratory system mechanics in inspiration and expiration. *In:* SCHMÜCKER, P., ELLSÄSSER, K.-H. & HAYNA, S., eds. 55. GMDS-Jahrestagung, 2010b Mannheim, Germany. Antares Verlag, 566-7.

MOLS, G., KESSLER, V., BENZING, A., LICHTWARCK-ASCHOFF, M., GEIGER, K. & GUTTMANN, J. 2001. Is pulmonary resistance constant, within the range of tidal volume ventilation, in patients with ARDS? *British Journal of Anaesthesia,* 86**,** 176-182.

NINANE, V. 1997. "Intrinsic" PEEP (PEEPi): role of expiratory muscles. *European Respiratory Journal,* 10**,** 516-518.

OTIS, A. B., FENN, W. O. & RAHN, H. 1950. Mechanics of Breathing in Man. *Journal of Applied Physiology,* 2**,** 592-607.

PARSONS, P. E., EISNER, M. D., THOMPSON, B. T., MATTHAY, M. A., ANCUKIEWICZ, M., BERNARD, G. R., WHEELER, A. P. & NETWORK, T. N. A. R. D. S. C. T. 2005. Lower tidal volume ventilation and plasma cytokine markers of inflammation in patients with acute lung injury. *Critical Care Medicine,* 33**,** 1-6.

PELOSI, P., CROCI, M., RAVAGNAN, I., VICARDI, P. & GATTINONI, L. 1996. Total Respiratory System, Lung, and Chest Wall Mechanics in Sedated-Paralyzed Postoperative Morbidly Obese Patients. *Chest,* 109**,** 144-151.

PELOSI, P., GOLDNER, M., MCKIBBEN, A., ADAMS, A., ECCHER, G., CAIRONI, P., LOSAPPIO, S., GATTINONI, L. & MARINI, J. J. 2001. Recruitment and derecruitment during acute respiratory failure: an experimental study. *American Journal of Respiratory and Critical Care Medicine,* 164**,** 122 - 30.

PETTY, T. L. & ASHBAUGH, D. G. 1971. The Adult Respiratory Distress Syndrome. *Chest,* 60**,** 233-239.

PILLET, O., CHOUKROUN, M. L. & CASTAING, Y. 1993. Effects of inspiratory flow rate alterations on gas exchange during mechanical ventilation in normal lungs. Efficiency of end-inspiratory pause. *Chest,* 103**,** 1161-1165.

PUYBASSET, L., CLUZEL, P., GUSMAN, P., GRENIER, P., PRETEUX, F. & ROUBY, J. J. 2000. Regional distribution of gas and tissue in acute respiratory distress syndrome. I. Consequences for lung morphology. CT Scan ARDS Study Group. *Intensive Care Medicine,* 26**,** 857 - 869.

RETAMAL, J., LIBUY, J., JIMENEZ, M., DELGADO, M., BESA, C., BUGEDO, G. & BRUHN, A. 2013. Preliminary study of ventilation with 4 ml/kg tidal volume in acute respiratory distress syndrome: feasibility and effects on cyclic recruitment - derecruitment and hyperinflation. *Critical Care,* 17**,** R16.

REYNOLDS, H. N., MCCUNN, M., BORG, U., HABASHI, N., COTTINGHAM, C. & BAR-LAVI, Y. 1998. Acute respiratory distress syndrome: estimated incidence and mortality rate in a 5 million-person population base. *Critical Care,* 2**,** 29–34.

ROSSI, A., POLESE, G., BRANDI, G. & CONTI, G. 1995. Intrinsic positive end-expiratory pressure ($PEEP_i$). *Intensive Care Medicine,* 21**,** 522-536.

ROUBY, J. J., LU, Q. & GOLDSTEIN, I. 2002. Selecting the Right Level of Positive End-Expiratory Pressure in Patients with Acute Respiratory Distress Syndrome. *American Journal of Respiratory and Critical Care Medicine,* 165**,** 1182-1186.

SCHILLER, H. J., STEINBERG, J., HALTER, J., MCCANN, U., DASILVA, M., GATTO, L. A., CARNEY, D. & NIEMAN, G. 2003. Alveolar inflation during generation of a quasi-static pressure/volume curve in the acutely injured lung. *Critical Care Medicine,* 31**,** 1126-1133.

SCHRANZ, C., DOCHERTY, P., CHIEW, Y. S., MOLLER, K. & CHASE, J. G. 2012. Iterative Integral Parameter Identification of a Respiratory Mechanics Model. *BioMedical Engineering OnLine,* 11**,** 38.

SCHULTZ, M., HAITSMA, J., SLUTSKY, A. & GAJIC, O. 2007. What tidal volumes should be used in patients with acute lung injury? *Anesthesiology,* 106**,** 1085 - 1087.

SCHUSTER, D. 1994. ARDS: clinical lessons from the oleic acid model of acute lung injury. *American Journal of Respiratory and Critical Care Medicine,* 149**,** 245-260.

SEBEL, P. 1985. *Respiration, the breath of life,* New York, Torstar Books.

SLUTSKY, A. 1993. Mechanical Ventilation. American College of Chest Physicians' Consensus Conference. *Chest,* 104(6)**,** 1833-1859.

STENQVIST, O., GRIVANS, C., ANDERSSON, B. & LUNDIN, S. 2012. Lung elastance and transpulmonary pressure can be determined without using oesophageal pressure measurements. *Acta Anaesthesiologica Scandinavica,* 56**,** 738-747.

STENQVIST, O. & ODENSTEDT, H. 2007. Alveolar Pressure/volume Curves Reflect Regional Lung Mechanics. *Intensive Care Medicine***,** 407-414.

STENQVIST, O., ODENSTEDT, H. & LUNDIN, S. 2008. Dynamic respiratory mechanics in acute lung injury/acute respiratory distress syndrome: research or clinical tool? *Current Opinion in Critical Care,* 14**,** 87 - 93.

STEWART, T. E., MEADE, M. O., COOK, D. J., GRANTON, J. T., HODDER, R. V., LAPINSKY, S. E., MAZER, C. D., MCLEAN, R. F., ROGOVEIN, T. S., SCHOUTEN, B. D., TODD, T. R. J., SLUTSKY, A. S. & THE PRESSURE- AND VOLUME-LIMITED VENTILATION STRATEGY GROUP 1998. Evaluation of a Ventilation Strategy to Prevent Barotrauma in Patients at High Risk for Acute Respiratory Distress Syndrome. *New England Journal of Medicine,* 338**,** 355-361.

STORSTEIN, O., FIELD, A. S. J., MASSUMI, R. & GRAY, F. D. J. 1959. Airway Resistance and Lung Compliance. *Yale Journal of Biology and Medicine,* 31(6)**,** 387-396.

SUAREZ-SIPMANN, F., BOHM, S. H., TUSMAN, G., PESCH, T., THAMM, O., REISSMANN, H., RESKE, A., MAGNUSSON, A. & HEDENSTIERNA, G. 2007. Use of dynamic compliance for open lung positive end-expiratory pressure titration in an experimental study. *Critical Care Medicine,* 35**,** 214 - 221.

SUNDARESAN, A., CHASE, J., SHAW, G., CHIEW, Y. S. & DESAIVE, T. 2011a. Model-based optimal PEEP in mechanically ventilated ARDS patients in the Intensive Care Unit. *BioMedical Engineering OnLine,* 10**,** 64.

SUNDARESAN, A. & CHASE, J. G. 2011. Positive end expiratory pressure in patients with acute respiratory distress syndrome - The past, present and future. *Biomedical Signal Processing and Control,* 7**,** 93-103.

SUNDARESAN, A., GEOFFREY CHASE, J., HANN, C. E. & SHAW, G. M. 2011b. Dynamic functional residual capacity can be estimated using a stress-strain approach. *Computer Methods and Programs in Biomedicine,* 101**,** 135-143.

SUNDARESAN, A., YUTA, T., HANN, C. E., GEOFFREY CHASE, J. & SHAW, G. M. 2009. A minimal model of lung mechanics and model-based markers for optimizing ventilator treatment in ARDS patients. *Computer Methods and Programs in Biomedicine,* 95**,** 166-180.

SWAN, A., HUNTER, P. & TAWHAI, M. 2008. Pulmonary Gas Exchange in Anatomically-Based Models of the Lung. *Integration in Respiratory Control,* 605**,** 184-189.

SWAN, A. J., CLARK, A. R. & TAWHAI, M. H. 2012. A computational model of the topographic distribution of ventilation in healthy human lungs. *Journal of Theoretical Biology,* 300**,** 222-231.

TAKEUCHI, M., GODDON, S., DOLHNIKOFF, M., SHIMAOKA, M., HESS, D., AMATO, M. B. P. & KACMAREK, R. M. 2002. Set Positive End-expiratory Pressure during Protective Ventilation Affects Lung Injury. *Anesthesiology,* 97**,** 682-692.

TALMOR, D., SARGE, T., MALHOTRA, A., O'DONNELL, C. R., RITZ, R., LISBON, A., NOVACK, V. & LORING, S. H. 2008. Mechanical Ventilation Guided by Esophageal Pressure in Acute Lung Injury. *New England Journal of Medicine,* 359**,** 2095-2104.

TAWHAI, M. H. & BURROWES, K. S. 2008. Multi-scale Models of the Lung Airways and Vascular System. *Integration in Respiratory Control,* 605**,** 190-194.

TAWHAI, M. H., HUNTER, P., TSCHIRREN, J., REINHARDT, J., MCLENNAN, G. & HOFFMAN, E. A. 2004. CT-based geometry analysis and finite element models of the human and ovine bronchial tree. *Journal of Applied Physiology,* 97**,** 2310-2321.

TERRAGNI, P. P., ROSBOCH, G., TEALDI, A., CORNO, E., MENALDO, E., DAVINI, O., GANDINI, G., HERRMANN, P., MASCIA, L., QUINTEL, M., SLUTSKY, A. S., GATTINONI, L. & RANIERI, V. M. 2007. Tidal Hyperinflation during Low Tidal Volume Ventilation in Acute Respiratory Distress Syndrome. *American Journal of Respiratory and Critical Care Medicine,* 175**,** 160-166.

THE ACUTE RESPIRATORY DISTRESS SYNDROME NETWORK 2000. Ventilation with Lower Tidal Volumes as Compared with Traditional Tidal Volumes for Acute Lung Injury and the Acute Respiratory Distress Syndrome. *New England Journal of Medicine,* 342**,** 1301-1308.

THE ARDS DEFINITION TASK FORCE 2012. Acute respiratory distress syndrome: The berlin definition. *JAMA: The Journal of the American Medical Association,* 307**,** 2526-2533.

TORTORA, G. J. & DERRICKSON, B. 2006. *Principles of Anatomy and Physiology,* J. Wiley.

VAN DRUNEN, E. J., CHASE, J. G., CHIEW, Y. S., SHAW, G. M. & DESAIVE, T. 2013a. Analysis of different model-based approaches for estimating dFRC for real-time application. *BioMedical Engineering OnLine,* 12**,** 9.

VAN DRUNEN, E. J., CHIEW, Y. S., CHASE, J. G., LAMBERMONT, B., JANSSEN, N. & DESAIVE, T. Model-based Respiratory Mechanics to Titrate PEEP and Monitor Disease State for Experimental ARDS Subjects. The 35th Annual International Conference of the IEEE Engineering in Medicine and Biology Society (EMBC'13), 3-7 July 2013b Osaka, Japan. IEEE, 4.

VAN DRUNEN, E. J., CHIEW, Y. S., CHASE, J. G., SHAW, G., LAMBERMONT, B., JANSSEN, N., DAMANHURI, N. & DESAIVE, T. 2013c. Expiratory model-based method to monitor ARDS disease state. *BioMedical Engineering OnLine,* 12**,** 57.

VAN DRUNEN, E. J., CHIEW, Y. S., PRETTY, C., SHAW, G. M., LAMBERMONT, B., JANSSEN, N., CHASE, J. G. & DESAIVE, T. 2013d. Visualisation of Time-Varying Respiratory System Elastance in Experimental ARDS Animal Models. *BMC Pulmonary Medicine,* (In Review).

VAN DRUNEN, E. J., CHIEW, Y. S., ZHAO, Z., LAMBERMONT, B., JANSSEN, N., PRETTY, C., DESAIVE, T., KNUT, M. & CHASE, J. G. Visualisation of Time-Variant Respiratory System Elastance in ARDS Models. Congress for the German Swiss and Austrian Society for Biomedical Engineering, 19-21 September 2013e Graz, Austria. BMT, 2.

VENEGAS, J. G., HARRIS, R. S. & SIMON, B. A. 1998. A comprehensive equation for the pulmonary pressure-volume curve. *Journal of Applied Physiology,* 84**,** 389 - 95.

VILLAR, J. 2005. Ventilator or physician-induced lung injury? *Minerva Anestesiologica,* 71**,** 255 - 258.

VILLAR, J., KACMAREK, R., PEREZ-MENDEZ, L. & AGUIRRE-JAIME, A. 2006. A high positive end-expiratory pressure, low tidal volume ventilatory strategy improves outcome in persistent acute respiratory distress syndrome: A randomized, controlled trial. *Critical Care Medicine,* 34**,** 1311 - 1318.

VINCENT, J.-L., CINEL, I., JEAN, S. & DELLINGER, R. P. 2007. Dynamic Lung Imaging Techniques in Mechanically Ventilated Patients. *Yearbook of Intensive Care and Emergency Medicine.* Springer Berlin Heidelberg.

WARE, L. B. 2008. Modeling human lung disease in animals. *American Journal of Physiology - Lung Cellular and Molecular Physiology,* 294**,** L149-L150.

WARE, L. B. & MATTHAY, M. A. 2000. The Acute Respiratory Distress Syndrome. *The New England Journal of Medicine,* 342**,** 1334-1349.

WERNER, R., EHRHARDT, J., SCHMIDT, R. & HANDELS, H. 2009. Patient-specific finite element modeling of respiratory lung motion using 4D CT image data. *Medical Physics,* 36**,** 1500-1511.

WIEST, P. W., LOCKEN, J. A., HEINTZ, P. H. & METTLER JR, F. A. 2002. CT scanning: A major source of radiation exposure. *Seminars in Ultrasound, CT and MRI,* 23**,** 402-410.

ZHAO, Z., GUTTMANN, J. & MOLLER, K. 2012. Adaptive Slice Method: A new method to determine volume dependent dynamic respiratory system mechanics. *Physiological Measurement,* 33**,** 51-64.

ZHAO, Z., MOLLER, K., STEINMANN, D., FRERICHS, I. & GUTTMANN, J. 2009. Evaluation of an electrical impedance tomography-based Global Inhomogeneity Index for pulmonary ventilation distribution. *Intensive Care Medicine,* 35**,** 1900-6.

ZHAO, Z., STEINMANN, D., FRERICHS, I., GUTTMANN, J. & MOLLER, K. 2010a. PEEP titration guided by ventilation homogeneity: a feasibility study using electrical impedance tomography. *Critical Care,* 14**,** R8.

ZHAO, Z., STEINMANN, D., MULLER-ZIVKOVIC, D., MARTIN, J., FRERICHS, I., GUTTMANN, J. & MOLLER, K. 2010b. A lung area estimation method for analysis of ventilation inhomogeneity based on electrical impedance tomography. *Journal of X-Ray Science and Technology,* 18**,** 171 - 182.